Utilizing Elastic System Properties for the Control of Posture and Movement

by

Joseph McIntyre

B.S. Engineering, California Institute of Technology (1982)
B.S. Biology, California Institute of Technology (1983)

Submitted to the Department of Brain and Cognitive Sciences
in partial fulfillment of the requirements for the degree of

Doctor of Philosophy

at the

MASSACHUSETTS INSTITUTE OF TECHNOLOGY

June 1990

Signature of Author_____
Department of Brain and Cognitive Sciences
May 7, 1990

Certified and Accepted by_____
Emilio Bizzi
Eugene McDermott Professor in the Brain Sciences
and Human Behavior
Chairman, Department of Brain and Cognitive Sciences

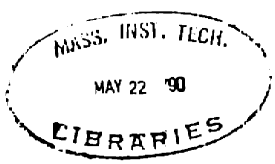

ARCHIVES

Utilizing Elastic System Properties for the Control of Posture and Movement

by

Joseph McIntyre

Submitted to the Department of Brain and Cognitive Sciences
on May 7, 1990, in partial fulfillment of the
requirements for the degree of
Doctor of Philosophy

Abstract

"What are the elastic properties of the human motor system, and how are they incorporated into the control of posture and movement?" Not only do the spring-like properties of the motor system affect the behavior of the limb, these properties can be exploited by the central nervous system to simplify the control task. The thesis addresses three main topics concerning the role of elastic system properties in the control of posture and movement.

First, the factors which affect limb stability are analyzed. The stiffness of the limb is shown to be a function of limb geometry and force output, as well as the intrinsic elastic properties of the muscles. The neuro-musculo-skeletal system must modulate joint stiffness in response to certain force loads in order to maintain stability. A number of potential control schemes are presented and compared with measured values of human arm stiffness.

Second, the issue of redundancy is addressed. Biological systems typically have more degrees of freedom than necessary for a given task. In the thesis an algorithm is analyzed which uses the passive elastic behavior of a system to resolve the redundancy. This algorithm has been extended to include the control of stiffness as well as posture. The control algorithm is used to predict the muscle activations for human subjects generating torques and forces with the arm. The model predictions are compared with published data from physiological experiments.

Finally, the concept of *movement from posture* is addressed. Can the elastic properties of the human motor system be utilized to provide a servomechanism for the control of movement as well as posture? A modification to the equilibrium point hypothesis is proposed that better predicts the behavior of the human arm during fast movements. The competence of the proposed model is tested via computer simulation of movement dynamics.

Thesis Supervisor: Emilio Bizzi
Title: Eugene McDermott Professor in the Brain Sciences and Human Behavior
Chairman, Department of Brain and Cognitive Sciences

Acknowledgments

The writing of this thesis is the culmination of what has been an exciting, fun-filled, if somewhat long, educational experience. My thanks goes to my advisor, Emilio Bizzi, for his continued support and generosity. I have very much appreciated the amount of freedom and encourgement I have been given to pursue my own interests. Thanks also to the members of my committee: Neville Hogan, Marc Raibert and Richard Anderson. Special thanks goes to Sandro Mussa-Ivaldi with whom I have collaborated extensively over the past few years, much of the motivation for the work described here is due to his influence.

I've had the pleasure of working and playing with many different people during my graduate career, I wish I could name you all. Thanks to each of you, especially Chris, who got me started and kept me fed, and Jenny, who I could always count on in a pinch, and who read the entire thesis. Simon and Sally, your comments and suggestions for the text of the thesis were greatly appreciated. Thank you Linda, Barb and Lee for unending levels of emotional and material support, especially during these last few months.

Life as a grad student would be unbearable without a few distractions, but I think I had more than my share. Thanks to all my friends in the department and at neurobeers, to the "group" at home, to my "kids" at the dorm, and to all the folks down at the pool. I've had more fun than I could stand, sometimes.

Final thanks must go to my family. To my siblings Patty, Frank and John, thanks for putting up with my student ways for such a long time, but don't expect things to change too much. Thank you Mom and Dad. You've always been supportive, and your help and encouragement over the last few months has been remarkable. I finish this work with warm feelings of love for you both. This thesis is for you.

This research was supported by NIH training grant NIH-GM07484, by a Graduate Fellowship from the Whitaker Health Sciences and Technolgy Fund, and by a Fairchild Foundation Graduate Fellowship.

Contents

1 Introduction **10**

1.1 Elastic Properties of Mechanical Systems 11

1.1.1 Stiffness and the Control of Posture 11

1.1.2 Geometry and Effective Stiffness 14

1.1.3 Multi-Dimensional Systems 15

1.1.4 Redundant Systems 16

1.1.5 Movement from Posture 18

1.2 Biological Motor Systems 19

1.3 Outline 21

2 The Modeling of Elastic Systems **22**

2.1 Model Structure 22

2.1.1 Primitive Elements 23

2.1.2 Causality 24

2.1.3 Summing Junctions 24

2.1.4 Transformers 25

2.2 Effective Stiffness 28

2.3 Numerical Methods 29

2.3.1 Newton-Raphson 30

2.3.2 Simulated Damping 30

2.4 Examples 31

2.4.1 Pendulum 31

2.4.2 Two Joint Arm 32

2.5 Implementation 33
2.6 Summary 33

3 Control of Limb Stability **34**
3.1 Previous Work 35
3.2 Factors Affecting Endpoint Stiffness 36
3.3 Materials and Methods 40
3.4 Simulation Results 43
3.4.1 Constant Joint Stiffness 43
3.4.2 Constant Endpoint Stiffness 44
3.4.3 Passive Stabilization 47
3.4.4 Summary 50
3.5 Experimental Results 50
3.6 Discussion 57
3.6.1 Stability Margin 58
3.6.2 Role of Double Joint Muscles 58
3.6.3 Local vs. Global Effects 59
3.6.4 Reflexes vs. Mechanical Properties 59
3.6.5 Model vs. Data Discrepancies 60
3.6.6 Modeling Errors 60
3.7 Conclusions 63

4 Redundant Motor Systems **64**
4.1 Previous Work 66
4.2 Control Update Algorithm 69
4.2.1 Example: A Linear Redundant System 70
4.2.2 Problems with Non-Linear Systems 70
4.2.3 Solutions for General Non-Linear Systems 72
4.2.4 Backdriving as a Pseudo-Inverse 79
4.3 Properties of the Backdriving Algorithm 80
4.3.1 Changing Moment Arms 80

4.3.2 Synergistic Behavior 82
4.3.3 Kinematic Singularities 83
4.3.4 Muscle Saturation 84
4.4 Control of Stiffness 84
4.4.1 Passive Stabilization 85
4.4.2 Active Impedance Modulation 85
4.5 Model Predictions and Biological Data 91
4.5.1 Comparison with Buchanan Data 92
4.6 Conclusions 99

5 Movement From Posture **100**
5.1 Definition of a Servo 101
5.2 Servo Models for Biological Motor Control 101
5.2.1 Reflex Servo Hypothesis 102
5.2.2 Equilibrium Point Models 104
5.3 Velocity Scaling 109
5.3.1 Stiffness Scaling 110
5.3.2 Equilibrium Trajectory Modification 110
5.3.3 Velocity Scaling and the Equilibrium Point Control Models . . 115
5.4 Enhancement of the Equilibrium Point Control Model 118
5.4.1 Simulation of the Proposed Controller 119
5.5 Conclusions 124

List of Figures

1-1 An example of position control via stiffness. 12

1-2 Effective stiffness of a pendulum. 14

1-3 Representations of two-dimensional stiffness fields. 16

1-4 A redundant elastic system. 17

1-5 Equilibrium point control of movement. 18

2-1 Model structure for a pendulum. 32

2-2 Model structure for a two joint arm. 33

3-1 Planar two-joint arm model. 37

3-2 Dependence of endpoint stiffness on output force. 39

3-3 Source of endpoint instability. 40

3-4 Force load apparatus. 42

3-5 Definition of joint stiffness components. 43

3-6 Simulation of constant joint stiffness control. 45

3-7 Simulation of constant endpoint stiffness control. 46

3-8 Exponential model of muscle length/tension properties. 48

3-9 Arm stiffness for the exponential model of muscle. 49

3-10 Exponential muscle model without double-joint muscles. 51

3-11 Stiffness data for subject SFG. 52

3-12 Stiffness data for subject JLM. 53

3-13 Stiffness data for subject SMB. 54

3-14 Effect of varying the ratio of moment arms. 61

4-1 Example of position redundancy. 65

4-2 Example of effort redundancy. 65
4-3 Control of a linear redundant system. 71
4-4 Effect of changing moment arm. 72
4-5 Backdriving with changing moment arms. 81
4-6 Defining synergies through backdriving. 82
4-7 Passive driving through kinematic singularities. 83
4-8 Passive driving of saturated muscles. 85
4-9 Model of planar two joint arm with six muscles. 86
4-10 Control of stiffness for a six muscle arm. 87
4-11 Torque measurement apparatus (from Buchanan 1986). 92
4-12 Comparison of Backdriving Model with EMG Data. 94
4-13 Comparison of Backdriving Model with EMG Data. 95

5-1 Definition of a servo. 101
5-2 Neural circuitry for the stretch reflex. 102
5-3 Merton's reflex servo control model. 103
5-4 Block diagram of α equilibrium model of motor control. 105
5-5 Invalid Formulations of the λ equilibrium point model. 107
5-6 Consistent formulation of the λ equilibrium point model. 108
5-7 Slow movement at low stiffness. 111
5-8 Fast movement at low stiffness. 112
5-9 Fast movement at high stiffness. 113
5-10 Fast movement with computed virtual trajectory. 114
5-11 Measured actual movement. 116
5-12 Estimation of the virtual trajectory for a monkey arm movement. . . 117
5-13 Proposed equilibrium point model with reflex feedback. 118
5-14 Fast movement with proposed reflex feedback model. 120
5-15 Lower muscle damping ratio. 121
5-16 Single feedback delay. 122
5-17 Single delay and low damping. 123

List of Tables

3.1 Comparison of control models for subjects SFG and JLM. 56

3.2 Comparison of control models for subject SMB. 57

4.1 Physiological data for elbow muscles (from An, et. al. 1981). 96

5.1 Control Model Parameters. 124

Chapter 1

Introduction

This thesis addresses the question "What are the elastic properties of the human motor system, and how are they incorporated into the control of posture and movement?" In recent years investigators of motor systems have emphasized the study of the mechanics of movements and the physical properties of the biological hardware used to produce them. An important finding has been that of describing the spring-like properties of muscles, and establishing a role for these properties in the biological control of movement (see Section 1.2 below). These studies have greatly enhanced our insight into the workings of biological motor systems, but a number of interesting questions remain open. For instance, what are the physical properties of biological motor systems, and how and why are they controlled? Are there a few simple control schemes that can be used to account for the broad range of motor behavior observed in humans?

The goal of this research is to address some of these questions with an approach best described as *analysis by design*. Following this approach, potential models for the control of movement are derived by an engineering analysis of the problem. These models are then tested via computer simulation, and the results compared with biological and psychophysical experiments. The models provide a theoretical framework for the organization and interpretation of experimental results, and can be used to drive the design of new experiments.

In this chapter I will describe the qualitative features of mechanical systems which

exhibit elastic behavior. I will define the terms *elastic properties* and *stiffness*, and relate them to the basic issues of *posture* [1], *movement* and *control*. I present a number of problems which are encountered when controlling any moving mechanical device, and discuss the relevance of these issues to the study of the human motor system. Finally, I provide an outline of the work to be presented in subsequent chapters.

1.1 Elastic Properties of Mechanical Systems

The term *system elastic properties* refers to the relationship between the forces acting on a mechanical system and the positions of the system elements. The force/length relationship of a simple spring is an obvious example of such a system. As the length of the spring changes, so does the force generated by the spring. Biological motor systems exhibit similar behavior. Displacement of a limb will cause changes in muscle lengths and moment arms, which result in changes in the forces and torques acting on the limb.

The elastic properties of a mechanical system can be exploited in order to control posture and movement. In this section simple mechanical examples will be used to identify the fundamental relationship between elastic properties and motor control. The following section will describe the elastic behavior of biological systems and the associated issues for motor control.

1.1.1 Stiffness and the Control of Posture

What is *stiffness* and how does it affect the control of limb positions? The answer is best illustrated by an example: consider a linear system composed of a mass attached to a spring and a viscous damper (Figure 1-1), and assume that the spring obeys Hooke's law. That is, the relationship between the force generated by the spring and

[1] The term posture will be used in its general sense to refer to the position of any limb, as opposed to the more common meaning of controlling the upright position of the body as a whole.

Definition of Stability in Terms of Stiffness

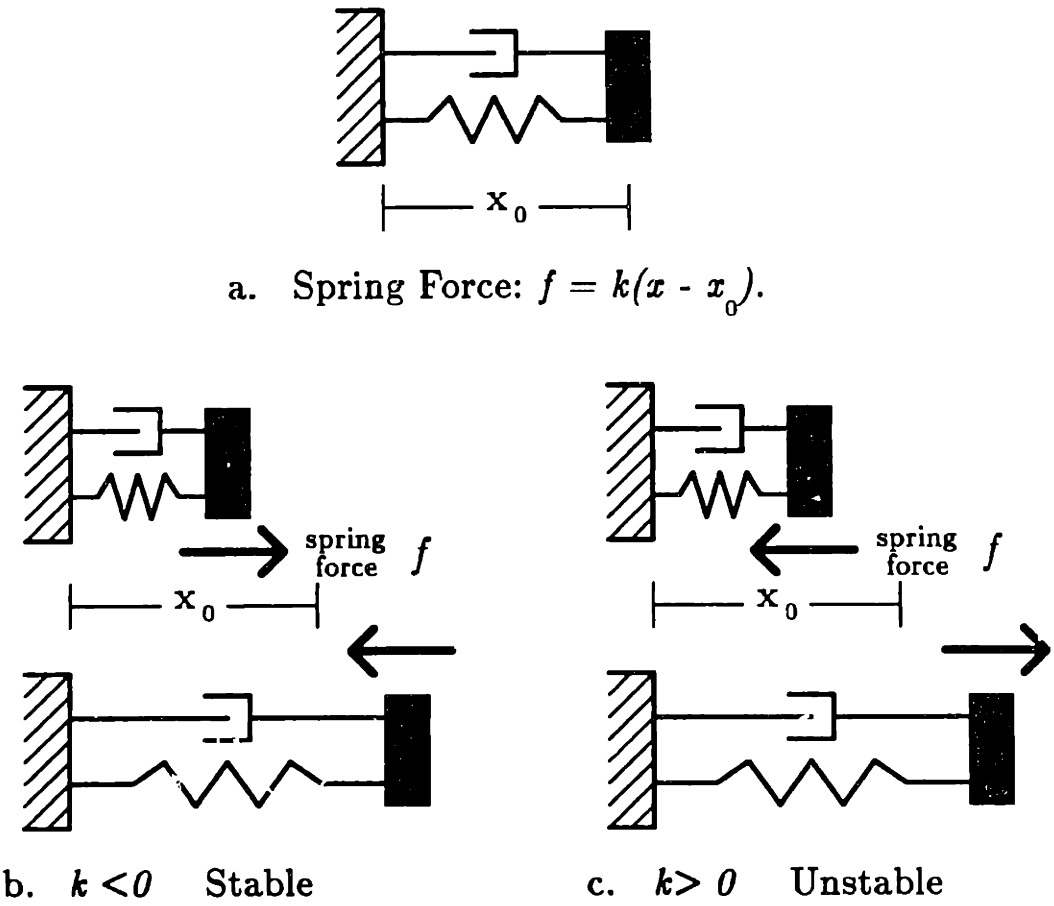

Figure 1-1: An example of position control via stiffness. A mass, spring, damper system at equilibrium (a). Displacement with a stable (b) and an unstable (c) stiffness.

the length of the spring is described by the equation

$$f = k(x - x_0). \tag{1.1}$$

If the goal is to control the position of the mass (x), a spring can be used with a rest-length (x_0) equal to the desired position of the mass. If the spring constant k is negative ($k < 0$), displacing the mass away from the desired position generates a force in the spring which acts to move the mass back to the original position (Figure 1-1b). The magnitude of the restoring force increases with the size of the

displacement. Thus, the spring can be used to *control* the position of the mass, returning the system to the desired location following a disturbance. The time course of the movement depends on the relative values of the mass, the stiffness, and the viscosity of the damper. However, a negative value of stiffness guarantees that the system will eventually settle back in the original position. Such a system can be described as statically *stable*[2].

One can imagine a system in which the spring constant is positive (Figure 1-1c). In such a case displacement of the mass results in a force that tends to move the system *away* from the initial position. This tendency to move away from the equilibrium position is clearly undesirable from the point of view of controlling position. Such a system is called *unstable.*

A system with zero stiffness produces no change of force when stretched or compressed. If such a system is displaced from the desired position, it will not move back toward the original position, but neither will it move farther away. A linear system with zero stiffness is *marginally stable.*

The static relationship between position and force defines the *elastic* behavior of a mechanical device. The stability of many mechanical systems can be assessed by examining this relationship between force and position. Furthermore, the analysis is not restricted to linear functions such as that exhibited by the ideal Hooke's law spring described above. The response of a non-linear system to small perturbations around an operating point can be approximated by a linearization of the force/position relationship at that point. Allowing force to be an arbitrary function of position

$$f = g(x).$$

The stiffness as a function of position is given by

$$k(x) = \frac{df}{dx} = \frac{d(g(x))}{dx}.$$

[2]For a reference on stability and control, see [49]. The association between stiffness and stability can be attributed originally to Lord Kelvin.

Figure 1-2: The effective stiffness of a pendulum in a stable (a) and unstable (b) configuration.

A system can be considered stable around a position x_1 if the value of the stiffness at that point is negative ($k(x_1) < 0$), a positive stiffness means the system is unstable. A nonlinear system having zero stiffness may or may not be stable.

1.1.2 Geometry and Effective Stiffness

Actual springs need not be present in a mechanical structure for the system to exhibit elastic (spring-like) behavior. Again, this situation is best explained by an example: Consider a pendulum consisting of a point mass suspended by a mass-less link of fixed length (Figure 1-2). Assume that the force due to gravity acting on the mass is constant with respect to the position of the mass ($f_g = mg$). The torque acting around the pivot point depends on the angular position of the pendulum θ

$$\tau = -f_g l \sin\theta.$$

If the pendulum is positioned vertically downward at zero angle (Figure 1-2a), the net torque is zero, and the system will remain at equilibrium. If the pendulum is rotated away from vertical, a torque will be generated in the direction of zero angle. The angular stiffness of the system is defined by

$$k_\theta = \frac{d\mathcal{T}}{d\theta} = -f_g l \cos\theta.$$

At zero angle, the angular stiffness is negative ($-f_g l$), resulting in stable elastic behavior around this point.

The stiffness generated by such a structure is not necessarily stable. Consider the same pendulum in an inverted position ($\theta = \pi$) (Figure 1-2b). In this position, the net torque is also zero, so the pendulum is at equilibrium. However, in this case, if small displacements are made around this point, the resulting torque is directed away from the equilibrium position. The angular stiffness at this position is positive ($k_\theta = -f_g l \cos\pi = f_g l$), resulting in an unstable equilibrium point.

It is important to note that the elastic behavior exhibited by the pendulum emerges even though the stiffness of the gravitational field is zero. This *effective* angular stiffness k_θ results from the non-linear transformation between the cartesian and angular coordinate frames (see Section 2.2). As can be seen in this example, the effective stiffness can act to stabilize or destabilize a mechanical system.

1.1.3 Multi-Dimensional Systems

The concept of stiffness can be extended to the control of multi-dimensional mechanical systems. In these cases, the position of the system and the force acting on the system are described by n-dimensional vectors X and F. If the force acting on the system is described by a vector function G

$$F = G(X).$$

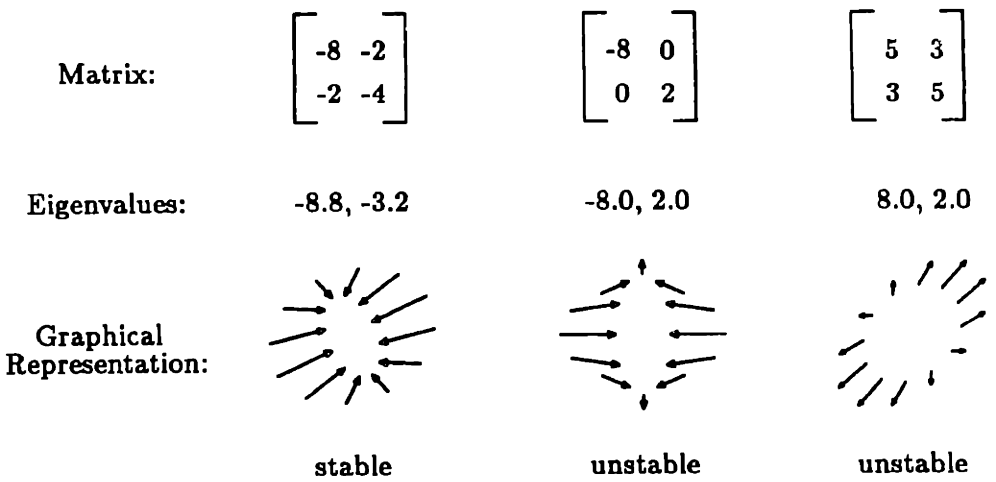

Figure 1-3: Representations of two-dimensional stiffness fields.

The stiffness of the system is an elastic field represented by the n by n matrix

$$K = \begin{bmatrix} \frac{\partial F_1}{\partial X_1} & \cdots & \frac{\partial F_1}{\partial X_n} \\ \vdots & \ddots & \vdots \\ \frac{\partial F_n}{\partial X_1} & \cdots & \frac{\partial F_n}{\partial X_n} \end{bmatrix}.$$

The stiffness field is stable if a small displacement in position ΔP results in a change in force ΔF that acts to restore the original position. A necessary and sufficient condition for stability is that K is negative definite. That is, all of the eigenvalues of K must be less than zero [49].

For a two dimensional system, the stiffness field can be represented graphically as in Figure 1-3. The base of each arrow represents a displacement of the system from the center position. The size and direction of each arrow corresponds to the size and direction of the change in force caused by that displacement. For a stable stiffness field, all of the arrows should point inward.

1.1.4 Redundant Systems

Mechanical systems can be made up of many elements, each having its own elastic properties. For a single point of interaction, the aggregate static behavior of such

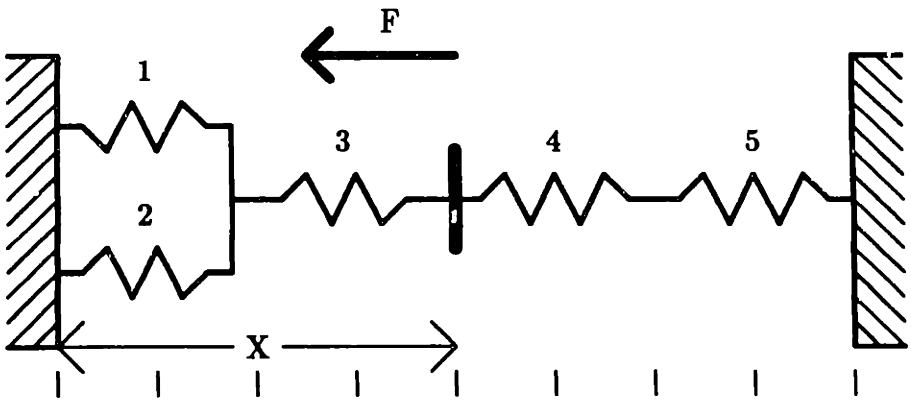

Spring parameters producing equivalent endpoint behavior.

Element	Stiffness	Restlength	Stiffness	Restlength	System Output
1	8	0	7	1	
2	4	0	9	1	$P = 4$
3	12	0	16	0	$F = -20$
4	8	1	3	1	$K = -10$
5	8	2	6	1	

Figure 1-4: A redundant elastic system.

a system can be described by a single relationship between force and position (Figure 1-4). Typically, the computation of the overall behavior of the system from the characteristics of its components is *well-posed* in the sense that there is typically a unique solution. That is, given the force/position relationship of each of the springs in the system, it is possible to compute analytically the net output force and the associated stiffness for a particular system configuration.

The inverse or *control* problem is, however, *ill-posed* in the sense that for a particular configuration of elastic elements, there may be an infinite number of combinations of force/position relationships which will result in the same net force and stiffness at a given position. The force and stiffness can be distributed in many different ways among the various springs. For example, the table in Figure 1-4 contains two sets of component characteristics which result in identical endpoint behavior.

In order to control the elastic behavior of the system, a choice must be made from among the possible solutions in order to resolve the redundancy.

1.1.5 Movement from Posture

The elastic properties of a mechanical system can be exploited to control movements as well as postures. By shifting the equilibrium position of the structure (imagine a tunable spring for which the rest length can be modified at will), forces will be generated to move the system toward the new desired position (Figure 1-5a). With the appropriate values of stiffness, it is possible to generate movements of the structure without an explicit computation of the movement inverse dynamics. One need specify only the desired positions as a function of time. The forces required to produce the movement are computed implicitly by the elastic behavior of the system – – this is the principle behind a position servo controller.

As stated above, the time course of a servo controlled movement is dependent on the value of the stiffness relative to the system's inertia and damping. Having a stable stiffness field guarantees only that the final position will eventually be achieved. If

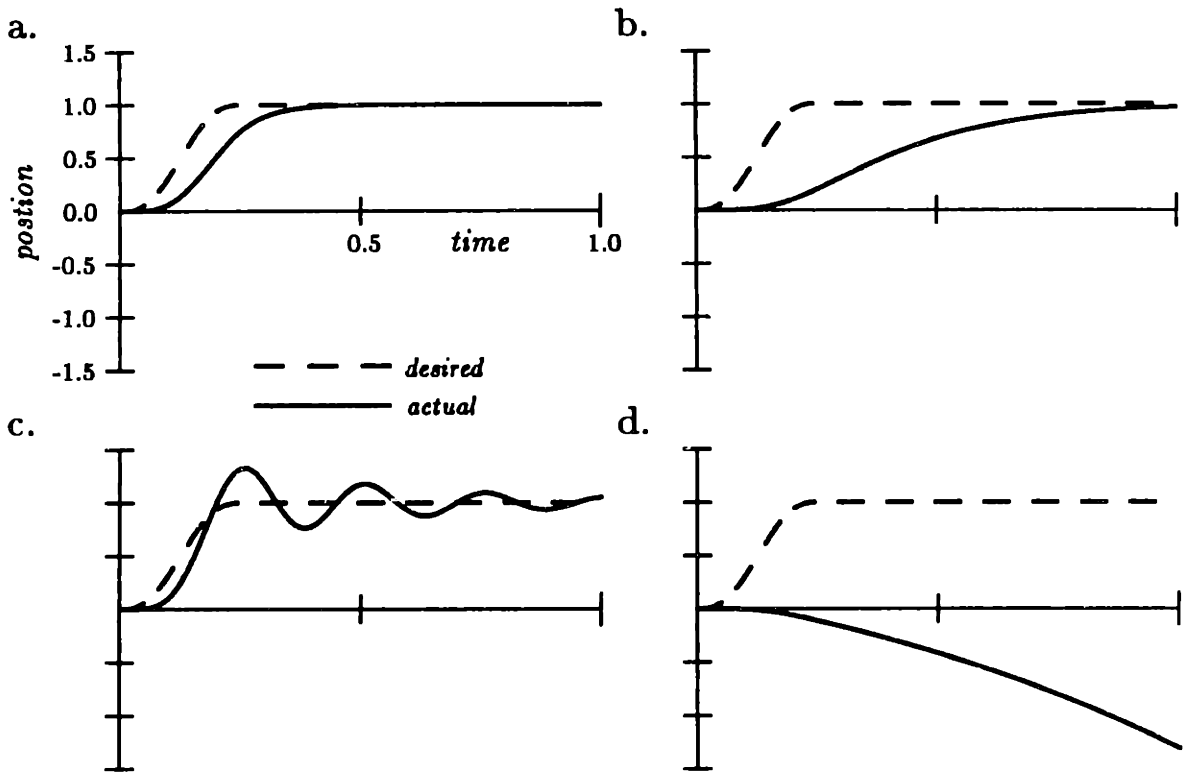

Figure 1-5: Equilibrium point control of movement.

the stiffness is too low, relative to the inertia and damping, the movement may be much slower than desired (Figure 1-5b). If the stiffness is too high, the structure may oscillate around the final position (Figure 1-5c), whiie an unstable stiffness will cause a movement in the opposite direction than is desired (Figure 1-5d). Servo control of movement requires the control of system stiffness as well as equilibrium position.

1.2 Biological Motor Systems

The concepts illustrated by the simple examples above are important issues for the control of biological systems. It has long been known that the actuators for biological motor systems act in a spring-like manner. The behavior of muscles in isolation [55], or in concert with the monosynaptic reflex arc [18, 48] can be described as a tunable spring in which the stiffness and rest-length can be varied via neuronal control. More recently the analysis of motor system elasticity has been extended to the study of multi-joint movements and postures. The static behavior of the neuro-musculo-skeletal system comprising the human or monkey arm can be described by a multi-dimensional, conservative stiffness field acting around a varying equilibrium position of the hand [47, 31, 5]. Establishing an appropriate endpoint stiffness is an important concern for controlling the interactive behavior of the limb [11, 12]. Of fundamental importance is the need to assure limb stability under a variety of conditions. Since a multi-joint limb has an inherently non-linear structure, the forces acting on the limb must be considered as well as the intrinsic stiffness of the actuators in order to insure stable limb behavior.

A number of researchers have proposed models for motor control that are based on the elastic properties of biological motor systems. Merton originally proposed a servo control model for generating movements based on the mono-synaptic stretch reflex [42]. The reflex acts to control posture by increasing the activation of the muscles in proportion to the amount of muscle stretch. It was proposed that movements are generated by altering the set-point of the posture control servo through the gamma motor neuron drive. Thus the tasks of controlling movement and posture were unified

under a single control scheme.

Merton's hypothesis is inconsistent with experimental observations of alpha-gamma co-activation as well as stability analysis in the face of significant feedback delays (see Chapter 5). While this theory has since been proven wrong for biological systems, the underlying concept of movement from posture remains. Feldman has proposed the *equilibrium point model* for motor control, based on the elastic properties of muscles [18]. The spring-like mechanical behavior of the muscles act without the problematic delays of the reflex circuitry. Bizzi, Hogan and colleagues have demonstrated that goal-directed movements can be performed in the absence of sensory feedback [9, 8, 6, 53] relying on the muscle mechanical properties alone. Feldman on the other hand has emphasized the combined role of stretch reflexes and muscle elastic properties for producing movements of the limb [18, 19]. Common to both of these models, muscle activities are chosen by the central nervous system to achieve a desired equilibrium position. Movements are executed by a gradual shift in the equilibrium position from the initial to the final position [5, 30]. Evidence suggests that the equilibrium point model for motor control is adequate for describing certain classes of multi-joint movements [21, 5].

Biological systems usually exhibit a high degree of redundancy. For instance, the human arm (excluding the hand) has seven rotational degrees of freedom (three at the shoulder, one at the elbow, three at the wrist), while only six degrees of freedom are required to determine arbitrarily the position and orientation of the hand. The number of muscles is significantly greater than the number of joints as well, with sixteen muscles acting across the elbow alone [1]. Thus, the central nervous system must solve Bernstein's problem [4] when performing motor tasks. That is, when there are more degrees of freedom in the motor system than necessary, the nervous system must select a particular solution from all the possibilities which accomplish a given task. This may include the selection of a set of joint angles for a redundant arm, or the problem may be to distribute forces among a redundant set of muscles. A number of strategies have been proposed and tested for resolving the redundancy in biological motor systems [51, 22, 35], but the issue remains an open area for research.

Control of movement and posture requires control of real physical devices. Understanding the dynamic behavior of the limbs is essential for understanding the overall system behavior. Furthermore, understanding the elastic characteristics of the system may provide the key to understanding the underlying control structure employed by the central nervous system.

1.3 Outline

This thesis addresses a number of issues concerning the control of movement and posture, with an emphasis on the role of the elastic behavior of the neuro-musculoskeletal system.

Chapter Two presents a mathematical framework for the analysis of elastic mechanical systems, including algorithms for simulating the behavior of such systems. Chapter Two provides the concepts necessary for the work presented in subsequent chapters.

Chapter Three contains an analysis of limb stability for the human arm. As in the case of the pendulum, the linkage has a non-linear geometrical structure, which adds an additional dimension to the problem of controlling stability. I discuss a number of strategies for controlling limb stability and compare them with experimental data.

Chapter Four addresses the issue of motor system redundancy. Muscle activities must be modified in a coordinated fashion so as to achieve a desired change in equilibrium position or output force. In this chapter I present a model in which the changes in activations are distributed among the various muscles based on the relative stiffness of each component. The model predicts the activations of different muscles used for the production of forces in the human arm. These predictions are compared with published experimental data.

Chapter five examines the theory of movement from posture. The ability of the equilibrium point control model to predict the performance of fast movements has recently be brought into question. In this chapter I extend the equilibrium point hypothesis to include the action of reflex control loops and test the ability of this model to predict the characteristics of fast movements.

Chapter 2

The Modeling of Elastic Systems

In this chapter I present a mathematical framework for modeling the mechanical properties of springs and linkages. These techniques can be used to model the static behavior of a manipulator interacting with its environment. In particular, the techniques can be used to compute the elastic properties of systems of arbitrarily connected springs and linkages.

2.1 Model Structure

I have taken a modular approach to modeling mechanical systems in which the characteristics of the manipulator are lumped in discrete elastic elements connected by rigid mechanical linkages. The basic building blocks are primitive elastic elements for which there are known relationships between an element's effort[1] e and position p. This relationship may be dependent on a control input u.

The action of an element may be transformed from one coordinate system to another by a rigid mechanical structure. e.g. For a muscle acting around a joint, the length/tension relationship of the muscle in transformed into a torque/angle relationship for the joint. To model this effect, a single composite element is created, composed of a *transformer* element coupled to a primitive elastic element. In a similar way, the action of multiple element connected together is modeled by a *junc-*

[1]Effort is a general term which for mechanical systems refers to either force or torque.

tion element connecting each of the components. The combined elements formed by transformers, junctions and their component elements have the same features as the primitive elements. There is a relationship between the overall position of the structure and its output effort which is computed from the properties of the component elements. The control input is simply a vector specifying the control input for each of the primitive elements that are involved. The behavior of the composite elements formed by junctions and transformers can be further transformed or coupled to other elements in order to simulate the behavior of more complicated mechanical systems.

The modeling approach used here is essentially equivalent to that of bond graphs [50]. Since we are interested primarily in the steady state elastic properties of the system, the variables of interest are the efforts and positions (e.g. forces and lengths) of the elements, instead of the efforts and flows (velocities). The goal is to compute either the net output effort for the system at a given position, or to compute the resultant position for a specified applied effort. In addition, we wish to compute the net stiffness (de/dp) at the endpoint, the net compliance (dp/de), or both.

2.1.1 Primitive Elements

The basic building blocks used in these model systems are described as tunable, generalized springs in which the *effort output* (e) of the element is a function of its *position* (p), or conversely, the position of the element is a function of the applied effort. Each element typically has a *control input* (u) which acts to modify this relationship between position and effort. Thus there are two types of elements, a stiffness element:

$$\begin{aligned} e &= f(p,u) \\ k &= \frac{\partial f}{\partial p} \\ c &= k^{-1}\ (k \neq 0), \end{aligned}$$

or a compliance element:

$$\begin{aligned} p &= g(e,u) \\ c &= \frac{\partial g}{\partial e} \\ k &= c^{-1}\ (c \neq 0). \end{aligned}$$

2.1.2 Causality

A stiffness element in which the effort is a non-monotonic function of position is described as having *position causality*, because given a position it is possible to analytically compute the resultant effort. The inverse problem (the position which gives a desired effort) may have multiple solutions. Numerical methods must be used to compute the appropriate solution under the assumption of quasi-static behavior for the system.

The dual of a position causal element is a compliance which has *effort causality*. For an effort causal element the position that produces a given effort can be computed analytically, while the effort that achieves a desired position must be computed numerically. In many cases the constraint equations are invertible, giving an element with *neutral causality*:

$$f(g(x,u),u) = g(f(x,u),u) = x.$$

2.1.3 Summing Junctions

Two or more elements may be connected together to form a single composite element by a *common position junction* in which the same position is imposed on each element. This corresponds to a set of springs connected in parallel. The resulting element is necessarily position causal. By specifying the position of the composite element, the positions of each of the components are known. An infinite number of different element efforts can produce a given overall effort for the combined system. Numerical methods must be used to compute the element configurations which will produce the

solution that minimizes the system potential energy.

The constraint equations describing common position junctions are [2]

$$\begin{aligned} p_i &= P \\ E &= \sum e_i \\ K &= \sum k_i. \end{aligned}$$

In a similar fashion a *common effort junction* (springs in series) generates an effort causal element via constraint equations:

$$\begin{aligned} e_i &= E \\ P &= \sum p_i \\ C &= \sum c_i. \end{aligned}$$

2.1.4 Transformers

The transformation of an element's actions from coordinate frame to another is described by a *transformer*. In general, the transformation can be non-linear, with the Jacobian matrix dependent on the configuration of the structure, and the transformation may involve a change in the number of dimensions ($p, e \in \mathcal{R}^m \Rightarrow P, E \in \mathcal{R}^n, m \neq n$). The form of the constraint equations depends on the dimensions of the coordinate frames and the computability of the transformation function.

Forward Transformations

The transformation from p to P will be defined as the *forward* direction. This may be the only direction wherein the transformation is analytically defined, as in the case where the transformation is from a higher to lower dimension, ($m > n$). The transformation from p to P is defined as $P = \mathcal{L}_f(p)$. [3] For example, when describing

[2] Upper case letters refer to the net values for the composite element, lower case refer to the individual components.

[3] The subscript f denotes a transformation in the *forward* direction ($p \rightarrow P$) The reverse transformation $P \rightarrow p$ will be indicated by an r subscript ($p = \mathcal{L}_r(P)$). This notation is useful for keeping

the transformation from joint coordinates to cartesian tip coordinates for a planar arm having more than two joints, a single tip position (P) can be achieved by many possible joint configurations (p); however a given joint configuration corresponds to only one tip position. Such a transformation is described by a *compliance transformer* which is effort causal. Its constraint equations are derived as follows:

Coordinate Transformations

$$\begin{aligned} P &= \mathcal{L}_f(p) \\ J_f(p) &= \frac{\partial \mathcal{L}_f(p)}{\partial p} \\ dP &= J_f(p)dp \\ e &= J_f^T(p)E \end{aligned}$$

Compliance Transformations

$$\begin{aligned} k &= \frac{\partial e}{\partial p} \\ &= \frac{\partial (J_f^T(p)E)}{\partial p} \\ &= J_f^T(p)\frac{\partial E}{\partial p} + \frac{\partial J_f^T(p)}{\partial p}E \\ &= J_f^T(p)\frac{\partial E}{\partial P}\frac{\partial P}{\partial p} + \frac{\partial J_f^T(p)}{\partial p}E \\ &= J_f^T(p)KJ_f(p) + \frac{\partial J_f^T(p)}{\partial p}E \\ k - \frac{\partial J_f^T(p)}{\partial p}E &= J_f^T(p)KJ_f(p) \\ \left[k - \frac{\partial J_f^T(p)}{\partial p}E\right]^{-1} &= \left[J_f^T(p)KJ_f(p)\right]^{-1} \\ J_f(p)\left[k - \frac{\partial J_f^T(p)}{\partial p}E\right]^{-1} J_f^T(p) &= J_f(p)\left[J_f^T(p)KJ_f(p)\right]^{-1} J_f^T(p) \end{aligned}$$

Note that $KJ_f(p)\left[J_f^T(p)KJ_f(p)\right]^{-1}$ is a generalized inverse of $J_f^T(p)$:

$$J_f(p)\left[k - \frac{\partial J_f^T(p)}{\partial p}E\right]^{-1} J_f^T(p) = (CK)\,J_f(p)\left[J_f^T(p)KJ_f(p)\right]^{-1} J_f^T(p)$$

track of the distinction, particularly in the cases when the transformation is invertible, meaning that both $\mathcal{L}_f$ and $\mathcal{L}_r$, and their associated Jacobians J_f and J_r are both defined.

$$C = J_f(p)\left[k - \frac{\partial J_f^T(p)}{\partial p}E\right]^{-1} J_f^T(p) \tag{2.1}$$

$$K = C^{-1},\ (|C| \neq 0). \tag{2.2}$$

The term $\frac{\partial J_f^T(p)}{\partial p}E$ reflects the change in effort resulting from the position dependence of the Jacobian. It is computed as follows:

$$\gamma_{ij} \triangleq \left[\frac{\partial J_f^T(p)}{\partial p}E\right]_{ij} = \sum_k \frac{\partial [J_f^T(p)]_{jk}}{\partial p_i}E_k = \sum_k \frac{\partial^2 P}{\partial p_i \partial p_j}E_k.$$

Reverse Transformations

When the transformation is from a low dimension to a higher one ($m < n$), or whenever the transformation from P to p is well defined, we define this transformation as $p = \mathcal{L}_r(P)$. A single muscle acting across two joints is an example of such a case. A given joint angle vector (P) can be transformed into a unique muscle length (p), however, a single muscle length may correspond to an infinite number of joint angle pairs. Such a transformation describes a *stiffness transformer* which is position causal. Its constraint equations are derived as follows:

Coordinate Transformations

$$p = \mathcal{L}_r(P) \tag{2.3}$$

$$J_r(P) = \frac{\partial \mathcal{L}_r(P)}{\partial P} \tag{2.4}$$

$$dp = J_r(P)dp \tag{2.5}$$

$$E = J_r^T(P)e \tag{2.6}$$

Stiffness Transformations

$$\begin{aligned} K &= \frac{\partial E}{\partial P} \\ &= \frac{\partial (J_r^T(P)e)}{\partial P} \\ &= J_r^T(P)\frac{\partial e}{\partial p} + \frac{\partial J_r^T(P)}{\partial P}e \\ &= J_r^T(P)\frac{\partial e}{\partial p}\frac{\partial p}{\partial P} + \frac{\partial J_r^T(P)}{\partial P}e \end{aligned}$$

$$K = J_r^T(P)kJ_r(P) + \frac{\partial J_r^T(P)}{\partial P}e \tag{2.7}$$

$$C = K^{-1},\ (|K| \neq 0) \tag{2.8}$$

$$\Gamma_{ij} \triangleq \left[\frac{\partial J_r^T(P)}{\partial P}e\right]_{ij} = \sum_k \frac{\partial [J_r^T(P)]_{jk}}{\partial P_i}e_k = \sum_k \frac{\partial^2 p}{\partial P_i \partial P_j}e_k.$$

Invertible Transformations

When the dimensions of the two domains are the same ($m = n$), either or both of the transformations $\mathcal{L}_f$ and $\mathcal{L}_r$ may be well defined (not when $\mathcal{L}_f$ or $\mathcal{L}_r$ is multi-valued, or when one of the Jacobians is singular). The dependence of the Jacobians on the configuration may be expressed in either coordinate system: $J_f(p)$ and $J_r(p)$ or $J_f(P)$ and $J_r(P)$. Either equation 2.1 or 2.7 may be used to compute the transformed stiffness or compliance.

2.2 Effective Stiffness

The effective stiffness of a transformer element arises from two sources: the linear transformation of the component element's stiffness and the non-linear transformation of the component element's effort. For a stiffness transformer, the net output effort is computed from the effort of the component element via the transform of the Jacobian (equation 2.6). If the transformation is non-linear, the Jacobian depends on the position of the system. As the position changes, the transformed effort will change, even if the effort of the component element does not. Thus an effective stiffness is seen at the output even if the component stiffness is zero.

In a general system, the net effective stiffness can be divided into two components, the *intrinsic* stiffness, obtained from the linear transformation of the component stiffnesses, and the *geometric* stiffness, from the non-linear transformation of efforts. For a stiffness transformer (from equation 2.7):

$$K_{intrinsic} = J_r^T(P)kJ_r(P) \tag{2.9}$$

$$K_{geometric} = \frac{\partial J_r^T(P)}{\partial P} e \tag{2.10}$$

$$K_{effective} = K_{intrinsic} + K_{geometric}. \tag{2.11}$$

For a compliance transformer (from equation 2.1):

$$\begin{aligned} k_{intrinsic} &= k \\ k_{geometric} &= -\frac{\partial J_f^T(p)}{\partial p} E \\ C_{effective} &= J_f(p) \left[k_{intrinsic} + k_{geometric}\right]^{-1} J_f^T(p). \end{aligned}$$

2.3 Numerical Methods

A real physical system produces a mechanical response to perturbations from the environment in both position and effort. The causality constraints may, however, prevent us from solving for this response analytically. In order to compute the time course of the movement for an imposed change in effort or position, it would be necessary to solve the dynamic equations which describe the mechanical system. This would require the estimation of additional parameters for the system which is being modeled, including inertial parameters and viscosities. If one is concerned with only the static or quasi-static behavior of the system, the static response can be computed without solving the full dynamic equations. The steady-state solution can be obtained by finding an equilibrium position for which the sum of all the efforts is zero. This reduces the problem to finding the roots of a non-linear equation. There may in fact be more than one root for a non-linear equation. For a quasi-static analysis one can assume that the system moves in the direction of the net effort until equilibrium is reached. A number of different numerical methods have been employed to solve for the response under these conditions, as described below.

2.3.1 Newton-Raphson

The simplest approach is to use the stiffness or compliance at the endpoint to search for the equilibrium response using the Newton-Raphson method. To drive a position causal element to a desired output effort (e_d), the algorithm is

$$while\ (e \neq e_d)\ do\ \{p_{n+1} = p_n + k_n(e_n - e_d)\}.$$

For an effort causal element, it is necessary to compute the effort output for a desired position change

$$while\ (p \neq p_d)\ do\ \{e_{n+1} = e_n + c_n(p_n - p_d)\}.$$

For a numerical simulation on a digital computer, perfect accuracy will never be reached. In the simulations, two vectors x and y are considered equal if $|x - y| < \epsilon$. Typically we will use an accuracy constraint of $\epsilon = .001$ for efforts in the range $e = \pm 10.0$.

This technique successfully computes the static or quasi-static behavior for small displacements in regions around the equilibrium point where the position-effort relationship are near linear. The robustness of this technique can be improved by reducing the size of the step when the output begins to diverge [54].

2.3.2 Simulated Damping

When the mechanical system is highly non-linear, the Newton-Raphson method may not converge. A second technique is used to simulate the relaxation of the mechanical system and the imposed external force acting against a pure viscous load. This is consistent with our quasi-static assumption that the system moves in the direction of the net force.

A system of this form will move with a time course described by the differential equation

$$\dot{p} = \frac{1}{\beta}(e - e_d) \tag{2.12}$$

where β is the magnitude of the fictitious viscous load. Numerically integrating equation 2.12 until $|e - e_d| < \epsilon$ yields the steady state position that produces the desired effort output. The actual value of β is not important, as it affects only the time course of the movement, not the steady state result. When numerically solving the differential equations, however, the integration time step must be chosen appropriately with respect to β in order to assure convergence. We arbitrarily set $\beta = 1$ and solve the equation using a variable step size Runge-Kutta integration to automatically adjust the step size as needed [54].

2.4 Examples

2.4.1 Pendulum

Consider the pendulum system described in Chapter 1 for a simple example of the modeling system. The gravitational field can be described as a primitive stiffness element having position causality. The equations which describe this element are

$$\begin{aligned} p &= \begin{bmatrix} x \\ y \end{bmatrix} \\ e &= \begin{bmatrix} 0 \\ f_g \end{bmatrix} \\ k &= 0. \end{aligned}$$

The transformation to angular coordinates [4] for the pendulum can be described by a stiffness transformer. Using equations 2.3 – 2.6:

$$\begin{aligned} \mathcal{L}_r(\theta) &= \begin{bmatrix} l\sin\theta \\ l\cos\theta \end{bmatrix} \\ J_r(\theta) &= \begin{bmatrix} -l\cos\theta \\ l\sin\theta \end{bmatrix} \end{aligned}$$

[4] An angle of zero corresponds to the pendulum hanging straight down.

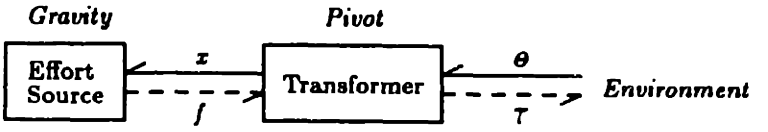

Figure 2-1: Model structure for a pendulum.

$$\begin{aligned} \tau &= [-l\cos\theta \quad l\sin\theta] \begin{bmatrix} 0 \\ -f_g \end{bmatrix} \\ &= -f_g l \sin\theta. \end{aligned}$$

From equation 2.7 the angular stiffness is

$$\begin{aligned} k_\theta &= J_\tau^T(\theta) k J_\tau(\theta) + \frac{\partial J_\tau^T(\theta)}{\partial \theta} e \\ &= [-l\cos\theta \quad l\sin\theta] 0 \begin{bmatrix} -l\cos\theta \\ l\sin\theta \end{bmatrix} + [-l\sin\theta \quad -l\cos\theta] \begin{bmatrix} 0 \\ f_g \end{bmatrix} \\ &= -f_g l \cos\theta. \end{aligned}$$

The structure of this model is represented in Figure 2-1. Each element is represented by a block in the graph. The lines connecting the blocks illustrate the flow of information for the analytical computation of the system's response. Since both elements are position causal, position information is passed down the tree (solid lines) and effort information propagates back up (dashed lines).

2.4.2 Two Joint Arm

A model of an arm provides a more complicated example in which the tree structure of the system is readily apparent. Figure 2-2 depicts a model of a two joint arm with six muscles. The length/tension properties of each muscle are represented by discrete stiffness elements. The action of each element on the appropriate joint is computed by each of six stiffness transformers. Common position junctions are used, first to form groups of muscles acting on the same joints, and then to produce a composite model of the arm at the joint level. Finally, one more transformer is used to represent

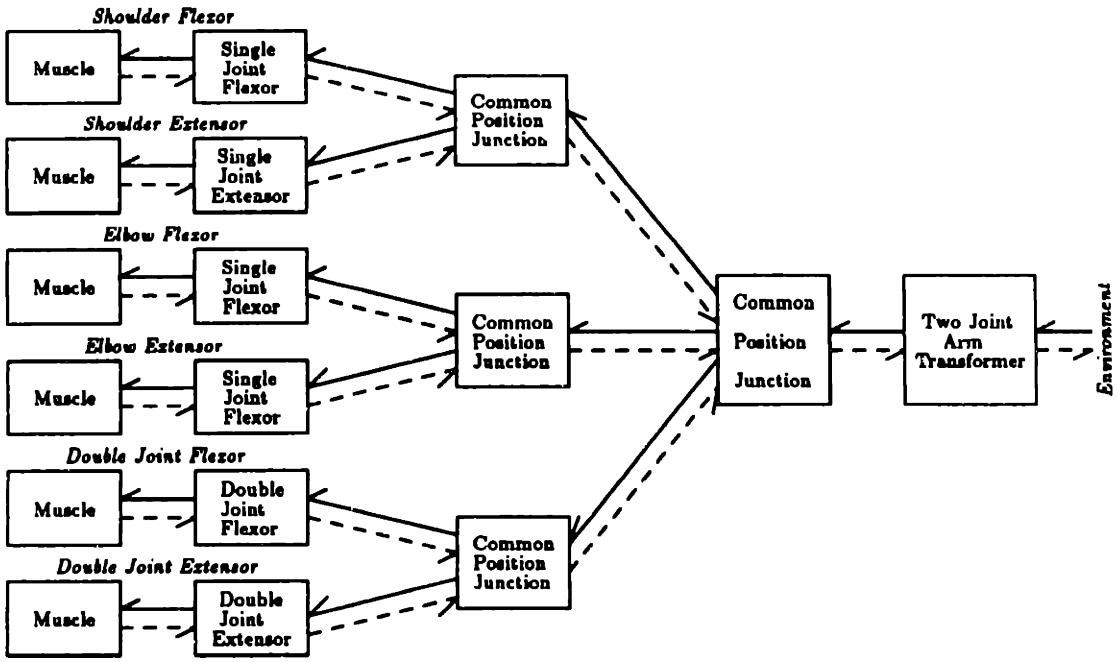

Figure 2-2: Model structure for a two joint arm.

the transformation from tip to joint coordinates.

2.5 Implementation

I have implemented a computer system for the simulation of elastic motor systems, based on the mathematics presented above. The system is written in LISP on a Symbolics 3600 series computer, using an object-oriented programming approach. The LISP environment easily supports the modular, tree-like structure of the simulation system.

2.6 Summary

In this chapter I have derived the mathematical formulas for computing the elastic behavior of mechanical systems, and described a method for modeling the behavior on a computer. These techniques will be applied in subsequent chapters to the study of the human motor system.

Chapter 3

Control of Limb Stability

The stiffness that is measured at the hand for a multi-joint arm emerges from combined effects of the elastic properties of the muscles and joints, the geometry of the linkages and muscle attachments, and the neural control circuits that act on the arm (i.e. reflex pathways). From Chapter 2 we know that the effective stiffness of a non-linear linkage such as a two-joint arm depends on the force acting on the system as well as the intrinsic stiffness of the actuators. This chapter presents an analysis of the factors which affect limb stiffness, including the effects of force load on the stiffness field. Potential strategies for controlling the stability of the limb are proposed and tested via computer simulations. The predictions from the simulations are then compared with measured stiffness values for human subjects working against a force load.

The role of multi-joint muscles in the control of posture and movement is unclear. The current study examines the contribution of these muscles to the control of overall limb stability. It will be shown that muscles which span several joints provide mechanical couplings which are necessary for the maintenance of stability. By utilizing multi-joint muscles, the neuro-musculo-skeletal system can control a global property of the system (stability) with a passive local strategy.

This chapter will show that human subjects must increase the stiffness at the joints in order to stabilize certain force loads at the hand. A local strategy may be used to accomplish this task, in which the muscle stiffness increases with muscle force.

Multi-joint muscles are a necessary component of this local strategy.

3.1 Previous Work

Since the observation that muscles act mechanically as tunable springs, both in isolation [55] and in connection with reflex feedback [18, 48, 59], considerable attention has been given to the analysis of limb impedance. This has led to the development of the equilibrium point hypothesis for the control of posture and movement [18, 9, 30]. The establishment of an appropriate mechanical impedance and equilibrium position for the limb is necessary to achieve stable limb postures and interactive behaviors [11, 12]. Control of limb impedance may in fact be the primary concern of the neuro-musculo-skeletal system [31, 26].

The human arm acting in the horizontal plane, is known to behave at the endpoint like a two-dimensional spring [47, 31, 21]. A control model has been proposed in which movements are produced via shifts in the equilibrium position of the limb [5, 21]. The effects of varying stiffness on the output of the model have been studied, suggesting that humans subjects use near optimal joint stiffnesses for the production of straight line trajectories [17]. Furthermore, it is known that human subjects can modify the stiffness behavior of the limb in only a limited number of ways [44].

In 1984 Hogan examined the possibility that joint impedance is modulated by the central nervous system (CNS) in order to stabilize certain loads [29]. In that study he has shown that: 1) joint stiffness can be increased via agonist/antagonist co-contraction, 2) under certain conditions co-contraction is the dynamically optimal solution for stabilizing the limb (subject to the modeling assumptions), and 3) electromyographic (EMG) measurements support the claim that subjects co-contract to stabilize unstable loads. The current study extends this analysis to include multiple joint limbs producing a net force at the endpoint.

3.2 Factors Affecting Endpoint Stiffness

What factors affect the stiffness of the limb observed at the hand? For a first order look at the problem the muscle properties and reflex actions can be lumped into a joint-level description of the elastic properties of the arm. The question then becomes: "Given the stiffness parameters at the joints, what factors affect the stiffness measured at the tip?" Applying Section 2.1.4, the derivation of the hand stiffness matrix for a two-joint arm is

Definitions

Cartesian Tip Coordinates:

$$\text{Tip Position } X = \begin{bmatrix} x \\ y \end{bmatrix}$$

$$\text{Tip Force } F = \begin{bmatrix} f_x \\ f_y \end{bmatrix}$$

$$\text{Tip Stiffness } K_X = \frac{\partial F}{\partial X}$$

Joint Coordinates:

$$\text{Joint Position } \Theta = \begin{bmatrix} \theta_1 \\ \theta_2 \end{bmatrix}$$

$$\text{Joint Torque } \tau = \begin{bmatrix} \tau_1 \\ \tau_2 \end{bmatrix}$$

$$\text{Joint Stiffness } K_\Theta = \frac{\partial \tau}{\partial \Theta}$$

Coordinate Transformations

$$X = \mathcal{L}(\Theta)$$

$$J(\Theta) = \frac{\partial \mathcal{L}}{\partial \Theta}$$

$$dX = J(\Theta)d\Theta$$

$$\tau = J^T(\Theta)F$$

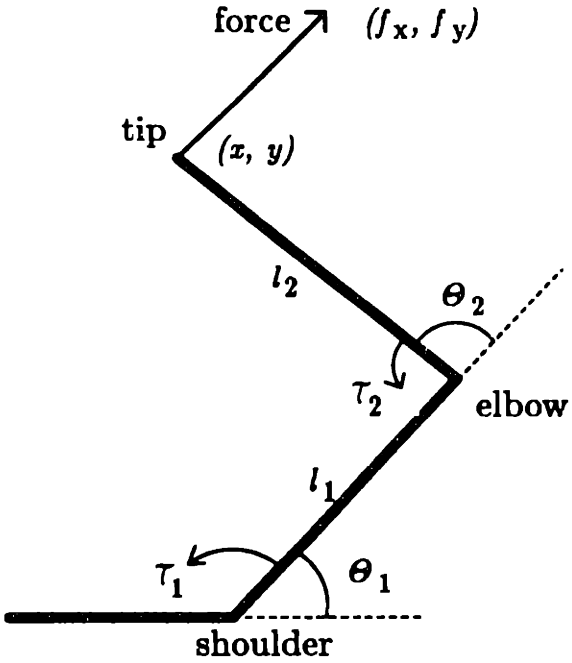

Figure 3-1: Planar two-joint arm model.

Stiffness Transformations

$$\begin{aligned} K_\Theta &= \frac{\partial \tau}{\partial \Theta} \\ &= \frac{\partial (J^T(\Theta)F)}{\partial \Theta} \\ &= J^T(\Theta)\frac{\partial F}{\partial \Theta} + \frac{\partial J^T(\Theta)}{\partial \Theta}F \\ &= J^T(\Theta)\frac{\partial F}{\partial X}\frac{\partial X}{\partial \Theta} + \frac{\partial J^T(\Theta)}{\partial \Theta}F \\ &= J^T(\Theta)K_X J(\Theta) + \frac{\partial J^T(\Theta)}{\partial \Theta}F \end{aligned}$$

$$K_X = J^{T^{-1}}(\Theta)\left[K_\Theta - \frac{\partial J^T(\Theta)}{\partial \Theta}F\right]J^{-1}(\Theta). \tag{3.1}$$

From equation 3.1 it can be seen that the stiffness at the hand depends not only on the value of the joint stiffness K_Θ, but on the position Θ and *tip force* F as well. The position and force effects both are a result of the dependence on position of the Jacobian $J(\Theta)$.

The dependence of the hand stiffness on position has been examined previously for a two joint arm with zero net output force [47]. Two primary features of the stiffness field which emerged from this analysis were the radial orientations of the stiffness field with respect to the shoulder, and the change in shape of the stiffness field as the hand approaches the limits of the workspace. Both of these features are captured to a large degree by a model of arm stiffness control in which the joint stiffness is held constant. Thus, the human motor system may adopt the control strategy of maintaining a constant joint (or muscle) stiffness independent of the position of the limb.

In terms of stability, a constant joint stiffness strategy for no force load is feasible, because maintaining a stable joint stiffness guarantees that the hand stiffness will be stable as well. Under the conditions of zero force load ($F = 0$), equation 3.1 reduces to

$$K_X = J^{T^{-1}}(\Theta) K_\Theta J^{-1}(\Theta).$$

If K_Θ is negative definite (has all negative eigenvalues, and is therefore stable), then K_X is also negative definite (stable) independent of the value of $J(\Theta)^{-1}$ [57].

Under conditions of varying force loads, stability of the joint stiffness matrix is no longer sufficient to guarantee stability of the hand stiffness. At high enough loads, the geometric stiffness terms ($\frac{\partial J^T(\Theta)}{\partial \Theta} F$) of equation 3.1 can significantly affect the hand stiffness field. Figure 3-2 shows the affect of output force on the stiffness of hand. The center field represents the stiffness of the tip for a particular value of joint stiffness operating against a zero force load. The surrounding fields illustrate what the measured tip stiffness would be for the arm in the same position with the same joint stiffness, but while producing a steady state force in the direction indicated by the large arrow. We can see from this figure that loads which cause the hand to *pull* (hand force directed toward the joints) tend to *stabilize* the limb, while hand forces that *push* (away from the joints) tend to *destabilize* the limb. In fact, for this combination of force magnitude and joint stiffness, the hand stiffness field is shown

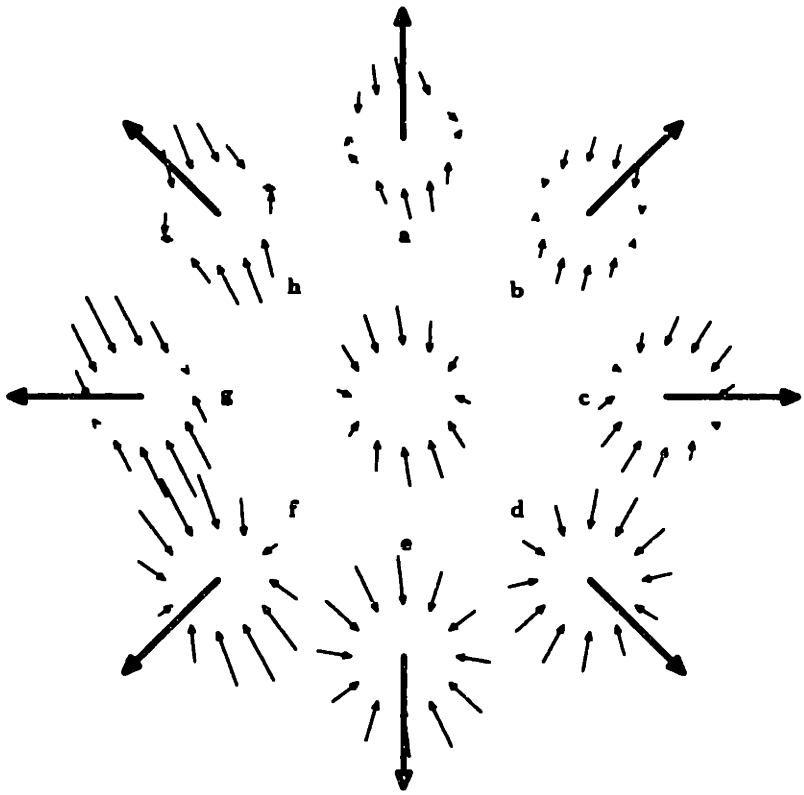

Figure 3-2: Dependence of endpoint stiffness on output force.

to be unstable for forces in certain directions (fields a and h).

An intuitive feel for the source of the instability can be gained by comparing the two joint arm system with the pendulum described in Section 1.1.2. Imagine a rigid link connecting the hand in a straight line to a pivot point at the shoulder (Figure 3-3). An external force acting inward along this line (i.e. the hand is pushing outward) would cause the system to behave like the inverted pendulum, generating an instability around the pivot point. Rotation around this pivot results in lateral motion of the endpoint. Thus, the effective stiffness generated by this geometrical effect produces instability at the hand perpendicular to the line of force. An applied force directed toward the pivot at the elbow would have a similar effect.

For non-linear linkages, such as a two joint arm, control of stability for the manipulator depends on the force output produced by the limb. A system which controls such a linkage must accommodate this dependence, although under certain conditions

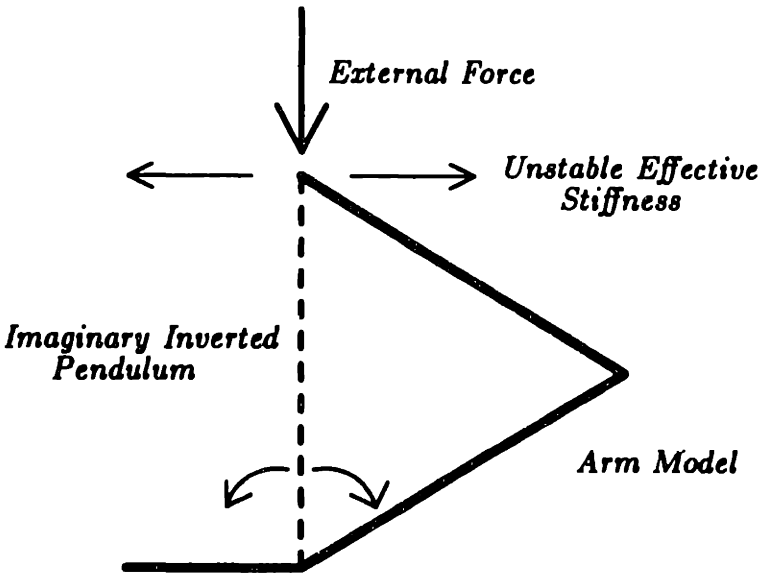

Figure 3-3: Source of endpoint instability.

ignoring the variation may be a perfectly viable solution. This chapter examines how the human motor system controls limb stiffness under varying load conditions.

3.3 Materials and Methods

The experiments performed for this chapter compared measurements of human motor responses with simulations of an ideal two-joint arm. Three normal, healthy volunteers, ages 25 – 35, participated in these experiments. The stiffness of the human arm was measured for each subject maintaining a specified posture against different force loads. The subject grasped the handle of a two-joint manipulandum, the end of which is free to move in the horizontal plane. The subject's elbow was supported by a sling suspended from the ceiling, restricting the movement of the arm to the horizontal plane as well. Stiffness was measured statically by imposing small displacements on the hand through servo control of torque motors acting at the two joints of the apparatus. The restoring force due to each displacement was measured by a six axis force/torque transducer mounted on the handle of the manipulandum. Displacements of two different magnitudes (7 and 10 mm) and in eight directions were applied for

each stiffness measurement. Linear regression of this data was used to compute a best fit, two by two matrix representing the stiffness field at the hand.

The symmetric and anti-symmetric components of the measured hand stiffnesses were compared for each subject, confirming that for the loads applied in this study the anti-symmetric component contributes little to the stiffness field (the field is conservative [47]). Only the symmetric component of this matrix was used in the subsequent analysis.

Force loads were generated by various lead weights attached to the subject's hand via a cable and pulley arrangement. The magnitude of the load was independently measured at the hand with a linear force transducer. While there is little or no intrinsic stiffness associated with the weight and cable, the geometry of the load apparatus generates a component of stiffness at the hand in the direction perpendicular to the direction of the cable. This effect was minimized by making the distance from the hand to the pulley as long as possible. In any case, the stiffness of the load apparatus is computed for each force value and subtracted from the measured stiffness to get the intrinsic hand stiffness:

$$\begin{aligned} K_X &= K_{measured} - K_{load} \\ K_{load} &= -mgl \end{aligned}$$

where l is the distance from the hand to the pulley, m is the mass of the weight and g is the acceleration due to gravity.

For these experiments, force loads were restricted to two directions along a single axis in the horizontal plane (Figure 3-4). A positive force value corresponds to an outward pushing of the hand, while a negative force value means the hand is pulling inward. Seven to twelve different load values were applied, ranging from -60 to +60 newtons.

Joint stiffness values were computed from the measured hand stiffnesses by in-

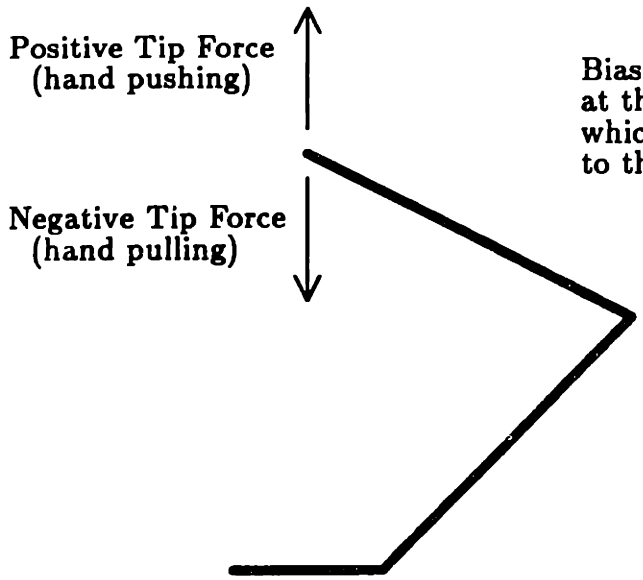

Figure 3-4: Force load apparatus.

verting equation 3.1:

$$K_\Theta = J^T(\Theta)K_X J(\Theta) + \frac{\partial J^T(\Theta)}{\partial \Theta}F. \tag{3.2}$$

The computed joint stiffness can be divided into three components corresponding to the net stiffness contributions of the single-joint shoulder muscles, the single-joint elbow muscles, and the double-joint muscles of the arm (Figure 3-5). This decomposition of the joint stiffness is based on the assumption that the muscles act with constant moment arms at the joints. Furthermore, it was assumed that the moment arms of the double-joint muscles are equal for each joint ($\frac{r_1}{r_2} = 1$). The sensitivity of the results to these assumptions will be discussed in a later section (3.6.6).

Simulations and analyses were performed on a Symbolics 3600 Lisp Machine using the algorithms described in Chapter 2.

Joint Stiffness Components

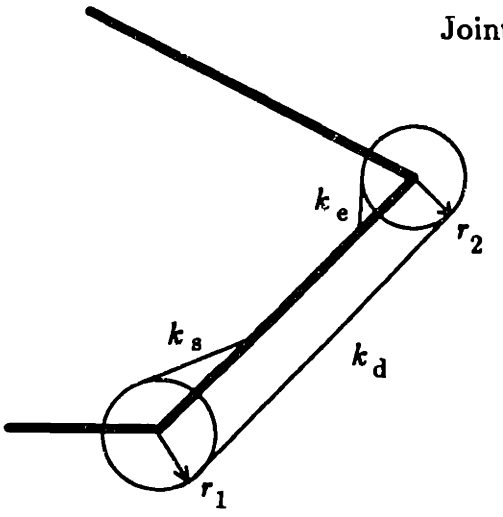

$$\text{Joint Stiffness } K_\Theta = \begin{bmatrix} k_s + \frac{r_1}{r_2} k_d & k_d \\ k_d & k_e + \frac{r_2}{r_1} k_d \end{bmatrix}$$

where k_s = single joint shoulder stiffness,

k_e = single joint elbow stiffness,

k_d = double joint stiffness.

Figure 3-5: Definition of joint stiffness components.

3.4 Simulation Results

A number of strategies can be hypothesized for the control of endpoint stiffness in the human arm. Three such strategies are described here, each of which has been simulated on the computer. These simulation results will be compared with the experimental data in the next section, in order to identify the control algorithm that best describes the strategy employed by the subject.

3.4.1 Constant Joint Stiffness

The simplest strategy that can be proposed is that of maintaining a constant joint stiffness independent of the output force. While this means that the hand stiffness will change with the force load, it is possible that the joint stiffness is high enough to maintain endpoint stability for loads of reasonable size.

Figure 3-6 shows the results of simulating a constant joint stiffness control strategy for two different values of joint stiffness. The lower magnitude joint stiffness is typical

of a human subject acting against a zero force load. The endpoint stiffness was simulated for conditions in which the limb maintains the same posture and joint stiffness, but produces a desired output force. The fields along the top of the figure represent the predicted stiffnesses for nine different specified force loads using the lower magnitude of joint stiffness. Below these figures is plotted a graph of the eigenvalues of the computed stiffness matrices. This plot shows that if the arm were to maintain a low constant joint stiffness (solid lines), the endpoint stiffness would become unstable at approximately 30 newtons of force. The system can be stabilized to a greater magnitude of applied force if a higher constant joint stiffness is used (dashed lines).

3.4.2 Constant Endpoint Stiffness

A more complicated strategy is that of controlling the joint stiffness so as to maintain a constant endpoint stiffness. The question here is: "How must each component of the joint stiffness be modified in order to maintain a constant endpoint stiffness with different force loads?" Again, starting with the tip and joint stiffnesses measured for a human subject with no load, we can use equation 3.2 to compute the joint stiffness necessary to maintain the initial tip stiffness while the arm produces a range of output forces.

Figure 3-7 shows the results of this simulation. Each joint stiffness component is plotted separately as a function of the force magnitude. The plots show that the shoulder and double-joint stiffness components must vary with the hand force in order to maintain a constant hand stiffness. This is interesting, because for force loads in these two directions, there is no torque being produced at the shoulder (the line of force passes through the shoulder, see Figure 3-4). In order to maintain a constant endpoint stiffness, *shoulder* stiffness must increase in response to an increase in torque at the *elbow*. Equally significant is the fact that elbow stiffness need not increase in this case in order to maintain stability.

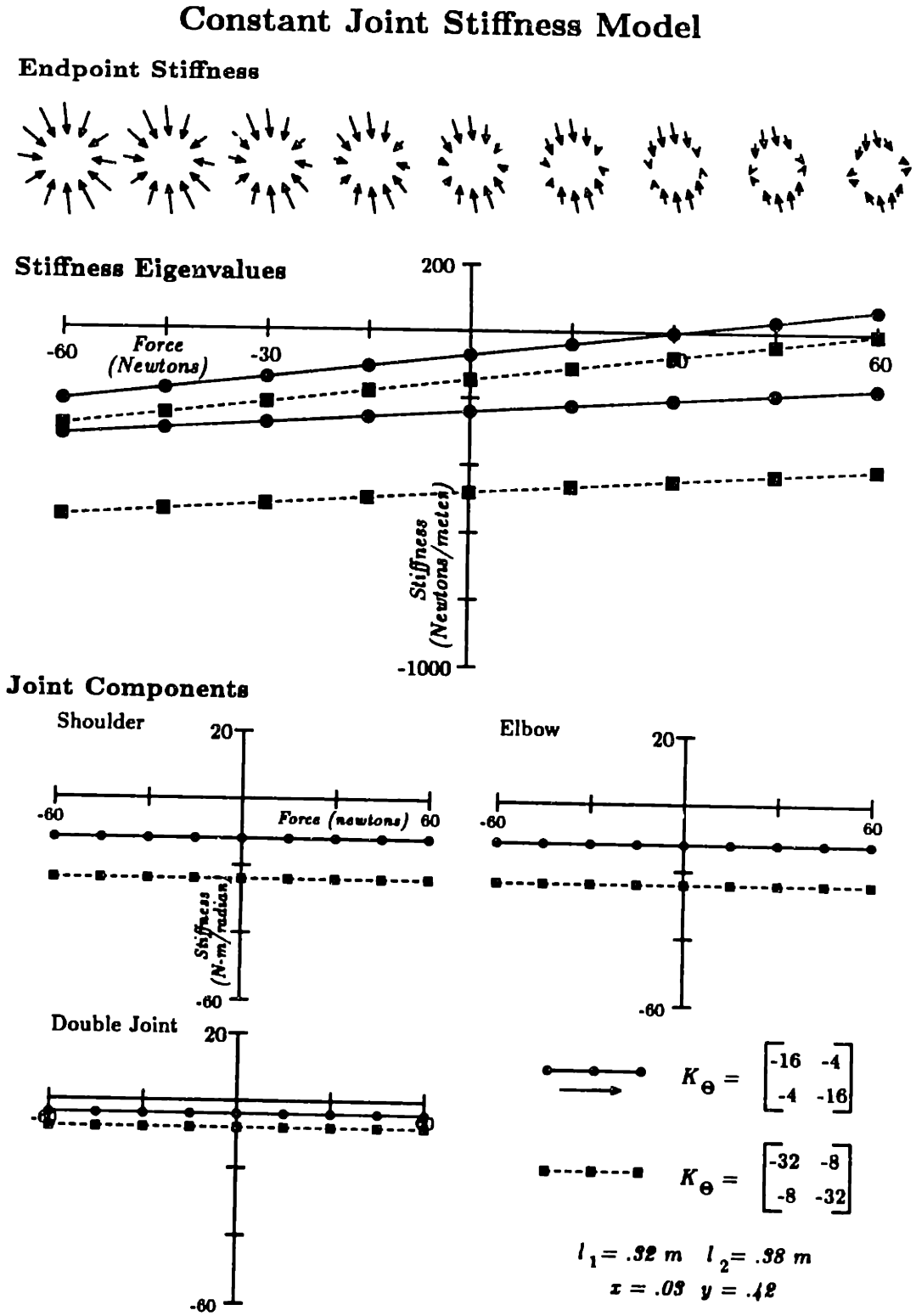

Figure 3-6: Simulation of constant joint stiffness control.

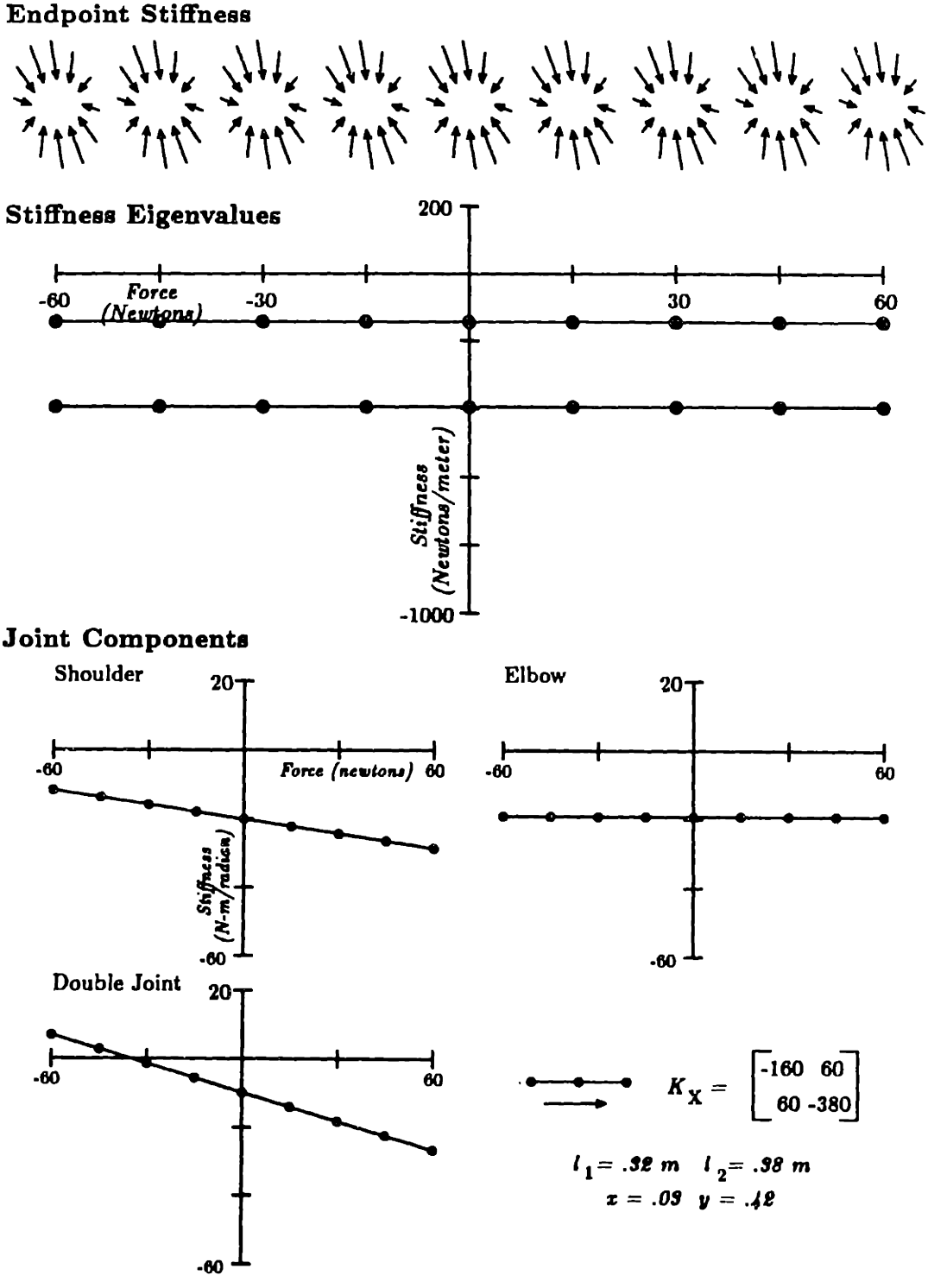

Figure 3-7: Simulation of constant endpoint stiffness control.

3.4.3 Passive Stabilization

I propose a third control strategy in which the hand stiffness is stabilized passively via the mechanical properties of the force producing elements. This model is based on two assumptions:

1. Muscle stiffness increases as the muscle force output increases.

2. Multi-articular muscles are active even when torque is produced only at a single joint.

The importance of these two conditions is apparent from the previous examples. Joint stiffness must increase with the force load in order to maintain hand stability. Furthermore, torque production at one joint must be coupled with stiffness changes at another. As torque is produced to generate the desired force, increases in muscle stiffness can produce the necessary change in joint stiffness, while multi-joint muscles can provide the required inter-joint coupling.

For the simulation of this strategy the muscle elastic response was modeled as an exponential relationship between muscle length and muscle force (Figure 3-8a). This relationship satisfies the assumption that stiffness ($\frac{\partial f}{\partial l}$) increases with muscle force (Figure 3-8b) and is consistent with observed biological data [55, 18]. The torque required to produce a desired force output is distributed between the uni-articular and bi-articular muscles based on the relative stiffness values of each. Again, this is in agreement with experimental observations [35, 10] (see Chapter 4).

Figure 3-9 shows the results of simulating a system with muscles that stiffen with output force. Unlike the constant joint stiffness model, stability is maintained despite increases in force load. The mechanics by which the hand stiffness is stabilized are apparent in the plot of the joint stiffness components. As the force load increases, the torque at the elbow must increase. This torque load is shared by the double-joint muscles. The increase in double-joint muscle force generates an increase in stiffness at both joints. In addition, because the double-joint muscle produces torque at both the shoulder and the elbow, the single-joint shoulder flexors must become active in

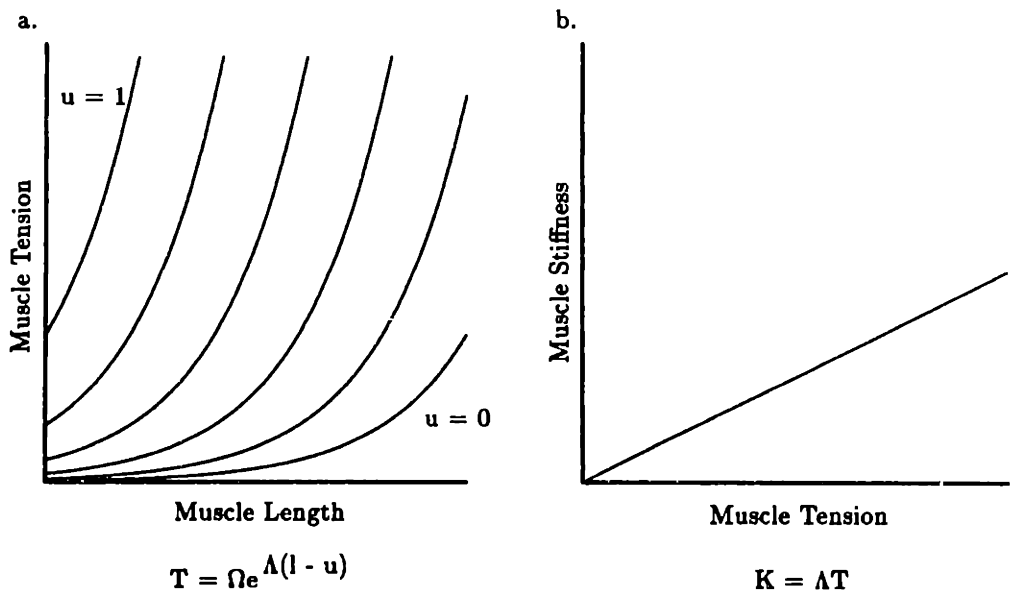

Figure 3-8: Exponential model of muscle length/tension properties.

order to counteract the shoulder torque. The resulting increase in stiffness of the single-joint shoulder muscles further stabilizes the limb.

In contrast to the constant tip stiffness model, the stiffness at the elbow also increases due to the increase in elbow single-joint muscle activity. Furthermore, the joint stiffness increases for hand forces in the negative direction as well. Each these affects tends to increase the overall stiffness of the hand. The tip stiffness will indeed change for different force loads, but the fundamental condition of stability will be satisfied.

The double-joint muscles play a key role in stabilizing the limb under this strategy. To emphasize this point, Figure 3-10 shows the simulated stiffness fields generated by a two-joint arm having only single-joint muscles. The stiffness at the elbow increases with the level of force output, but since the shoulder muscle generates no torque, there is no change in shoulder stiffness. The pattern of tip stiffness is different from the constant joint stiffness model, however the stiffness can still become unstable as

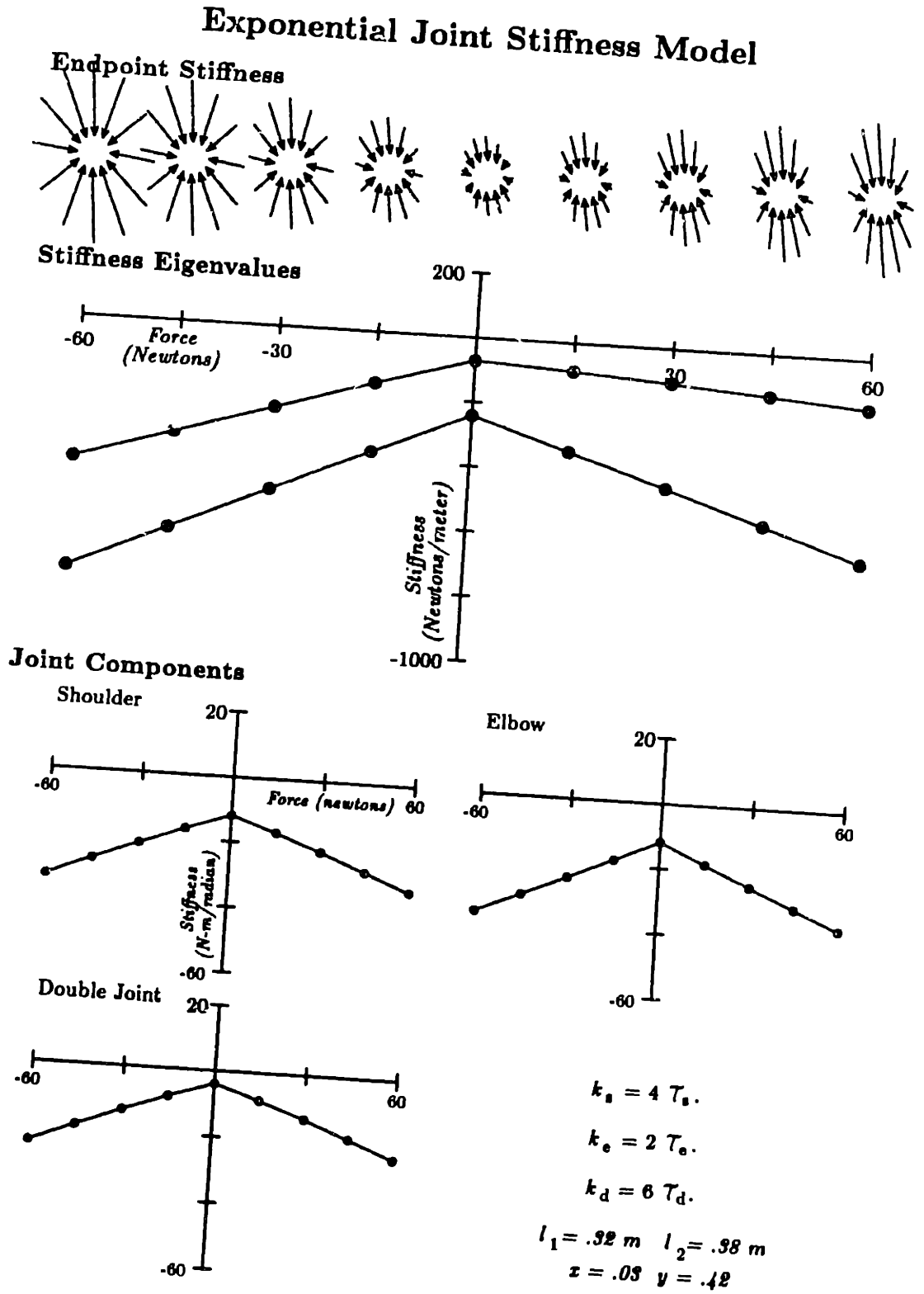

Figure 3-9: Arm stiffness for the exponential model of muscle.

the force level increases.

3.4.4 Summary

The predictions that can be made from these simulations are summarized as follows:

- Maintaining a constant joint stiffness will yield a destabilization of the hand stiffness when operating against certain force loads, possibly to the point of instability.
- Stabilizing the hand stiffness requires the coupling of torque changes at one joint with stiffness changes at another.
- A local strategy in which muscle stiffness increases with output force, can effectively stabilize the limb.
- Multi-articular muscles provide the inter-joint coupling necessary to stabilize the limb.

3.5 Experimental Results

The stiffness parameters were measured for three human subjects working against a range of torque loads. Figures 3-11 through 3-13 show the results of these experiments. Measured hand stiffnesses are plotted as vector fields, along with the stiffness eigenvalues and compute joint stiffness components for each measurement. (Not all of the measured stiffness values are plotted as vector fields.)

Experiment 1: Must the joint stiffness change in order to maintain stiffness at the endpoint? This question was answered by simulating a constant joint stiffness model, using the measured resting joint stiffness for each subject. The simulated constant joint stiffness results are plotted as broken lines superimposed on the measured data. From these simulations we can see that a constant joint stiffness strategy would produce an unstable hand stiffness at force loads within the range achieved by subjects SFG and JLM. (Subject SMB was not tested above the potentially unstable

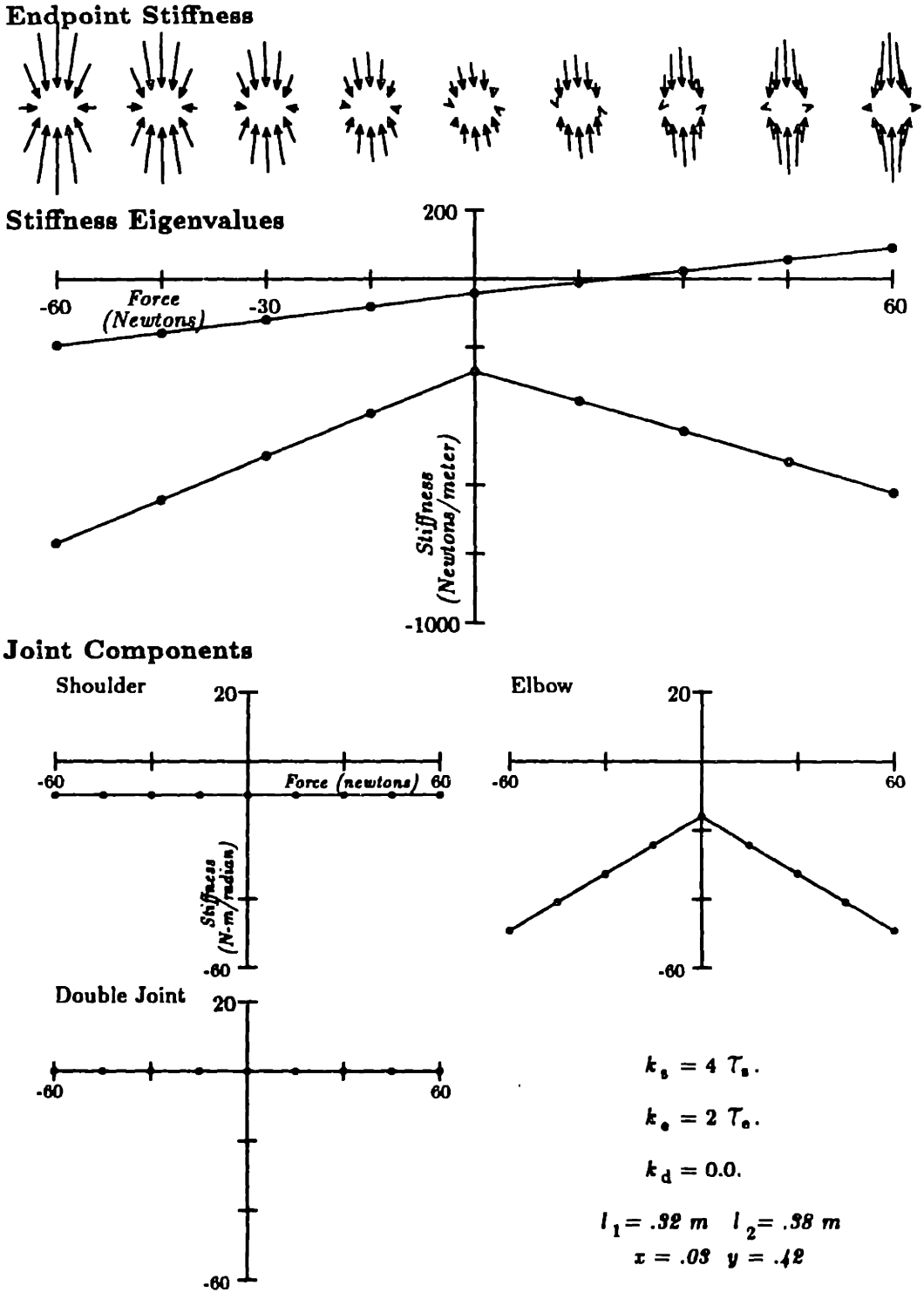

Figure 3-10: Exponential muscle model without double-joint muscles.

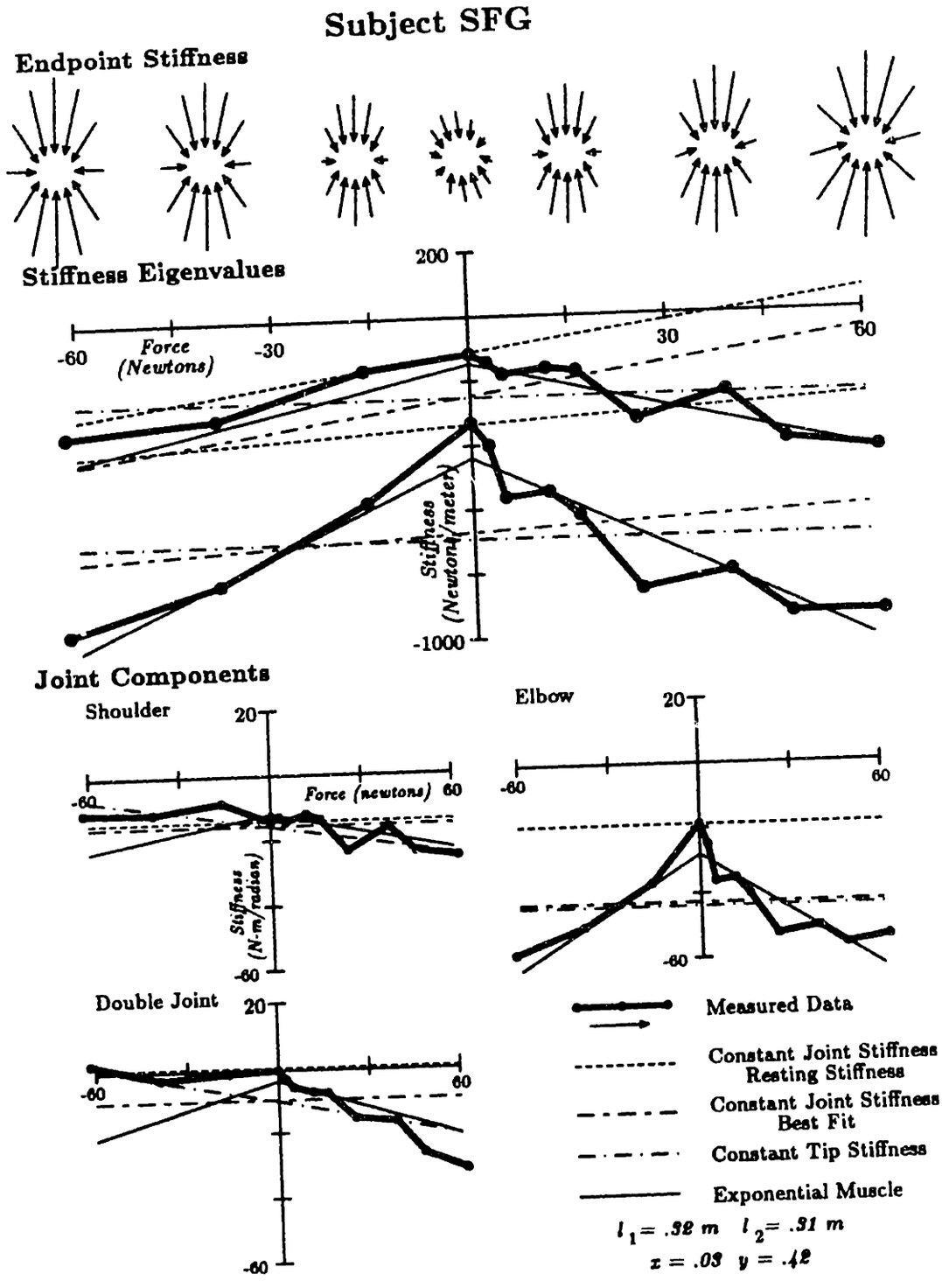

Figure 3-11: Stiffness data for subject SFG.

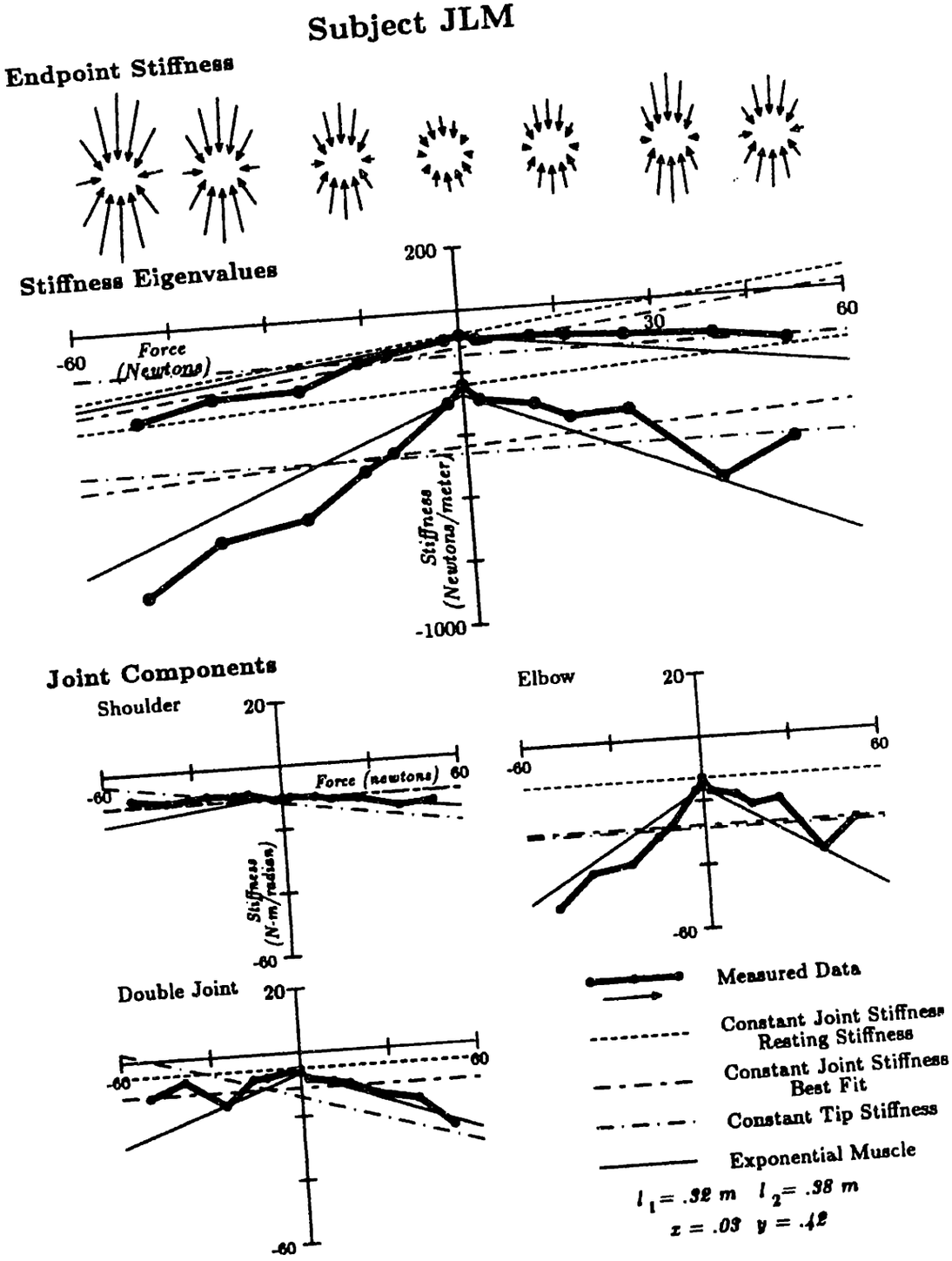

Figure 3-12: Stiffness data for subject JLM.

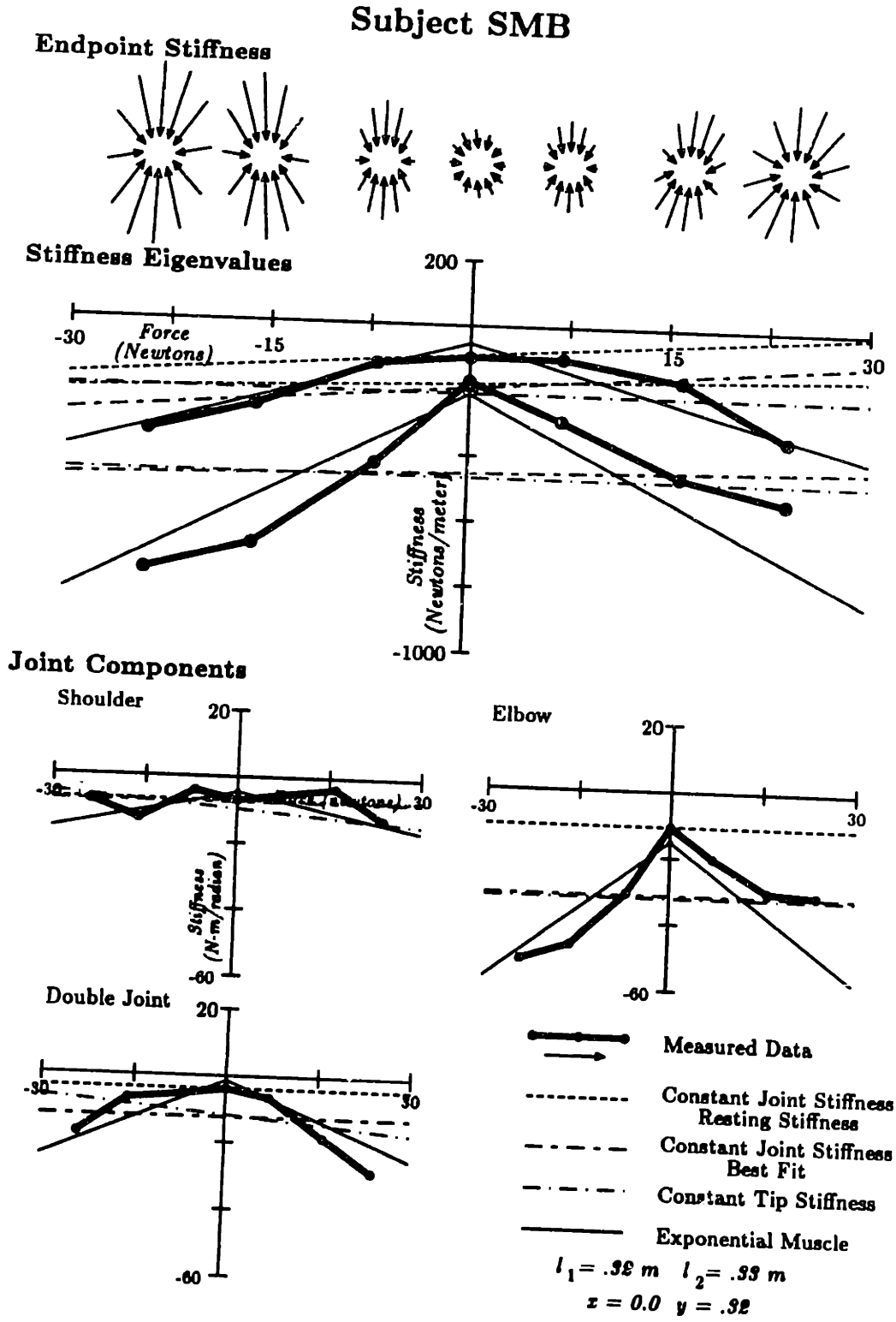

Figure 3-13: Stiffness data for subject SMB.

level of force.) To test the reliability of this result, the hand stiffness was sampled on subject SFG five times each at loads of 0.0 and 2.5 newtons. For each of these loads the mean and standard deviation of each component of the hand stiffness were computed. The arm would become unstable at one or more of the test force loads even if each component of the stiffness field were increased from the mean by three times the measured standard deviation. That is, assuming that the variations in resting stiffness are due to random noise, the prediction of an unstable hand stiffness is reliable to a confidence level of $p < .01$, based on the sampled data.

Experiment 2: What model best describes the experimental data? Four such models were considered for comparison. The first is the constant joint model described above, using the measured resting joint stiffness of the subject. A second constant joint stiffness model was also tested, using the average joint stiffness measured for all the trials. A constant tip stiffness model was considered, using the average measured hand stiffness and finally, a model in which the muscles stiffen with output force was examined.

The four control models produce different predictions for the hand and joint stiffnesses measured for different force loads. Lines representing the predicted responses are superimposed on the plots of measured data for each subject. In tables 3.1 and 3.2, the accuracy of the models are compared quantitatively. The error between the predictions and the data is defined as:

$$\varepsilon = K_{measured} - K_{model}.$$

Defining the norm of a matrix to be equal to its largest eigenvalue [57], the average magnitude of the error matrices for a given model was used as a measure of its fit to the data. For all three subjects the best model was that of increasing muscle stiffness with output force.

Subject	Model	Constraints	Average Error
SFG	Constant Joint Stiffness Rest Stiffness	$K_\Theta = \begin{bmatrix} -14.9 & -0.7 \\ -0.7 & -19.5 \end{bmatrix}$	409
	Constant Joint Stiffness Best Fit	$K_\Theta = \begin{bmatrix} -25.4 & -9.9 \\ -9.9 & -52.7 \end{bmatrix}$	210
	Constant Tip Stiffness	$K_X = \begin{bmatrix} -251.5 & -16.0 \\ -16.0 & -690.3 \end{bmatrix}$	197
	Exponential Muscle Stiffness	$k_s = -.183F - 11.8$ $k_e = -.583F - 28.1$ $k_d = -.284F - 3.9$	84
JLM	Constant Joint Stiffness Rest Stiffness	$K_\Theta = \begin{bmatrix} -15.4 & -5.11 \\ -5.11 & -18.0 \end{bmatrix}$	233
	Constant Joint Stiffness Best Fit	$K_\Theta = \begin{bmatrix} -21.6 & -11.2 \\ -11.2 & -38.9 \end{bmatrix}$	144
	Constant Tip Stiffness	$K_X = \begin{bmatrix} -145.7 & -5.9 \\ -5.9 & -461.0 \end{bmatrix}$	149
	Exponential Muscle Stiffness	$k_s = -.111F - 9.4$ $k_e = -.555F - 16.0$ $k_d = -.334F - 6.70$	88

Table 3.1: Comparison of control models for subjects SFG and JLM.

Subject	Model	Constraints	Average Error
SMB	Constant Joint Stiffness Rest Stiffness	$K_\Theta = \begin{bmatrix} -10.9 & -3.9 \\ -3.9 & -14.5 \end{bmatrix}$	319
	Constant Joint Stiffness Best Fit	$K_\Theta = \begin{bmatrix} -20.0 & -12.4 \\ -12.4 & -43.9 \end{bmatrix}$	195
	Constant Tip Stiffness	$K_X = \begin{bmatrix} -210.3 & -3.8 \\ -3.8 & -469.3 \end{bmatrix}$	193
	Exponential Muscle Stiffness	$k_s = -.385F - 4.6$ $k_e = -1.38F - 15.1$ $k_d = -.774F - 1.40$	107

Table 3.2: Comparison of control models for subject SMB.

3.6 Discussion

It is immediately clear from the cartesian representation of the measured stiffness that subjects did not become unstable under any of the force loads tested. This is not surprising, as it would have been very difficult for the subject to perform the task if the arm were not stable. The question is not so much "*Does* the arm remain stable?" as "*How* does the arm remain stable?" That the joint stiffness must be varied in order to maintain stability is demonstrated by Experiment 1. If the joint stiffness observed for the arm at low force levels were maintained for all applied loads, the arm would become unstable for high levels of force.

Using the experimental data from Experiment 2, one can reject the hypotheses that the central nervous system controls the limb so as to maintain either a constant joint stiffness or a constant endpoint stiffness. The constant joint stiffness model would predict a monotonic change in the effective hand stiffness with respect to the applied force. A model in which the endpoint stiffness is held constant would require

a monotonic increase in shoulder and double-joint stiffnesses, and no change in elbow stiffness. None of these predictions are in concert with the qualitative features of the observed data.

The data are in good agreement with the increasing force/stiffness model for the control of stability. The fact that the elbow stiffness goes up dramatically with elbow torque, *even though this is not required to maintain stability*, is consistent with this model for the control of stiffness. Furthermore, the stiffness in each joint component is seen to increase for force loads in either direction.

3.6.1 Stability Margin

The *margin of stability* is defined as the magnitude of the smallest eigenvalue of the stiffness field. This corresponds the minimum stiffness that would be observed for disturbances in any direction. In all cases the subject apparently increases joint stiffness with force load so as not to reduce the margin of stability. The human nervous system may control the limb stiffness in such a way as to guarantee a given stability margin, thus providing a minimum level of disturbance rejection. Whether or not this observation holds for different limb configurations and experimental conditions will be the topic of future research.

3.6.2 Role of Double Joint Muscles

The need for multi-articular muscles in biological systems has not yet clearly been established. Multi-joint muscles are not necessary for the production of arbitrary force vectors by a two joint arm, the necessary torque could be provided by the single-joint muscles alone. On the other hand, double-joint muscles are necessary for generating an endpoint stiffness of arbitrary shape and orientation [31]. Yet the human motor system seems unable to take advantage of this flexibility. Human subjects are not able to significantly alter either the shape or the orientation[1] of the stiffness field at the hand [44]. It has, however, been shown that optimal trajectory following

[1]See [47] for a definition of stiffness field shape, size and orientation.

with a fixed joint stiffness requires the presence of a significant level of double-joint stiffness [17, 20].

The current study presents an alternative view of the role of muscles which span two or more joints. The presence of these muscles allows for the mechanical coupling of torque and stiffness across joints. To achieve a passive stabilization of the limb through the actuator mechanical properties, multi-joint muscles must be present. This is perhaps a more compelling reason for the existence of multi-joint muscles.

3.6.3 Local vs. Global Effects

The destabilizing effect of the endpoint force is a global property of the system resulting from the non-linear nature of the linkage. If either joint were studied in isolation, or if pure torque loads were used, the effects on stability would not be observed. The level of torque being produced at one joint can affect the stiffness required at the other. Yet the human motor system seems to adopt a local strategy for controlling stability. Muscle stiffness need be a function only of muscle force. Again, it is the multi-articular muscles that provide the necessary coupling between joints. This is an example of where a clever mechanical design can be used to simplify the control problem.

3.6.4 Reflexes vs. Mechanical Properties

These experiments have not addressed the question of how the changes in joint stiffness are achieved. A particularly elegant solution would be to have muscles which mechanically stiffen as the force increases. Stiffness control would be achieved *passively* with no additional intervention from the nervous system. On the other hand, Hogan found that load stabilization was achieved through co-contraction at the elbow [29]. In that single joint case, no net change in torque was required to support the change in load, so passive stabilization via increased force output would not accomplish the task. Another possibility does exist, joint stiffness could increase through changes in the reflex feedback gains which contribute to the stiffness around the joint.

Additional experiments will be needed to distinguish between these possibilities for the multi-joint arm producing a net force output.

3.6.5 Model vs. Data Discrepancies

In the measured data the increase in stiffness seen for each of the joint components is asymmetric with respect to the direction of force. This is in contrast to the symmetric patterns of stiffness change predicted by the exponential muscle force model. In the model, however, torques and stiffnesses were produced by ideal spring-like actuators acting at the joints, one for each of the joint components. In reality, the joint torques are produced by agonist/antagonist groups of muscles. The torque produced in one particular direction would be generated by a different set of muscles than for torque in the opposite direction. Thus, it is reasonable to expect a different torque vs. stiffness relationship for forces in different directions.

3.6.6 Modeling Errors

How are the conclusions drawn from this data affected by the modeling assumptions we have made?

Equal Moment Arms

The computation of the joint stiffness components was based on the assumption that the double joint muscles act at each joint with equal moment arms ($\frac{r_1}{r_2} = 1$). This assumption can be relaxed without altering the conclusions, neither the observed hand stiffness values nor the overall joint stiffness matrix is affected by this assumption. The conclusion that the subject maintains neither a constant hand stiffness, nor a constant joint stiffness are valid regardless of the value of $\frac{r_1}{r_2}$.

Variations in the value of $\frac{r_1}{r_2}$ affect only the relative contribution of each type of muscle to the overall joint stiffness. Figure 3-14 shows the joint stiffness components computed for subject JLM using three different values for the moment arm ratio. The change in ratio quantitatively affects the shoulder and elbow components, but

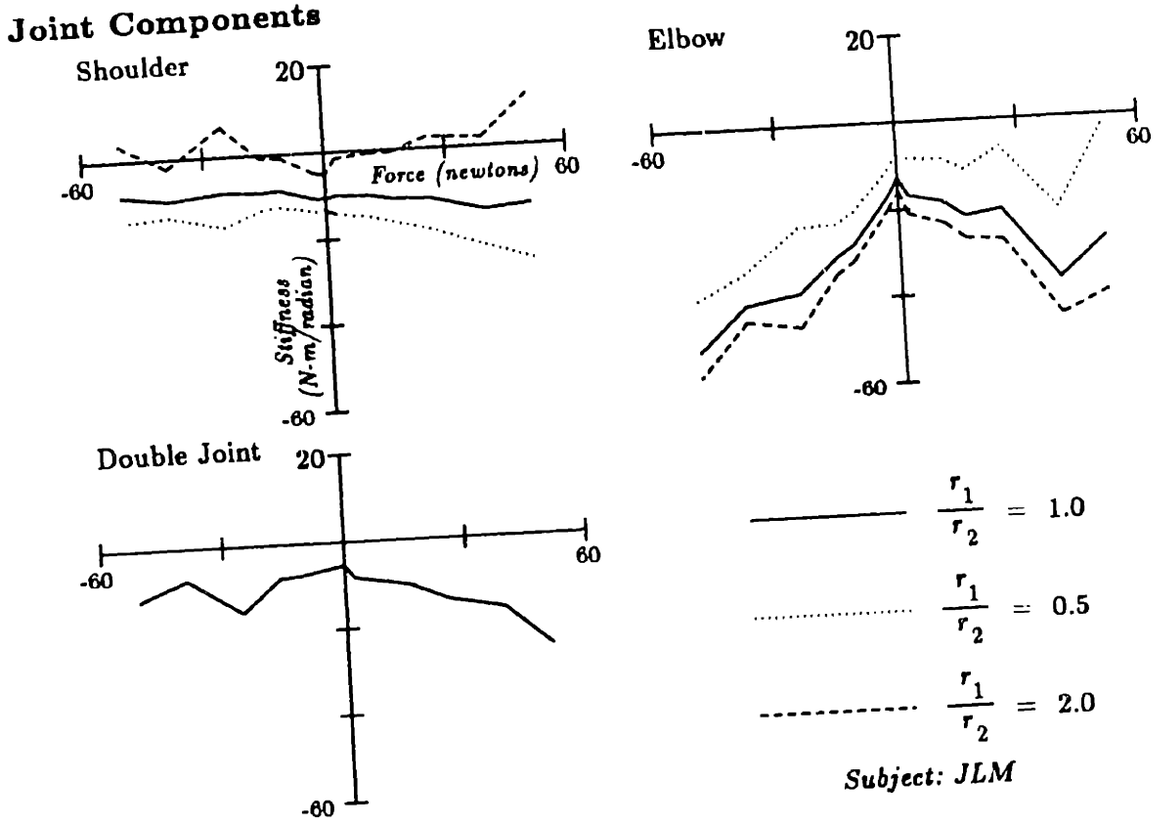

Figure 3-14: Effect of varying the ratio of moment arms.

qualitatively the results are the same. The elbow stiffness continues to increase for forces in either direction. The values for the double joint stiffness components are unaffected by the choice of the moment arm ratio.

Constant Moment Arms

For the analysis of the measured data, we assumed that the muscles acted at the joints with constant moment arms and attributed observed changes in joint stiffness to changes in muscle stiffness. A muscle acting with a non-constant moment arm around a joint would produce an effective joint stiffness component dependent on both the intrinsic muscle stiffness and the muscle force. It is conceivable that the

observed changes in joint stiffness can be attributed solely to this mechanical effect, but it is unlikely that it would be sufficient to stabilize the limb in all areas of the workspace. A muscle attachment which tends to increase joint stiffness with muscle force for one joint configuration could decrease the stiffness for another.

Additional analysis and experiments will be necessary to fully elucidate the effect of non-constant muscle moment arms in the stability of the limb. Yet even if the observed data could be attributed entirely to geometrical effects of muscle attachments, the significance of this study would not be diminished. Instead of solving the control problem with cleverly designed muscle mechanical properties, the neuro-musculoskeletal system would now have a solution which arises from a cleverly designed mechanical linkage. Limb stability is still maintained passively through increases in muscle force, and the double-joint muscles still form an essential component of the control scheme.

Linear Force/Stiffness Variation

The destabilizing effect of the applied load increases linearly with the force magnitude, as does the joint torque required to counteract the load. Thus, an appropriate linear relationship between the joint stiffness components and the applied torque could guarantee stability for any level of force. Other non-linear relationships between stiffness and force may also be sufficient to guarantee stability, the key assumption is only that stiffness must increase with muscle force.

Force Distribution

For a force load acting radially about the shoulder, the shoulder joint stiffness must increase, although the only net torque required is at the elbow. Passive stabilization of the limb through muscle mechanical properties requires that the double joint muscles participate in torques produced at either joint. Measurements of EMG signals during production of torques in the human arm support this assumption [22, 35].

3.7 Conclusions

To adequately control the stability of a multi-joint limb, the force being produced by the limb must be considered. These experiments have shown that for human subjects joint stiffness must increase with force output in order to maintain stability at the hand.

The mechanism by which human subjects maintain limb stability is not known. A potential control model has been proposed in which muscle stiffness increases with muscle force. This strategy is biologically plausible and the competence of the model has been demonstrated by computer simulations.

The stability of the limb is a global property of the motor system, depending on limb configuration and net output force. The proposed model, on the other hand, is a local strategy in which a muscle's stiffness is dependent only on that muscle's force output. The ability of this local strategy to stabilize the hand depends on the mechanical coupling provided by the two-joint muscles of the arm, suggesting an important role for multi-articular muscles in the control of limb posture.

In human subjects, the central nervous system maintains neither a constant joint stiffness, nor a constant endpoint stiffness when faced with different force loads. Of the control models tested, stiffness control in human subjects is best described by the passive stabilization of the endpoint through increasing muscle stiffness.

Chapter 4

Redundant Motor Systems

Biological motor systems are redundant with respect to many of the tasks required of them. A mechanical system can be considered redundant with respect to a specified task if the number of degrees of freedom which can be controlled by the system is greater than the number of constraints imposed by the task. As an example, consider a planar positioning task as shown in Figure 4-1. To arbitrarily position and orient an object requires three degrees of freedom (two translational and one rotational). A planar manipulator having four or more revolute joints is redundant with respect to this task. A given position and orientation of the end effector can be achieved by an infinite number of limb configurations. Similarly, a particular velocity at the endpoint can be obtained by an infinite number of different joint velocities.

The above example illustrates the concept of motor redundancy with respect to limb positions (position redundancy). A motor system may be redundant with respect to the production of effort (force or torque) as well (effort redundancy). If the number of actuators exceeds the number of positional degrees of freedom in the system, the effort required from each of the actuators to produce a particular net output is not uniquely determined. For example, consider two muscles acting in opposition around a single joint (Figure 4-2). If the force being produced by each of the muscles is the same, the net torque acting around the joint is zero. In order to generate a net positive torque, the force in the flexor could increase, the force in the extensor could decrease, or both muscle force levels (in the appropriate combination) could change.

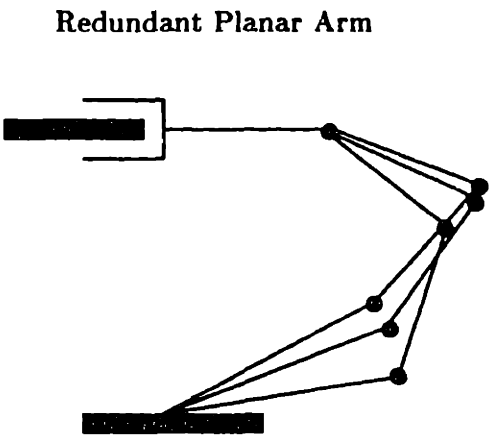

Figure 4-1: Example of position redundancy.

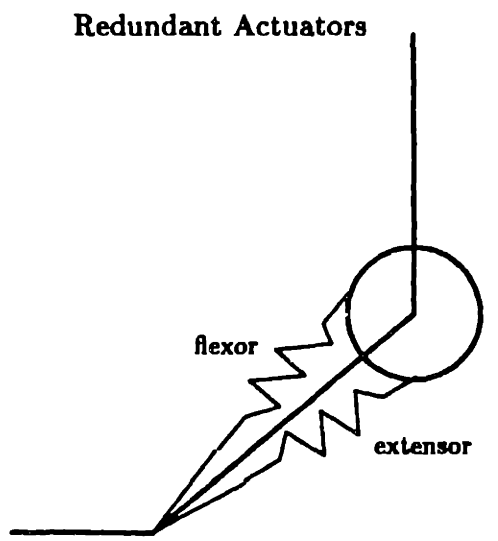

Figure 4-2: Example of effort redundancy.

Biological systems, and in particular the human arm, are redundant with respect to both positions and efforts. Typically the number of joints and the number of muscles in the system exceed the minimum numbers required to complete a particular task. The central nervous system (CNS) faces the problem of resolving the redundancy in order to achieve a particular solution. In terms of the human arm, the neuro-musculo-skeletal system must select an appropriate set of joint angles to achieve a desired hand position, and the CNS must determine a set of muscle activations which results in the desired force and torque output.

An algorithm has recently been proposed, called *backdriving*, that provides a method for the control of redundant motor systems [45, 46, 41]. Under this strategy, the elastic properties of the system are used to determine the active coordination of the individual mechanical elements. The algorithm unifies the control of position and effort redundancies into a single computational framework.

In this chapter I will demonstrate some of the advantages of the backdriving method, which include solutions to problems of kinematic singularities, variations of muscle moment arms, and muscle saturation. I will extend the algorithm to include the control of system impedance (stiffness or compliance) as well as position and effort. Finally, I will test the biological plausibility of the control scheme by comparing model predictions with published experimental data.

4.1 Previous Work

In general a biological limb will have more degrees of freedom at the joints than are needed for a particular positioning task. In some cases, the workspace may impose additional hard constraints which which will determine the allowable values for the free degrees of freedom. For instance, an obstacle in the workspace may preclude certain limb configurations which would otherwise achieve the desired endpoint position. When such constraints are not present, the control system is free to choose any of the allowable configurations.

Bernstein observed that the frog hindlimb is redundant with respect to the spinal

wiping reflex [4]. To reach a particular location on the body in order to remove a noxious stimulus, the limb may assume one of many different joint configurations. Feldman and colleagues observed that the spinal frog retains the ability to adapt the selection of joint configuration for trials to the same target location. They use the term *motor equivalence* to describe different kinematic behaviors which accomplish the same task [18, 3].

In our laboratory, the issue of kinematic redundancy has been examined for the spinal frog as well. We observed that, while the spinal frog may switch between discrete motor equivalent strategies for a given stimulus location, there was little continuous variation between joint configurations for a given approach. It was suggested that the free degrees of freedom for the task were exploited in order to simplify the computational complexity of the inverse kinematics problem. Due to the system redundancy, a simple linear relationship between the target location and each joint angle is sufficient to accomplish the task [23].

In robotics the resolution of kinematic redundancy is an active area of research. A popular solution to the problem is to use the excess degrees of freedom available in the manipulator to optimize control in terms of secondary performance criteria. Numerous optimization criteria have been proposed to resolve the extraneous degrees of freedom, including minimizing joint velocities [37], avoiding joint limits [39], and minimizing torque loads [32]. It has also been demonstrated that the choice of joint configuration can be used to modify the effective endpoint impedance of the limb [31].

The above examples fit into a conceptual framework in which movement *planning* and *execution* are computed separately and sequentially [33, 25]. A desired trajectory of joint angles is computed (perhaps in real time) and then fed to a control system which ensures that the manipulator follows this plan. An alternative strategy is to plan the movement in task coordinates only, and allow the controller to determine the joint configurations as the movement progresses. Such a strategy has been used to successful control a redundant robot [28]. The Jacobian (J_f^T) of the forward model is used to translate positional errors at the tip directly into torque commands at the joint. Inversion of the non-square Jacobian matrix is not needed. By appropriately

selecting the control law for the endpoint, this strategy can also be used to avoid workspace obstacles and singularities. Control laws such as these have been proposed for the control of biological motor systems [43].

Another approach might be to learn the inverse kinematic solutions necessary to accomplish a given task. Jordan has proposed a learning algorithm in which incremental adjustments are made in articulatory (joint) space in response to errors generated in task space [36]. Errors from one trial are used to improve the performance in the next attempt. In this model, the task level errors are translated into joint level corrections, again through the forward model of the system.

Redundancy with respect to force production is more of an issue for biological control systems than it is for artificial systems. Mechanical linkages are usually designed with only one actuator per joint. Recently, however, redundancy in terms of force has become an issue due to the development of tendon driven robot arms and hands [34].

For biological systems, the means by which forces and torques are distributed among the various muscles of the limb is unknown. Bernstein suggested that the CNS must lump muscles having similar actions into single control entities (synergies), thus reducing the number of available degrees of freedom. Experimental evidence shows, however, that rigid coupling of the activations of different muscles is rare when the muscles are observed performing different tasks or operating under different conditions. The concept of a *task group* [40] by which parts of different muscles (i.e. motor units) are controlled as single units preserves the idea of a classical muscle synergy, but the question remains as to how these synergies are defined and activated for different motor tasks.

A number of optimization criteria have been proposed to describe the how the CNS resolves redundancy with respect to muscle force. These include minimizing a weighted sum of forces and torque [56, 52], minimizing energy [24], minimizing fatigue [16], and maximizing endurance [13]. Another approach has been to relate the active coordination of muscles to the afferent sensory feedback generated by the muscles [51, 22].

This chapter analyses a new strategy for the control of redundant motor systems, called *backdriving* [46]. Under the backdriving model the complementary problems of resolving redundancy with respect to positions and efforts are combined under a single computational framework. The generation of a particular control pattern is based on the passive mechanical properties of the mechanism, providing a natural solution to the problem of motor system indeterminacy. By incorporating the mechanical properties of the motion execution system into the planning of the movement, certain problems associated with other control strategies, such as kinematic singularities and joint limits, can be avoided.

4.2 Control Update Algorithm

The motions of a mechanical system made up of elastic elements are well defined for passive interactions between the system and the environment. For instance, a redundant arm can be controlled by placing springs across each of the joints. If an external force displaces the endpoint of the arm to a new position, the joints will settle into a configuration which minimizes the amount of potential energy stored in the springs (provided that the system is stable, see Chapter 3). Similarly, if several springs act around a single joint, a change in torque imposed by the environment will cause a shift in the position of the joint. At the new position the torque will be distributed to each of the elements, again so as to minimize the sum of the potential energies stored in each of the springs. By obeying fundamental physical laws, a passive elastic system in effect resolves redundancy by minimizing the total potential energy stored in the system.

Control of a redundant system requires a solution to the inverse of the passive motion problem. What is the active change needed in each element which will produce a desired change in output at the endpoint? Under the proposed backdriving algorithm, the active change in each element is computed based on the response to an equivalent passive change imposed by the environment. To illustrate the concept, I will apply the algorithm to a simple linear system. Subsequently I will derive the

equations necessary to compute the solution for arbitrary non-linear systems.

4.2.1 Example: A Linear Redundant System

Consider the system of linear springs shown in Figure 4-3a. Each spring obeys Hooke's law, and each spring has a control input which determines the rest length of the spring. The behavior of each spring is described by the equation

$$f_i = k_i(x_i - u_i).$$

The sensitivity of the force in each spring to changes in input is given by

$$\sigma_i \triangleq \frac{\partial f_i}{\partial u_i} = -k_i.$$

If the stiffness is non-zero, a desired change in force Δf_i can be achieved by a change in input:

$$\Delta u_i = -\sigma_i^{-1}\Delta f_i = k_i^{-1}\Delta f_i. \tag{4.1}$$

In this example the goal is to compute a change in inputs which will produce a desired change in endpoint position ΔX without changing the net output force F_0. Since there are more elements than free degrees of freedom at the endpoint, this problem is ill-posed. Conceptually, the proposed control algorithm resolves the indeterminacy as follows: If the endpoint of the system is passively displaced to the new desired position $(X_0+\Delta X)$, the system will settle to a configuration consistent with a minimum change in potential energy(Figure 4-3b). Each spring will experience a change in output force due to the passive displacement. The control update is computed by equation 4.1 so as to cancel the change in force in each element. Because the system is linear, the net output force will return to its initial value F_0 (Figure 4-3c).

4.2.2 Problems with Non-Linear Systems

When the system is non-linear, the solution cannot be so simple. The problem is demonstrated by the mechanism shown in Figure 4-4. As the joint angle varies, the

Backdriving Algorithm

a. Start at the initial desired force.

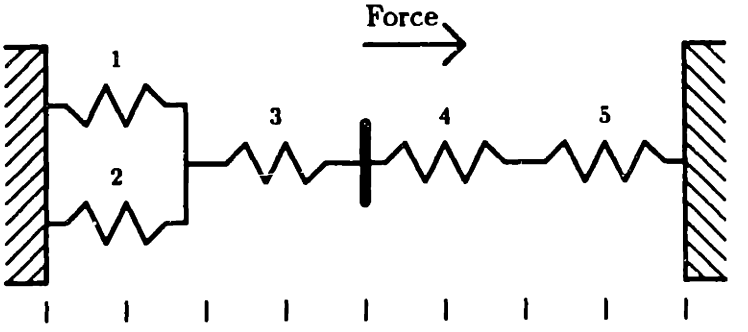

b. Displace to the new desired position.

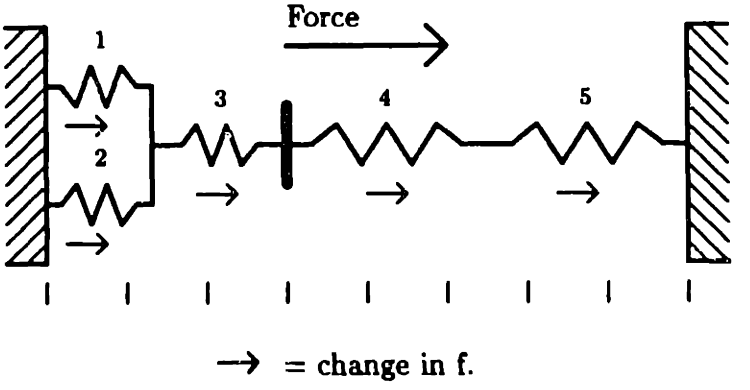

c. Update control inputs to cancel changes in f.

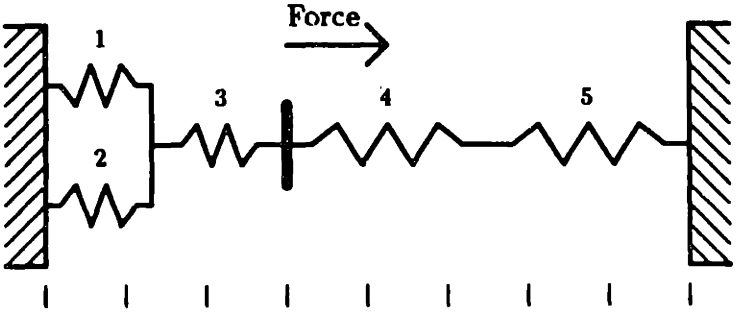

Figure 4-3: Control of a linear redundant system.

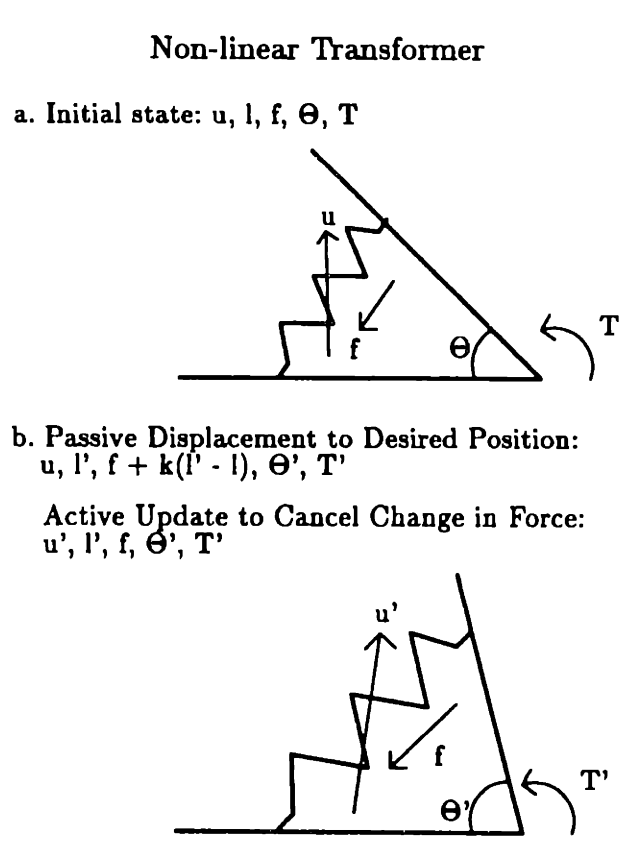

Figure 4-4: Effect of changing moment arm.

torque around the joint changes due to both the change in spring force and the change in moment arm. Applying the simple algorithm described above, after the passive displacement and active control update the force in the spring will be restored to its original value. The torque, however, will not be restored, due to the change in moment arm (Figure 4-4b). The final torque value is the product of the original spring force and the new moment arm. In the derivation of the control algorithm that follows, accommodation of changing moment arms will be a significant issue.

4.2.3 Solutions for General Non-Linear Systems

Two fundamental operations must be defined in order to control the position and effort of a mechanical device. It is necessary to compute a change in input that

will achieve a desired change in position at constant effort, or compute a change in input which produces a change in effort at a constant position. Compound changes in both position and effort can be achieved by sequential application of these two basic functions.

The control solution for a system of arbitrary complexity can be computed recursively using the same modular structure that was used to model elastic systems (Chapter 2). The two basic operations are defined as differential relationships between positions or efforts and inputs:

$$\begin{aligned} du &= \pi dp \\ du &= \psi de. \end{aligned}$$

where in general du, dp and de are vectors and π and ψ are matrices. Causality constraints may preclude the direct computation of π or ψ. In these cases, the stiffness or compliance of the element can be used to transform from one computation to the other. For stiffness and compliance elements we have, respectively:

$$\begin{aligned} du &= \pi \frac{\partial p}{\partial e} de \\ \psi &= \pi c \end{aligned}$$

$$\begin{aligned} du &= \psi \frac{\partial e}{\partial p} dp \\ \pi &= \psi k. \end{aligned}$$

The control law is computed for compound elements from the known relationships for each of the component elements and from the mechanical properties of the junction elements.

Primitive Elements

It is assumed that at least one of the two sensitivity functions is known for each primitive element in the system:

$$\sigma_e \triangleq \frac{\partial e}{\partial u}$$
$$\sigma_p \triangleq \frac{\partial p}{\partial u}.$$

For a primitive stiffness element, the control update relationships are

$$\psi = \sigma_e^{-1} \tag{4.2}$$
$$\pi = \sigma_e^{-1} k. \tag{4.3}$$

For a compliance element:

$$\pi = \sigma_p^{-1} \tag{4.4}$$
$$\psi = \sigma_p^{-1} c. \tag{4.5}$$

Junctions

Junction elements combine the appropriate transformations from each component element to compute a change in input for each element. For a common position junction, the displacement in each element is the same for a change in the overall position dP. Since the efforts sum linearly, it is sufficient to cancel the change in effort in each element:

$$dU = \Pi \, dP$$
$$\Pi = \begin{bmatrix} \pi_1 \\ \pi_2 \\ \vdots \\ \pi_n \end{bmatrix}.$$

Since a common position junction is position causal, changes in effort must be transformed into changes in position via the compliance:

$$\Psi = \begin{bmatrix} \pi_1 C \\ \pi_2 C \\ \vdots \\ \pi_n C \end{bmatrix}.$$

By a similar argument, a common effort junction yields

$$dU = \Psi\, dE$$

$$\Psi = \begin{bmatrix} \psi_1 \\ \psi_2 \\ \vdots \\ \psi_n \end{bmatrix}$$

$$\Pi = \begin{bmatrix} \psi_1 K \\ \psi_2 K \\ \vdots \\ \psi_n K \end{bmatrix}.$$

Transformers

As pointed out in Section 4.2.2, straightforward application of the backdriving procedure would not produce the appropriate result for a non-linear stiffness transformation. The effect of changing moment arm must be accounted for when general, non-linear transformations are involved.

Consider a non-linear transformation with position causality. For an initial input u_0 and initial position P_0, the state of the system is given by

$$\begin{aligned} p_0 &= \mathcal{L}_r(P_0) \\ e_0 &= f(p_0, u_0) \\ E_0 &= J_r^T(P_0) e_0. \end{aligned}$$

For a small displacement in position P^*, the change in state is given by

$$\begin{aligned}
P &= P_0 + dP^* \\
p &= p_0 + J_r(P_0)dP^* \\
e &= e_0 + kJ_r(P_0)dP^* \\
E &= E_0 + KdP^* \\
&= E_0 + \left[J_r^T(P_0)kJ_r(P_0) + \frac{\partial J_r^T(P)}{\partial P}e_0\right]dP^* \\
&= J_r^T(P_0)e_0 + J_r^T(P_0)kJ_r(P_0)dP^* + \frac{\partial J_r^T(P)}{\partial P}e_0\,dP^* \\
&= J_r^T(P_0)e + \frac{\partial J_r^T(P)}{\partial P}e_0\,dP^*.
\end{aligned}$$

Applying the input update rule so as to cancel the change in element effort e:

$$\begin{aligned}
du &= \pi dp \\
&= \pi J_r(P_0)dP^* \\
e &= e_0 \\
E &= J_r^T(P_0)e_0 + \frac{\partial J_r^T(P)}{\partial P}e_0\,dP^*.
\end{aligned}$$

Now impose the condition that the output effort effort E_1 must be equal to the initial effort E_0:

$$\begin{aligned}
E_1 &= E_0 \\
&= E - \frac{\partial J_r^T(P)}{\partial P}e_0\,dP^* \\
P_1 &= P - C\frac{\partial J_r^T(P)}{\partial P}e_0\,dP^* \\
&= P_0 + dP^* - C\frac{\partial J_r^T(P)}{\partial P}e_0\,dP^* \\
dP &= \left[I_n - C\frac{\partial J_r^T(P)}{\partial P}e_0\right]dP^*.
\end{aligned}$$

where I_n represents the identity matrix of appropriate dimensions. By imposing a displacement dP^* and applying the input update rule a displacement of dP with zero

change in effort has been achieved. The dP^* required to produce a desired dP is

$$\begin{aligned} K\,dP &= \left[K - \frac{\partial J_r^T(P)}{\partial P} e_0\right] dP^* \\ dP^* &= \left[K - \frac{\partial J_r^T(P)}{\partial P} e_0\right]^{-1} K\ dP. \end{aligned}$$

For a non-linear transformation, the change in input which will achieve a desired change in position is given by

$$\begin{aligned} du &= \Pi\ dP \\ &= \pi J_r(P)\ dP^* \\ &= \pi J_r(P) \left[K - \frac{\partial J_r^T(P)}{\partial P} e_0\right]^{-1} K\ dP. \end{aligned}$$

Simplifying, using equation 2.7, the control input update rule for a non-linear stiffness transformer is

$$\Pi = \pi J_r(P) \left[J_r^T(P) k J_r(P)\right]^{-1} K \tag{4.6}$$

$$\begin{aligned} \Psi &= \Pi C \\ &= \pi J_r(P) \left[J_r^T(P) k J_r(P)\right]^{-1}. \end{aligned} \tag{4.7}$$

Note that $J_r^T(P)kJ_r^T(P)$ is defined by equation 2.9 to be the *intrinsic* stiffness of the mechanism. That is, it is the stiffness that would be observed for the mechanism if all the forces and torques acting on the system were zero. Using this definition, the relationship between change in position and input becomes

$$\begin{aligned} \Pi &= \pi J_r(P) C_{intrinsic} K \\ \Psi &= \pi J_r(P) C_{intrinsic}. \end{aligned}$$

By a similar argument, the backdriving solution for a compliance transformer with effort causality is derived as follows: The goal is to compute a change in input which

produces a desired change in effort dE. Beginning with the mechanism in an initial stable state in which

$$\begin{aligned} e_0 &= J_f^T(p_0)E_0 \\ p_0 &= g(e_0, u_0) \\ P_0 &= \mathcal{L}_f(p_0). \end{aligned}$$

A small change in effort at the endpoint dE yields a displacement in the element position p:

$$\begin{aligned} E &= E_0 + dE \\ P &= P_0 + J_f^T(p_0)\ dp \\ p &= p_0 + dp \\ e &= e_0 + J_f^T(p_0)\ dE + \frac{\partial J_f^T(p_0)}{\partial p} E_0\ dp. \end{aligned}$$

Compute a change in input to cancel the change in element position:

$$\begin{aligned} dP &= C\ dE \\ J_f(p_0)dp &= J_f(p_0)\left[k - \frac{\partial J_f^T(p_0)}{\partial p} E_0\right]^{-1} J_f^T(p_0)\ dE \\ dp &= \left[k - \frac{\partial J_f^T(p_0)}{\partial p} E_0\right]^{-1} J_f^T(p_0)\ dE \\ du &= \pi dp \\ &= \pi\left[k - \frac{\partial J_f^T(p_0)}{\partial p} E_0\right]^{-1} J_f^T(p_0)\ dE, \end{aligned}$$

leaving the system in a consistent state:

$$\begin{aligned} E_1 &= E_0 + dE \\ P_1 &= P_0 \\ p_1 &= p_0 \end{aligned}$$

$$
\begin{aligned}
e_1 &= e_0 + J_f^T(p_0)\, dE \\
&= J_f^T(p_0)E_0 + J_f^T(p_0)\, dE \\
&= J_f^T(p_0)E_1.
\end{aligned}
$$

The control update relationships for a compliance transformer are

$$\Psi = \pi \left[k - \frac{\partial J_f^T(p_0)}{\partial p} E_0 \right]^{-1} J_f^T(p_0)\, dE \tag{4.8}$$

$$\Pi = \pi \left[k - \frac{\partial J_f^T(p_0)}{\partial p} E_0 \right]^{-1} J_f^T(p_0) K\, dP. \tag{4.9}$$

4.2.4 Backdriving as a Pseudo-Inverse

The computation of a change in posture from a change in input is a well-posed problem. There exist analytical solutions to the problem of computing the changes in position or effort resulting from a given change in input. For a compound element formed by a stiffness element and transformer, the relationship between effort and force at a constant position is given by

$$
\begin{aligned}
de &= \sigma_e du \\
dE &= J_r^T(P)\, de \\
&= J_r^T(P)\sigma_e du.
\end{aligned}
$$

The inverse problem, computing a change in input for a desired change in effort dE', is ill-posed since, in general, $J_r^T(P)\sigma_e$ is non-square and therefore non-invertible. Using the backdriving algorithm (equations 4.3 and 4.7) to substitute for du, it can be seen that the backdriving relationship forms a stiffness weighted pseudo-inverse for $J_r^T(P)\sigma_e$:

$$
\begin{aligned}
dE &= J_r^T(P)\sigma_e \left(\sigma_e^{-1} k\right) \left(J_r(P) \left[J_r^T(P) k J_r(P) \right]^{-1} \right) dE' \\
&= \left(J_r^T(P) k J_r(P) \right) \left[J_r^T(P) k J_r(P) \right]^{-1} dE' \\
dE &= dE'.
\end{aligned}
$$

The pseudo-inverse minimizes the quadratic form $de^T kde$, which corresponds to the minimization of the change in potential energy.

4.3 Properties of the Backdriving Algorithm

The mechanical structures of biological motor systems are intrinsically non-linear. One example is the action of a muscle around a joint. The moment arm by which the muscle exerts torque around the joint is dependent on the position of that joint. Another example is that of muscle saturation. Muscles cannot push, nor can they produce force above a certain maximum. Because of these non-linearities, a given change in control input can have widely different effects on the overall behavior of the system, depending upon the initial state of the components.

The backdriving algorithm provides a solution to the problem of computing a change of control input in order to cause a desired change in the state of the system. Because the solution is based on both the Jacobians of the geometrical transformations and on the elastic properties of the actuators, the non-linearities of the system are naturally accommodated by the control strategy. The following simulation examples will illustrate how the backdriving algorithm handles changing moment arms and muscle saturation.

4.3.1 Changing Moment Arms

Consider two identical spring-like muscles acting around a single joint as shown in Figure 4-5. The muscles obey the control law

$$f_i = k(l_i - (l_0 - u_i)).$$

Thus, the input to a muscle determines the rest-length of the spring. An increase of input u_i generates a decrease in rest-length. At constant length, this will cause an increase in muscle tension.

As the position of the joint changes, the moment arms for each of the muscles

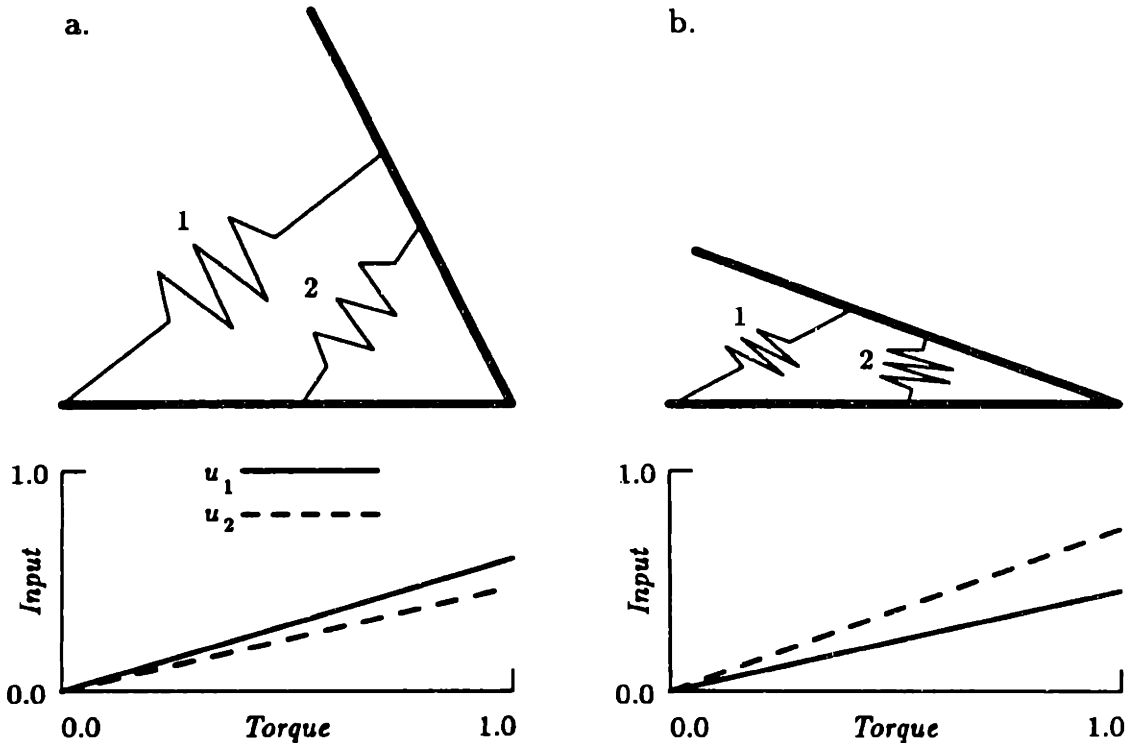

Figure 4-5: Muscle effectiveness affects muscle activity for the backdriving algorithm. The relative activations of muscles 1 and 2 change as the moment arms change.

change as well. Figure 4-5 shows the joint in two positions. In position a, muscle 1 has a greater mechanical advantage for producing torque than does muscle 2. At position b, however, the relative effectiveness of these two muscles is reversed. The backdriving algorithm has been applied to the structure for each of these two positions in order to produce one unit of flexion torque. The modifications of control input predicted by the algorithm are shown in the figure. In position a, the change in input to muscle 1 is larger than the change for muscle 2. For position b, the input change for muscle 1 is decreased, with muscle 2 contributing more to the total production of torque. This illustrates a basic property of the backdriving algorithm: as an actuator becomes more effective in producing an output effort, the contribution of that actuator increases relative to other effort producing elements in the system.

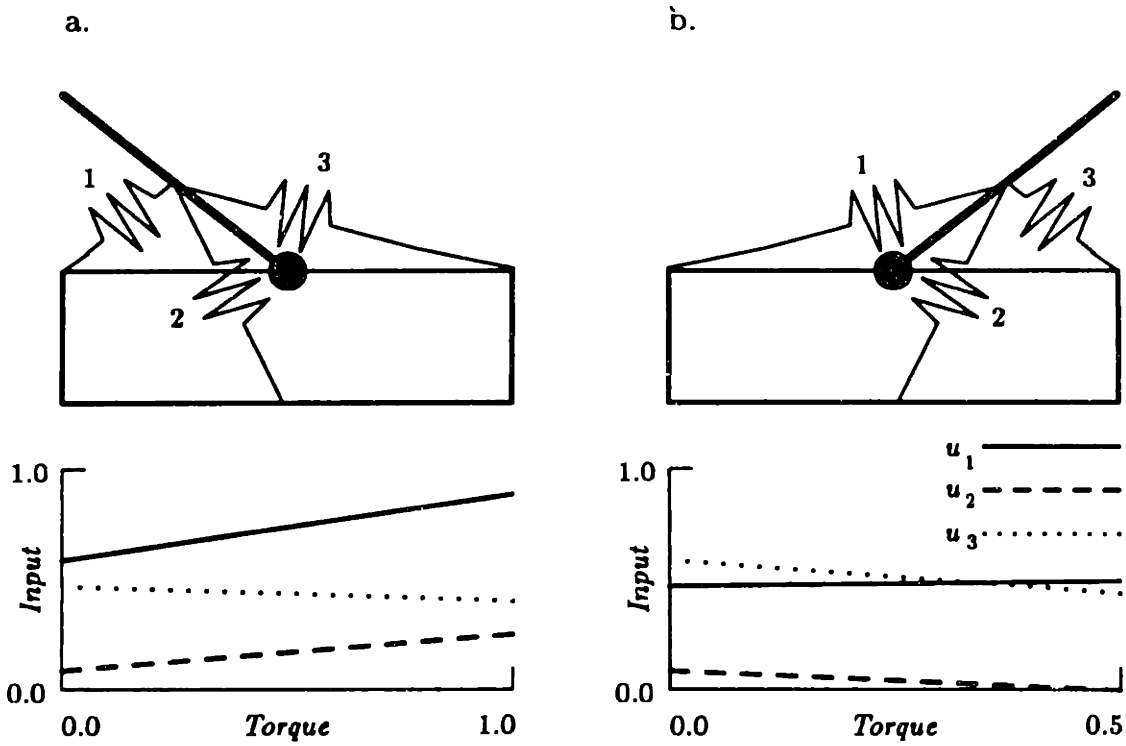

Figure 4-6: Defining synergies through backdriving.

4.3.2 Synergistic Behavior

Figure 4-6 demonstrates how synergies are defined by the backdriving algorithm. In position a, muscles 1 and 2 both act to flex the limb, while muscle 3 is an extensor. In position b, muscle 1 is the only flexor, while muscles 2 and 3 act to extend the limb. The change in action of muscle 2 is reflected in the Jacobian of the joint angle to muscle length transformation at each of these positions. In position a, the value of the Jacobian will be positive for muscles 1 and 2, and negative for muscle 3. At position b, the sign of the Jacobians is unchanged for muscles 1 and 3, but the Jacobian for muscle 2 is now negative.

The computed input for a change in joint torque is shown under each figure. At position a, muscles 1 and 2 act synergistically, while at position b muscles 1 and 2 are antagonists and muscle 3 acts synergistically with muscle 2. Under the backdriving algorithm, synergies are defined by the passive mechanical properties of the system:

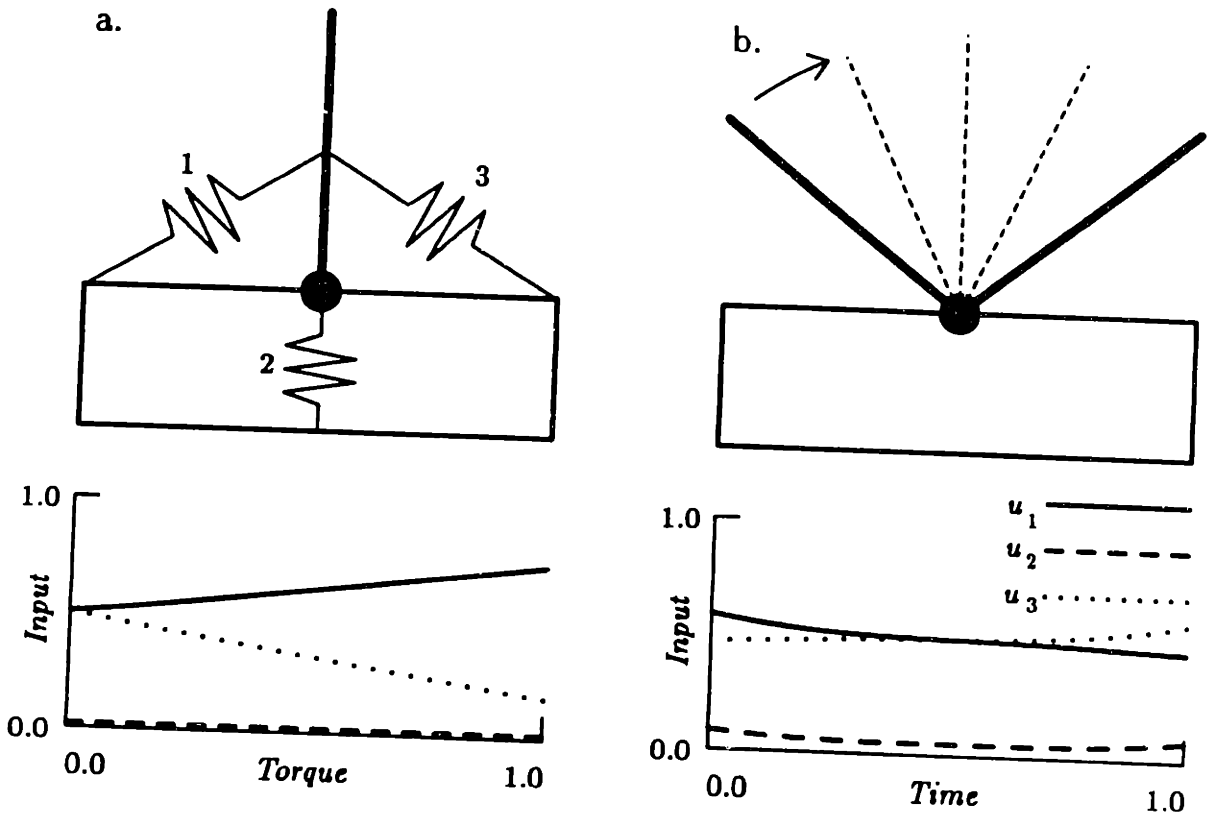

Figure 4-7: Passive driving through kinematic singularities.

Elements which respond in the same manner to a passive displacement of the system act as synergists during active control of the system.

4.3.3 Kinematic Singularities

The same mechanism is used to illustrate another feature of the backdriving algorithm in Figure 4-7. For the position of the joint shown in figure 4-7a, muscle 2 is at a kinematic singular point. Small displacements around this point generate no change in muscle length. Similarly, the muscle can contribute no torque at this position. At positions near the singular point, producing small changes in torque with muscle 2 would require very large changes in muscle input. The backdriving algorithm accommodates kinematic singularities of this sort, again due to its dependence on the Jacobian of the transformations. As the limb approaches the singular point for a

particular muscle, the Jacobian of that muscle approaches zero. Provided that there are other muscles acting on the joint which are not near singularities, the muscle in question is not required to contribute to the production of movement or torque at this point. Under the backdriving algorithm, actuators are passively driven through kinematic singularities (see Figure 4-7b).

4.3.4 Muscle Saturation

The force produced by a muscle cannot be modulated over an infinite range. Muscles cannot push, therefore the minimum tension which can be generated in a muscle is zero. Similarly, muscles have maximum activation levels, above which no additional force can be generated. A system which controls actuators having these properties should not try to drive the elements outside the effective range of activities.

The backdriving algorithm effectively handles actuator saturation as well. When a muscle saturates, the stiffness of the muscle drops to zero. A muscle acting in this region of operation undergoes no change in muscle force in response to a passive displacement of the system. Thus, the backdriving algorithm computes a zero change in input for the actuators in this state.

Figure 4-8 demonstrates the backdriving principle for a model of muscle which exhibits saturation. In the initial state, both of the muscles are active. Each of the muscles contributes to the change in output torque by changing its control input. As a muscle reaches a limit in force production, its stiffness goes to zero. Further increases in torque require no additional change in activation for that muscle. The rate of input change for muscles which are still active increases, to compensate for the lack of change in the saturated elements.

4.4 Control of Stiffness

The backdriving algorithm provides a means of controlling effort and position only. As was demonstrated in Chapter 3, control of a limb requires consideration of the endpoint impedance as well. Due to non-linear transformations in the system, limb

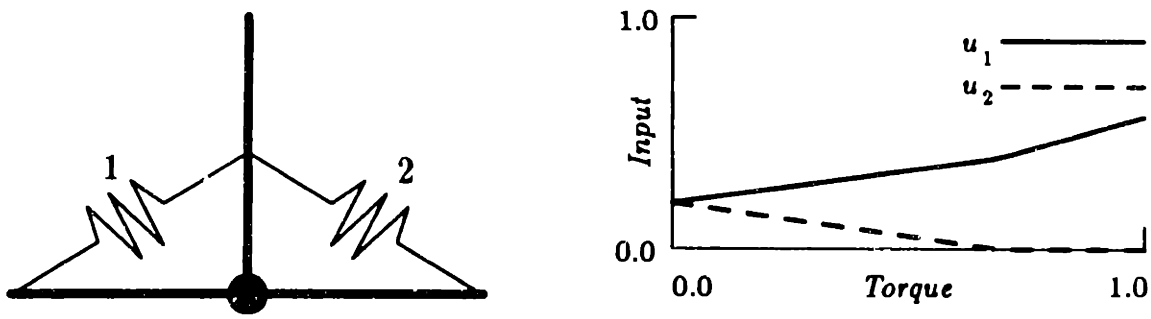

Figure 4-8: Passive driving of saturated muscles.

stiffness will change as a function of limb configuration or output force.

4.4.1 Passive Stabilization

The backdriving algorithm is compatible with the passive stabilization scheme proposed in Chapter 3. Figure 4-9 shows a model of a planar two-joint arm having six muscles. If the muscles are described by an exponential relationship between force and length, the backdriving algorithm produces stable endpoint behavior for the six muscle arm (Figure 4-10).

4.4.2 Active Impedance Modulation

The passive changes in actuator stiffness may be insufficient to meet the control constraints of the motor system. For instance, if the rate of stiffness increase versus force output is small, the passive strategy may not produce a change in joint stiffness sufficient to stabilize the load. Alternatively, it may be necessary to increase endpoint stiffness without changing endpoint force. Finally, the control system may wish to exert more precise control over the shape and orientation of the endpoint stiffness field. All of these cases would require active modulation of the actuator inputs to control the endpoint behavior.

Section 4.2.3 defined two basic operations for the control of a mechanical system: $du = \pi dp$, which computes a change in input to produce a desired change in position

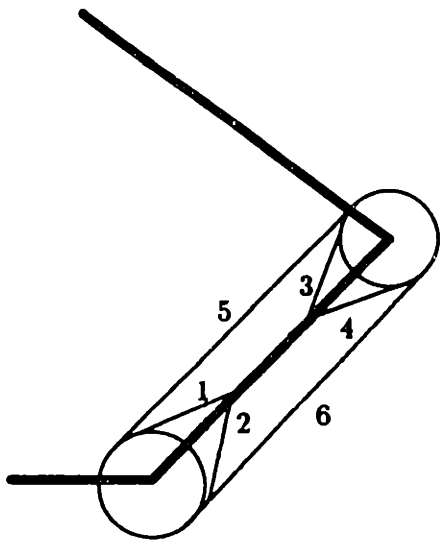

Figure 4-9: Model of planar two joint arm with six muscles.

at constant effort, and $du = \psi de$, which produces a change in effort at constant position. The goal of this section is to derive a third fundamental operation which produces a change in stiffness without affecting position or effort:

$$du = \kappa\, dk.$$

Consider a system that is redundant with respect to efforts: $u \in \mathcal{R}^m, e \in \mathcal{R}^n, m > n$. Provided that the control inputs have an effect on actuator stiffness ($\frac{\partial k}{\partial u} \neq 0$), the additional $m - n$ degrees of control freedom can be used to modulate the stiffness of the system.

Nullspace Input Changes

Given a transformation from control input to effort $\sigma_e = \frac{\partial e}{\partial u}$, let ψ be any pseudo-inverse relationship which maps a desired change in effort to a desired change in input. The backdriving algorithm provides a specific example of such a mapping, but the

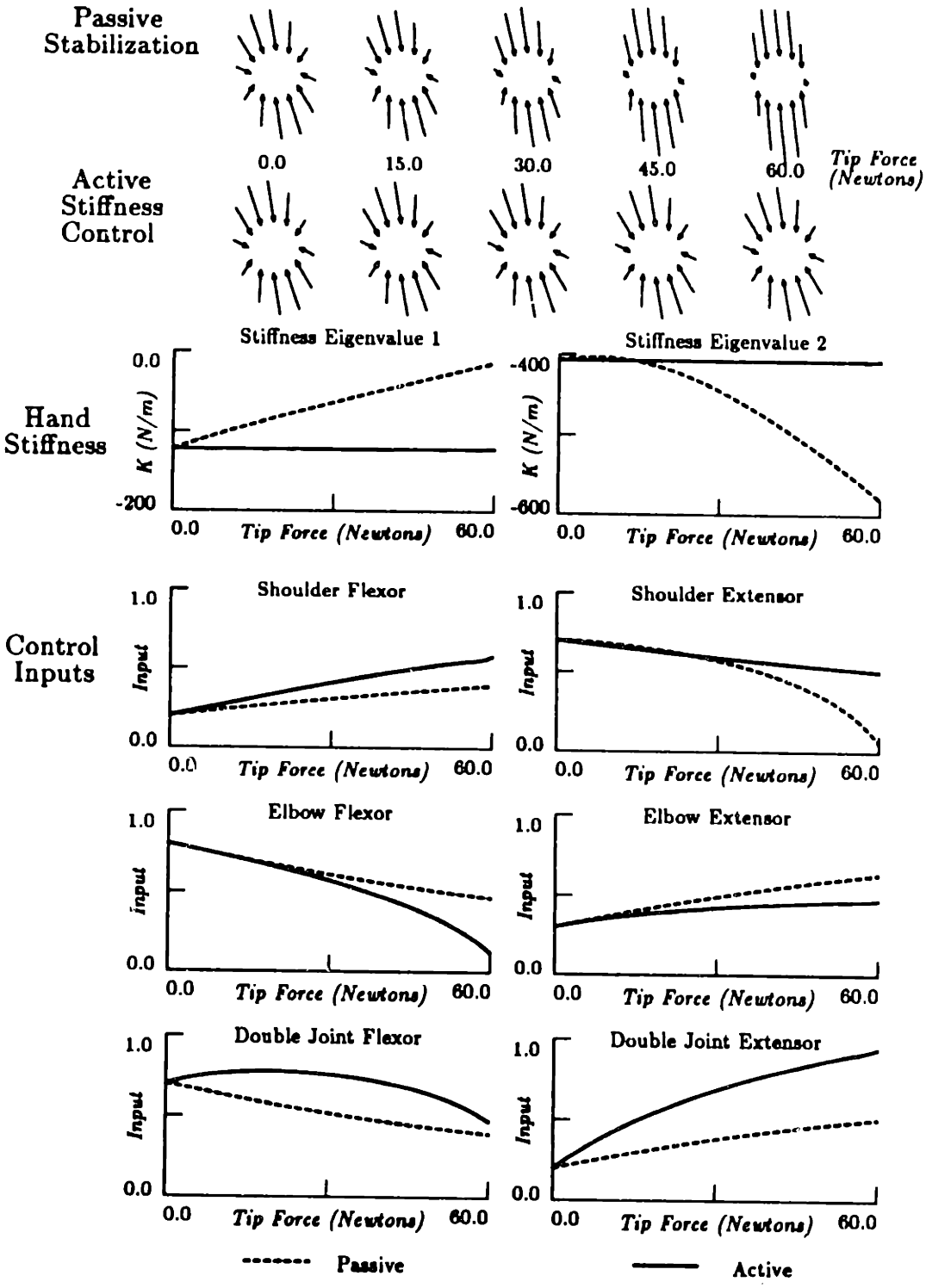

Figure 4-10: Control of stiffness for a six muscle arm.

following analysis applies to any inverse transformation which satisfies the condition

$$\sigma_e \psi = I_m.$$

The matrix ψ maps a desired change in effort to a particular change in input, from an infinite number of possible input changes. The more general solution can be given by the expression

$$du = \psi de + (I_n - \psi\sigma_e)u^*$$

where I_n is the nxn identity matrix and u^* is an arbitrary vector in $\mathcal{R}^n$ [37]. By varying the value of the vector u^*, all possible changes in input that will produce a given change in effort can be computed. The matrix $[I_n - \sigma_e\psi]$ projects the vector u^* into the null space of ψ. A change in input du' computed by the expression

$$du' = (I_n - \psi\sigma_e)u^*$$

will produce no change in the effort output of the system.

Control of Stiffness

In order to control the endpoint stiffness of a position causal element, it is necessary to know the relationship between the control input and the impedance of an element. First, consider the stiffness of an n dimensional system. The stiffness k is an $n \times n$ matrix. If the element behaves in a passive manner, the stiffness field must be conservative, and therefore the stiffness matrix is symmetric. Thus, the $n \times n$ stiffness matrix k has only $(n^2 + n)/2$ elements which can be controlled independently.

Let $\mathcal{S}(m)$ represent a matrix operator which produces a vector from the independent elements of the symmetric matrix m. A vector $\hat{k}$ can be defined which represents each of the independent elements of k. For example, if k is a two dimensional symmetric matrix,

$$k = \begin{bmatrix} a & b \\ b & c \end{bmatrix}$$

the vector $\hat{k}$ is the three dimensional vector

$$\hat{k} = S(k) = \begin{bmatrix} a \\ b \\ c \end{bmatrix}.$$

The sensitivity of an element effort and stiffness to changes in control input is assumed to be known for a primitive element having an n-dimensional control input:

$$\begin{aligned} \sigma_e &\triangleq \frac{\partial e}{\partial u} \\ &= \left[\frac{\partial e}{\partial u_1} \cdots \frac{\partial e}{\partial u_n} \right] \\ &\triangleq \left[\sigma_e^1 \cdots \sigma_e^n \right] \end{aligned}$$

$$\begin{aligned} \sigma_k &\triangleq \frac{\partial k}{\partial u} \\ &= \left[\frac{\partial k}{\partial u_1} \cdots \frac{\partial k}{\partial u_n} \right] \\ &\triangleq \left[\sigma_k^1 \cdots \sigma_k^n \right] \end{aligned}$$

where σ_e^n denotes the nth component of the row vector σ_e. For a common position junction with m elements the sensitivities are simply

$$\begin{aligned} \sigma_E &= \left[\sigma_{e_1}^1 \cdots \sigma_{e_1}^n \cdots \sigma_{e_m}^1 \cdots \sigma_{e_m}^n \right] \\ \sigma_K &= \left[\sigma_{k_1}^1 \cdots \sigma_{k_1}^n \cdots \sigma_{k_m}^1 \cdots \sigma_{k_m}^n \right] \end{aligned}$$

where $\sigma_{e_m}^n$ denotes the nth component of the sensitivity row vector σ_e for element m. The effort and stiffness sensitivities for a position causal transformer under conditions of constant position are

$$\sigma_E = \left[J_r^T(P)\sigma_e^1 \cdots J_r^T(P)\sigma_e^n \right]$$

$$\sigma_K = \left[\left(J_r^T(P)\sigma_k^1 J_r(P) + \frac{\partial J_r^T(P)}{\partial P} e_0\ \sigma_e^1\right) \cdots \left(J_r^T(P)\sigma_k^n J_r(P) + \frac{\partial J_r^T(P)}{\partial P} e_0\ \sigma_e^n\right)\right].$$

The sensitivity of the independent elements of k to the input is defined by

$$\sigma_{\dot{k}} \triangleq \left[\mathcal{S}(\sigma_k^1) \cdots \mathcal{S}(\sigma_k^n)\right].$$

A change in input produces a change in stiffness given by

$$d\dot{k} = \sigma_{\dot{k}}\ du.$$

If the change in input is first projected into the null space of ψ, the change in stiffness can be computed for which there is no change in effort:

$$\begin{aligned} d\hat{k}|_{de=0} &= \varsigma_{\dot{k}}\ du \\ &= \sigma_{\dot{k}}\left(I_n - \psi\sigma_e\right)\ du \\ \varsigma_{\dot{k}} &= \sigma_{\dot{k}}\left(I_n - \psi\sigma_e\right). \end{aligned}$$

A weighted pseudo-inverse can then be used to compute a change of input that will produce a desired change in stiffness at zero change in force:

$$\begin{aligned} du &= \kappa\ dk \\ &= \omega\varsigma_{\dot{k}}^T\left(\varsigma_{\dot{k}}\omega\varsigma_{\dot{k}}^T\right)^{-1}\ \mathcal{S}(dk) \end{aligned}$$

where ω is a diagonal matrix of weights. If $\omega = I_n$ the mapping κ produces a minimum norm change in input which will produce a desired change in endpoint stiffness. Another option would be to weight the contribution of each control input

by the force sensitivity:

$$\omega = \begin{bmatrix} \sigma_{e_1} & & 0 \\ & \ddots & \\ 0 & & \sigma_{e_n} \end{bmatrix}$$

which would tend to minimize the change in muscle force for a given change of stiffness.

Arbitrary changes in position, effort, and now stiffness can be computed by sequentially applying the three update rules:

$$\begin{aligned} u_{n+1} &= u_n + \pi\ dp \\ u_{n+2} &= u_{n+1} + \psi\ de \\ u_{n+3} &= u_{n+2} + \kappa\ dk. \end{aligned}$$

The control of stiffness can be applied to the six muscle arm described above. Figure 4-10 shows the changes in hand stiffness that occur when simple force backdriving is used with an exponential relationship between muscle length and force. Figure 4-10 also shows the same force task implemented with active control of stiffness in order to maintain a constant endpoint stiffness.

4.5 Model Predictions and Biological Data

The above sections have described an algorithm which can be used to control the posture and impedance of a redundant motor system. The question remains as to whether the backdriving algorithm can be considered as a model for the control of the human motor system. To test this hypothesis I will compare the change in muscle activations that would be predicted by the backdriving algorithm to the actual levels of activation measured in human subjects. This section will make use of data from a published study [10] in which the activation of muscles acting around two joints was measured during the production of torques in different directions.

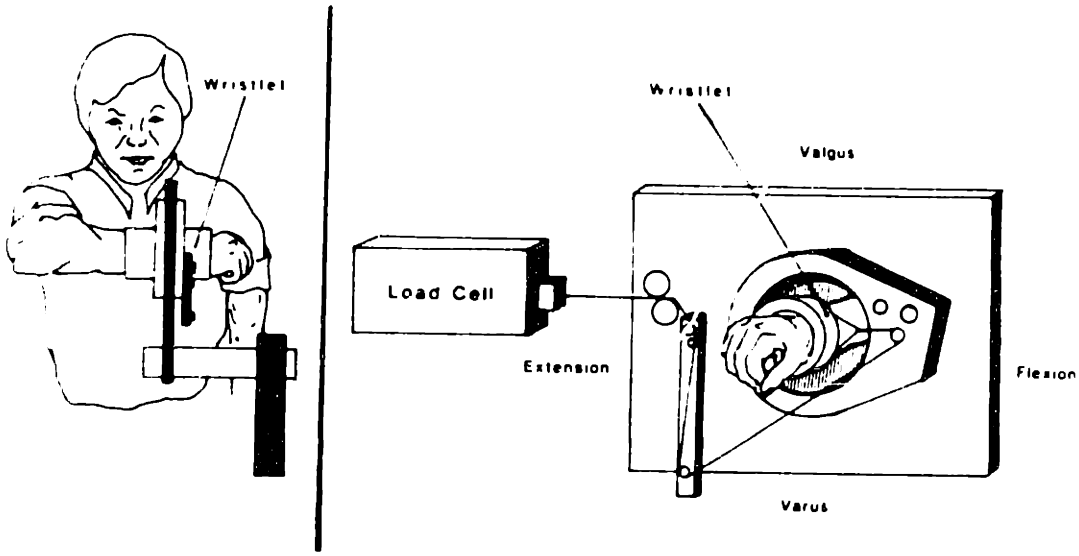

Figure 4-11: Torque measurement apparatus (from Buchanan, et. al. 1986 [10]).

4.5.1 Comparison with Buchanan Data

Buchanan and colleagues built an apparatus with which they could measure the torque generated by a subject around two joint axes of the arm (Figure 4-11). The torques which were measured acted to flex or extend the elbow, or to generate varus or valgus rotation around the axis of the humerus. While subjects were asked to generate specific target combinations of torque, intra-muscular electrodes were used to measure the electromyographic (EMG) signal from the muscles acting around these joints. (See the Buchanan paper [10] for details of the experimental procedure.) While the exact relationship between muscle activation and EMG is not known, this technique can be used to compare the relative activity of a given muscle during the production of torque in one direction versus another. The ability to make this comparison depends only on the condition that muscle force is a monotonically increasing function of EMG for a muscle at a fixed length. Quantitative comparison of the relative activation of two different muscles cannot be made based on EMG, but qualitative observations about patterns of muscle coordination can be made. It is possible to test for which directions of torque two muscles are concurrently active, and for which directions

they are not. In this way it is possible to assess the synergistic and antagonistic relationships generated by a group of muscles.

The data from the Buchanan experiments are displayed in the polar plots of Figures 4-12 and 4-13, as they were in the original paper. A data point is plotted at the tip of a vector, the direction of which corresponds to the direction of torque which was generated for that trial. The magnitude of the vector is proportional to the amount of EMG measured in a particular muscle during torque production in that direction. Data were collected from nine muscles (eight of which are shown), for torques generated in ten different directions and four different magnitudes. Data points for torques of the same magnitude are connected by solid lines in the figure.

Backdriving Predictions

Can the backdriving algorithm predict the patterns of muscle activations observed for this task? Knowledge of the muscle stiffness properties,and the muscle attachment geometries is necessary in order to compute the activations predicted by the backdriving algorithm. In 1981, An and colleagues measured the moment arms for the muscles acting around the elbow by serial sectioning cadaver arms [1]. In addition, they measured the cross-sectional area and rest-length of each muscle. From these measurements it is possible to estimate the relative stiffness properties for each muscle.

Stiffness Scaling

If one assumes that muscle sarcomeres each have identical stiffness properties, the stiffness of a muscle is directly proportional to the number of sarcomeres in parallel and inversely proportional to the number of sarcomeres in series. The cross-sectional area provides an estimate of the number of sarcomeres in parallel, while the rest-length corresponds to the number in series. Given a reference muscle with stiffness k_{ref}, cross-sectional area α_{ref} and rest-length λ_{ref}, the stiffness of another muscle k_i

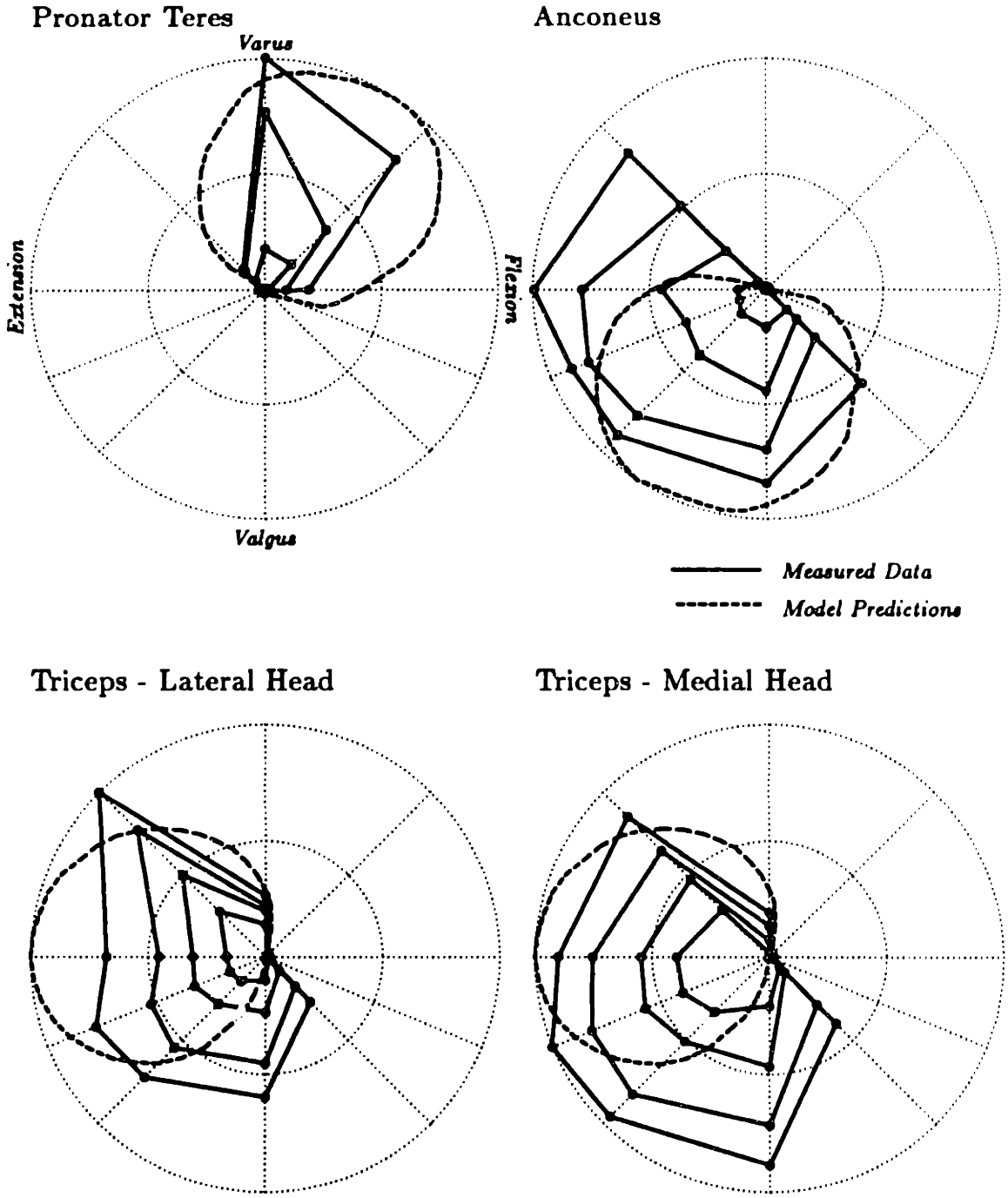

Figure 4-12: Comparison of Backdriving Model with EMG Data. EMG data is from Buchanan, et. al. 1986 [10].

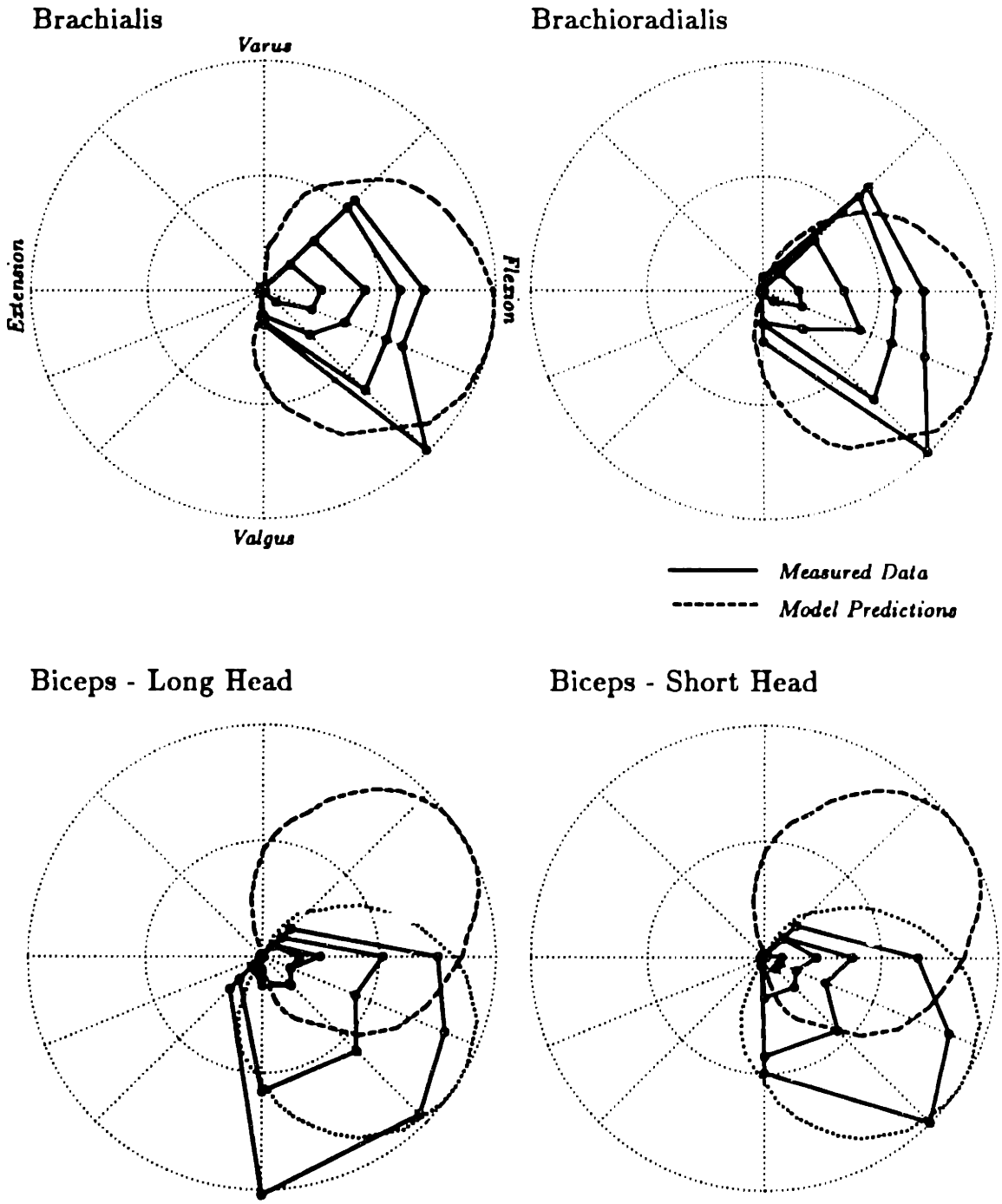

Figure 4-13: Comparison of Backdriving Model with EMG Data. EMG data is from Buchanan, et. al. 1986 [10].

Muscle	Moment Arm		Physiological Data		
	Flexion / Extension	Varus / Valgus	Cross Section α	Rest Length λ	Stiffness k
Brachialis	2.052	0.129	7.0	9.0	0.8
Brachioradialis	4.164	-0.182	1.5	16.4	0.09
Biceps - Long	3.431	1.133	2.5	13.6	0.18
Biceps - Short	3.431	1.133	2.1	15.0	0.14
Pronator Teres	1.646	1.528	3.4	5.6	0.61
Anconeus	-1.126	-1.762	2.5	2.7	0.93
Triceps - Lateral	-2.039	-0.027	6.0	8.4	0.71
Triceps - Medial	-2.039	-0.027	6.1	6.3	0.97
Triceps - Long	-2.039	-0.027	6.7	10.2	0.66
ECRL	2.871	-0.462	2.4	7.8	0.31
ECRB	2.871	-0.462	2.9	5.3	0.55
FCR	0.923	2.294	2.0	5.8	0.34
FDS	0.027	1.887	4.2	6.4	0.66
FCU	-1.326	1.611	3.2	4.8	0.66
ECU	-0.659	-2.873	3.4	4.5	0.76
EDC	0.443	-2.045	1.0	6.1	0.16

Table 4.1: Physiological data for elbow muscles (from An, et. al. 1981 [1]).

can be computed by scaling according to its geometrical parameters α_i and λ_i:

$$k_i = \frac{\alpha_i}{\alpha_{ref}} \frac{\lambda_{ref}}{\lambda_i} k_{ref}.$$

Since we are concerned only with relative stiffness values, the reference values can be set to unity in arbitrary units, yielding a simple formula for relative muscle stiffness:

$$k_i = \frac{\alpha_i}{\lambda_i}.$$

The physiological data from [1] and the computed stiffness values are shown in Table 4.1.

Model Predictions

The physiological data was used to generate a model of the human elbow with seventeen muscles. The backdriving algorithm was applied to the model to predict the

activation of each muscle for a given level of joint torque. The simulated procedure is based on the following model assumptions:

- **Constant Moment Arms:** Lacking specific data to the contrary, I assumed that each muscle acts with a constant moment arm for joint angles in the neighborhood of the tested posture:

$$\frac{\partial J_r^T(\theta)}{\partial \theta} = 0.$$

  Since $\frac{\partial J_r^T(\theta)}{\partial \theta}$ does not enter into the expression for ψ (Equation 4.7), this assumption has no effect on the results.

- **Constant Muscle Stiffness:** An active muscle (that is, a muscle which is producing force) is assumed to have a constant level of stiffness, i.e. force is a linear function of position. Muscles cannot push, therefore the stiffness of an inactive muscle is zero:

$$\frac{\partial f_i}{\partial l_i} = \begin{cases} k_i & f_i \geq 0 \\ 0 & \text{otherwise} \end{cases}.$$

- **Activation Equivalent to Muscle Force:** Since the length of each muscle is held constant for the task, the observed activation of the muscle was assumed to be simply the force generated by that muscle:

$$\text{EMG}_i = f_i.$$

Results

The predicted activations for each of the muscles included in the Buchanan study are plotted as dashed lines on the polar plots of Figures 4-12 and 4-13. The backdriving algorithm predicts three of the main features apparent in the measured EMG data. First, each muscle is broadly tuned with respect to the direction of torque production. Each muscle is active for a wide range of torque directions. Second, for a given

magnitude of torque load, both the model and the data show a unimodal pattern of activation level as the direction of the load is varied. Finally, the direction of maximum activation is predicted by the backdriving algorithm for each muscle. For six of the tested muscles, the predicted direction of maximum activation agrees with the experimental data.

The two heads of the biceps are the exception to the third finding. The anatomical data from [1] predicts that the biceps contributes to humeral rotation in the varus direction, while the EMG data shows that the biceps is active during valgus torque generation. Buchanan noted this anomaly as well and suggested that the An paper may be in error, citing additional evidence for a positive biceps moment in the valgus direction [10]. A brief experiment was performed in our laboratory to verify that the biceps is active when a valgus torque is produced. The biceps shows little activity during production of torque in the varus direction. If the sign of the varus/valgus moment arm was changed for the biceps, the backdriving algorithm would produce a much closer fit to the measured EMG data (shown as a dotted line in Figure 4-13), as is to be expected. This modification in the model parameters had no noticeable affect on the predicted activations for each of the other muscles.

On the other hand, the observed pattern of EMG activity can be more broadly tuned than predicted by the model, specifically in this case for the triceps. One possible explanation is that the CNS is actively controlling stiffness as described in Section 4.4.2. Co-contraction of the elbow flexors and extensors may be needed to maintain limb stability. Note also that the triceps acts at the shoulder as well as the elbow. The additional measured activity may be related to its function at this joint.

The Buchanan study illustrates a basic property of the human motor system. Muscle coordination is based on the mechanical properties of the system, and is not necessarily organized into fixed synergistic relationships. A muscle is most active when it is mechanically most effective. The backdriving algorithm predicts the same sort of behavior, and as such is a biologically plausible model for the control of biological motor systems.

4.6 Conclusions

The backdriving algorithm has been presented for the control of redundant motor systems. The control solution is derived from the passive elastic behavior of the mechanism, providing a natural basis by which motor system indeterminacies are resolved. By including the mechanical properties of the controller in the planning of movement, certain problems with system nonlinearities can be avoided.

In addition to controlling the position and force output of a limb, the CNS must control the limb impedance as well. An algorithm has been presented by which the excess degrees of freedom in the actuators can be used to modulate the limb stiffness at a given posture.

Backdriving is a biologically plausible model for the behavior of the human motor system. Predictions about muscle activations, based on the elastic properties of the muscles are in good agreement with observed biological behavior.

Chapter 5

Movement From Posture

Merton's hypothesis first brought forth the idea of *movement from posture*; the same neuro-muscular system which acts to control the stationary position of the limb (i.e. the stretch reflex) could be used, with appropriate modulation of the set point, to control movements as well. While Merton's original hypothesis has been rejected, the idea of movement from posture has not. The *equilibrium point* model for motor control, as first proposed by Feldman [18] is based on the same principle – – the muscles and reflexes acting around a joint form a feedback servo mechanism which acts to control the position of the limb. Under these models the CNS generates movements by specifying an appropriate reference signal to the servo control circuit.

An on-going discussion in the field of human motor control concerns feedforward versus feedback models of movement control. Does the CNS represent movements in dynamic terms, with explicit representations of the forces and torques required for a movement, or does the motor system rely on feedback only to generate the appropriate muscle forces from a central representation of the desired movement? This chapter address the question by examining quantitatively the performance of several feedback based control hypotheses. Can feedback control alone account for the observed behavior of the human arm?

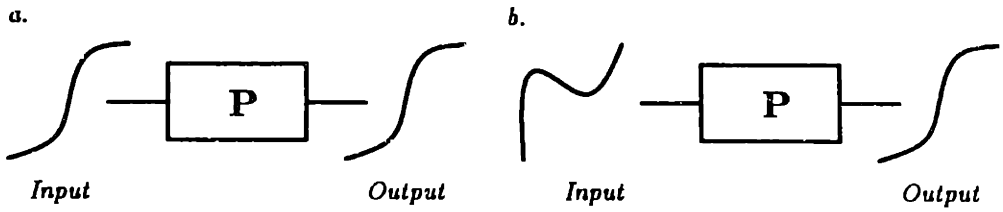

Figure 5-1: Definition of a servo. (a) meets the criteria, (b) does not.

5.1 Definition of a Servo

What exactly defines a servo system? "A servomechanism is an automatic device for controlling and correcting the performance of a mechanism."[1] Typically, the correcting aspect of the controller is achieved through feedback. The output of the system is compared with a reference input, and corrective control signals are generated accordingly. The interpretation of the term *automatic* may generate some ambiguity about the definition of a servo mechanism. To focus the ensuing discussion on the issue of feedforward versus feedback control, I will adopt a strict working definition of a servo which states: "A servomechanism is an automatic control system for which the input to the system is simply a representation of the desired system output." Figure 5-1 illustrates this point. The system in Figure 5-1a fits the definition of a servo, the system in Figure 5-1b does not. Appropriate control via circuit b requires knowledge of the system characteristics,thus requiring an element of feedforward control to achieve satisfactory performance.

5.2 Servo Models for Biological Motor Control

Can the human motor system be described as a servomechanism? There is no question that the human motor system employs feedback to control movements. Perturbations to movements and postures are effectively corrected for by the neuromuscular system. The question is, "To what extent does the peripheral motor system form a position

[1] Webster's Dictionary

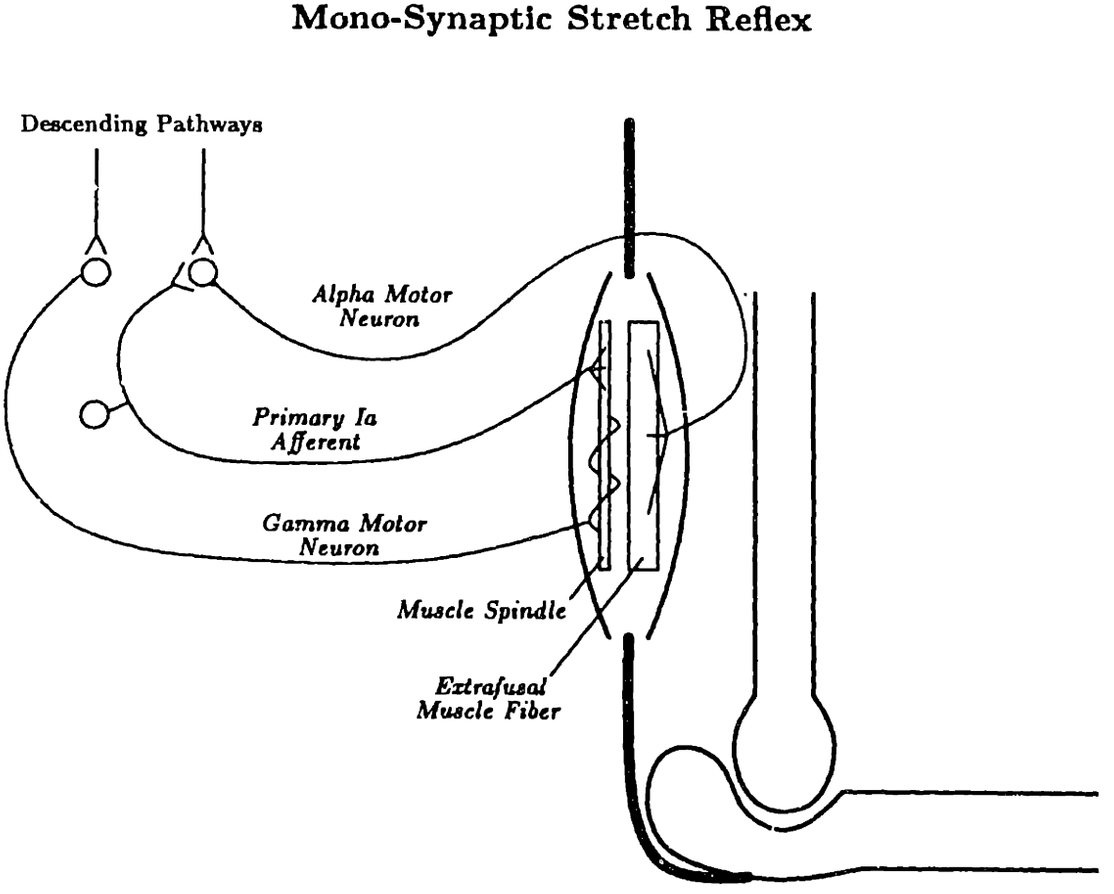

Figure 5-2: Neural circuitry for the stretch reflex.

servo for the control of movement?" Can feedback alone account for the movements, or must the CNS provide a feedforward component based on the dynamics of the desired motion?

5.2.1 Reflex Servo Hypothesis

The reflex servo loop proposed by Merton was an interesting hypothesis for the control of movement, based on feedback alone. The theory was based on the parallel alpha and gamma motor drives to muscles in the human motor system (Figure 5-2). Under this scheme, the gamma motor neurons would drive the muscle spindles through the desired trajectory of the limb. The error between the spindle movement and the actual muscle movement would generate the neural activity in the alpha motor

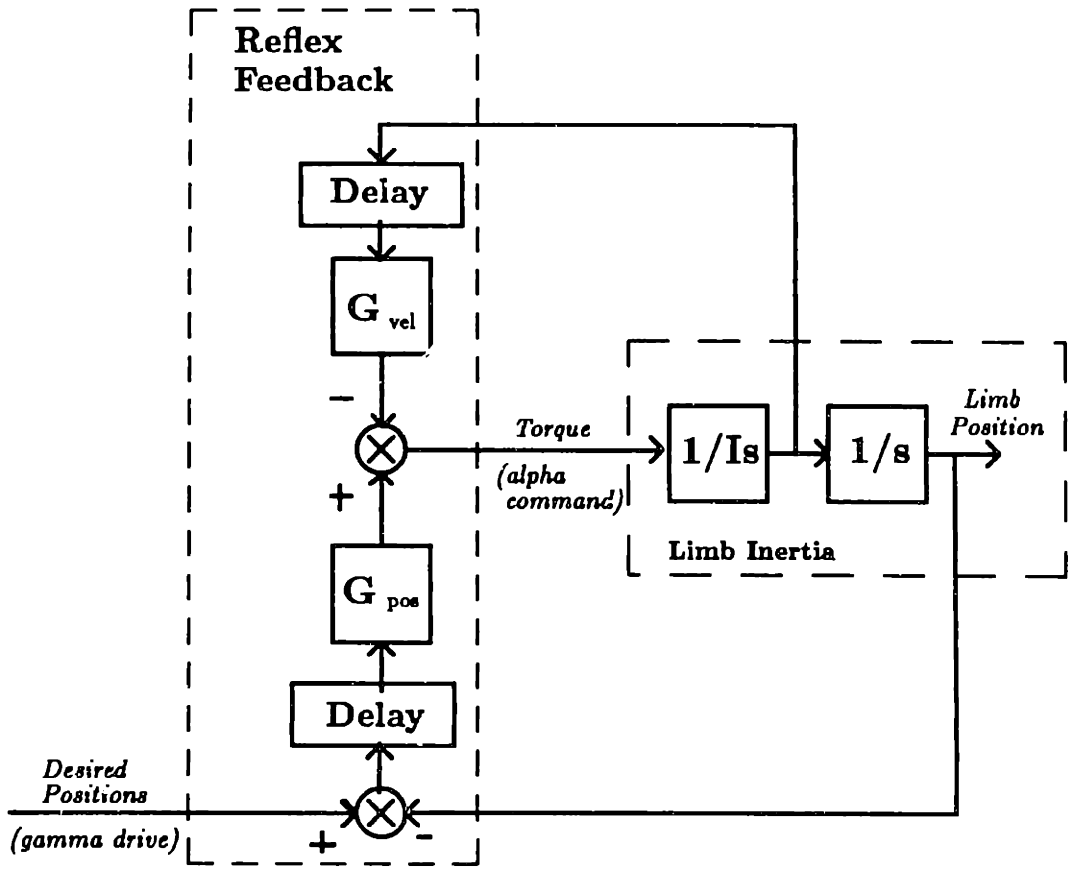

Figure 5-3: Merton's reflex servo control model.

neurons (via the monosynaptic spinal reflex) that actually drives the limb. This method is attractive from a computational point of view because it produces the desired movement without an explicit solution of the *inverse dynamics*. In order to produce a limb movement, the CNS commands a time series of positions for the muscle spindles via the gamma motor neurons. The muscle forces and resulting joint torques are generated ***implicitly*** by reflex feedback onto the alpha motor neurons. Figure 5-3 shows a block diagram representation of the Merton reflex servo model of motor control.

Experimental and analytical evidence does not support Merton's theory, however. Feedback loop delays are too long to allow for the stable operation of such a system. In addition, alpha and gamma motor units are known to become active simultaneously (alpha-gamma co-activation) at the initiation of movement [58]. The reflex servo

hypothesis would predict a slight lead in the activation of the gamma motor neurons. Alpha motor neurons would fire only after the stretch reflex signal had reached the spinal cord, a delay of approximately twenty milliseconds for the human arm. Finally, deafferented monkeys are known to be capable of directed movement of their limbs in the absence of reflex feedback [9, 8] This would not be possible if reflex feedback were the sole source of alpha motor activation.

5.2.2 Equilibrium Point Models

Alternatives to Merton's hypothesis are described by the equilibrium point models for motor control. Under these models the mechanical properties of muscles and the myotactic reflexes generate equilibrium positions for the limb, at which the net force and torque acting on the limb is zero. Movements are generated as shifts in the equilibrium posture of the limb. The equilibrium point hypotheses are in better agreement with the experimental data, yet they maintain the computational simplicity of Merton's reflex servo hypothesis.

Currently there are two formulations of the equilibrium point hypothesis under consideration. The α model, as proposed by Bizzi, Hogan and colleagues [9, 5, 30, 31] relies on the spring-like properties of muscles to generate the forces required to cause movement. Feldman's λ model, on the other hand, emphasizes the combined role of stretch reflexes and muscle elastic properties for producing movements of the limb [18, 19]. Each model will be considered separately in the following sections.

α Model

The α equilibrium point model is based on the mechanical properties of muscles. As a muscle is stretched, the tension in the muscle increases [55, 26]. The muscle acts like a spring for passive displacements. For two muscles acting in opposition around a joint there exists an equilibrium position at which the net torque acting on the joint is zero. The location of the equilibrium point is determined by the rest lengths and relative stiffness of the two muscles, which are in turn determined by their activation levels [7, 30]. If the limb is displaced from this position, the spring-like properties of the

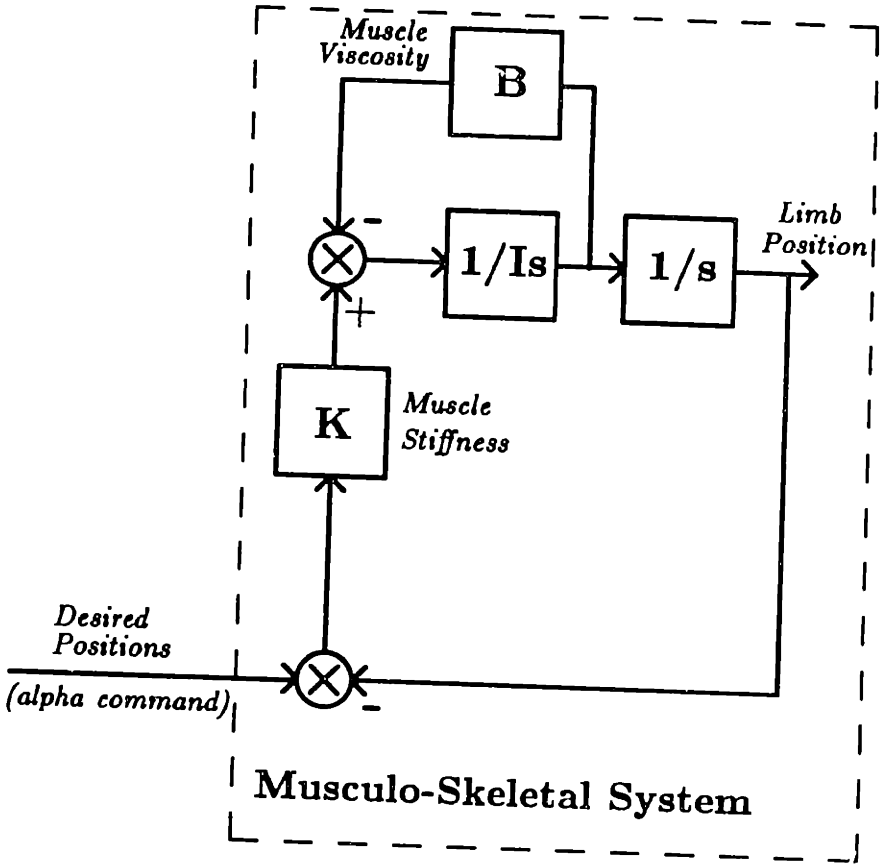

Figure 5-4: Block diagram of α equilibrium model of motor control.

muscles generate the appropriate restoring torques to return the limb to equilibrium.

Figure 5-4 is a simplified model of the musculo-skeletal system of a single joint. The position feedback gain K corresponds to the net stiffness of all the muscles acting around the joint, while B is the net viscosity. The inputs to this model system consist of a reference trajectory which specifies the equilibrium position of the joint as a function of time and a stiffness level determined by the level of agonist/antagonist co-activation. (I will assume for simplicity that the viscosity B is dependent on K so as to produce a constant damping ratio with no load.)

Limb movements can be generated by adjusting the muscle activations so as to smoothly vary the equilibrium point along the desired path. As in Merton's reflex servo model, no explicit computation of inverse dynamics is performed. In contrast to the reflex based model, however, stability is not an issue. Because the servo action

which generates the movement is based on the mechanical properties of the muscles, there is no problem with feedback delays.

The experimental evidence for the α equilibrium point model is quite strong. Deafferented monkeys can make pointing movements to visually selected targets in the absence of any sensory feedback about the location of the limb [9, 7, 6, 30]. Furthermore, the production of such movements is robust with respect to perturbations imposed by the experimenters [6, 5, 27, 30]. The fact that the monkey can achieve a desired target position regardless of the starting point of the limb belies the idea that movements are generated by centrally generated torque commands.

The α formulation of the equilibrium point hypothesis is not completely satisfactory, however. Experiments with deafferented monkeys and humans have shown that motor performance in the absence of sensory feedback is seriously degraded. While the limb may reach the final desired position, the trajectory of the arm is much more erratic than in normal subjects. Clearly, reflexes play an important role in the production of movements and should be included in any model of motor control.

λ Model

Under the λ equilibrium point model for motor control movements are also generated by shifts in the equilibrium posture of the limb. The λ model differs from the α model in the way that the equilibrium position is defined. Under the λ model changes in equilibrium position are generated by adjustments to the threshold of the monosynaptic stretch reflex [19, 3]. The simplest possible interpretation of this formulation is shown in the block diagram of Figure 5-5a. At first glance, this model appears to be identical to the Merton hypothesis. The model in Figure 5-5a differs from the Merton circuit of Figure 5-3 in one subtle way. Because the subtraction of the CNS generated reference signal and the spindle generated position signal occurs in the spinal cord, there is no delay required between the initiation of the central motor program and the alpha motor signal. This model is consistent with the experimentally observed alpha-gamma co-activation.

Model 5-5a has the same inherent feedback delays as the Merton model, and

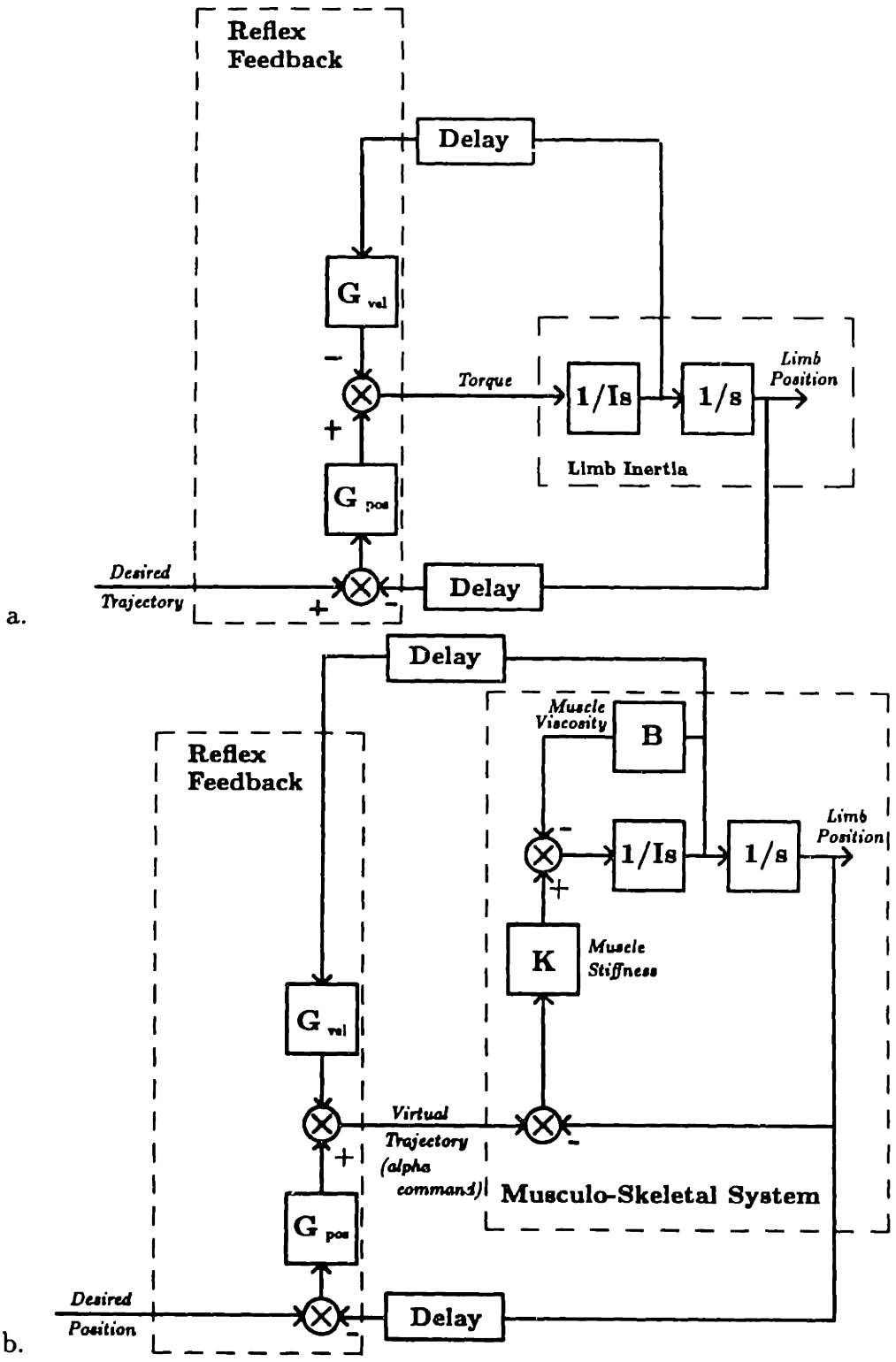

Figure 5-5: Formulations of the λ equilibrium point model which do do not adequately reflect known properties of the human motor system - (a) has the same stability problems as the Merton hypothesis, (a) and (b) fail to explain performance of deafferented monkeys.

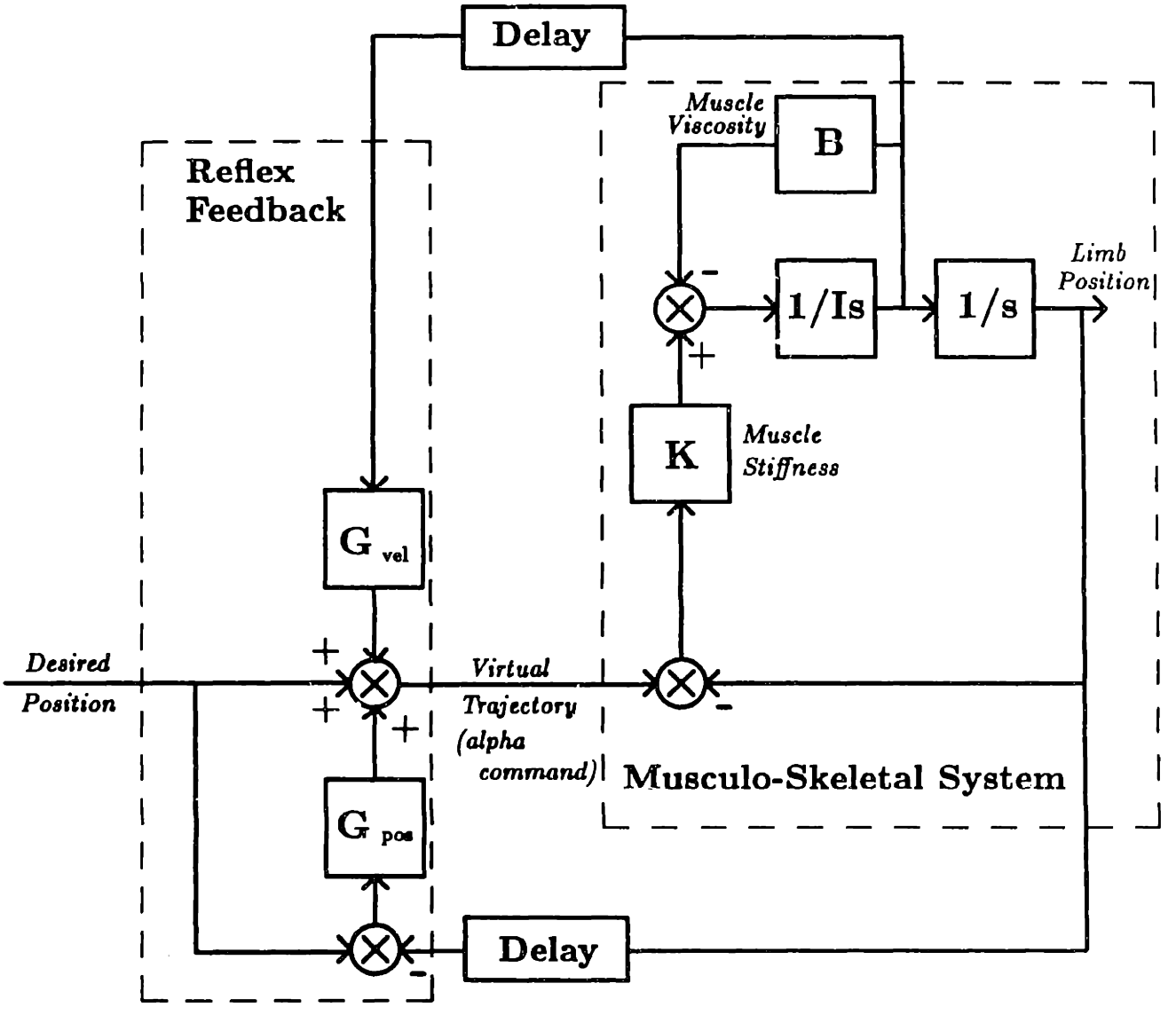

Figure 5-6: Consistent formulation of the λ equilibrium point model. The model is consistent with alpha-gamma coactivation, and deafferented monkey experiments. The α model is a integral component of this formulation.

therefore suffers from the same problems of stability. The equilibrium point model is dependent on the mechanical properties of the muscles to provide stability to the system.

Figure 5-5b shows a second interpretation of the λ hypothesis. The reflex circuit computes an equilibrium position for the musculo-skeletal system based on the sensory feedback from the limb. This equilibrium point is fed to the muscles via an appropriate combination of agonist and antagonist alpha motor commands. This model is, however, inconsistent with the experiments in deafferented monkeys. If the reflex pathways were cut, the muscles would no longer receive an alpha motor command that is consistent with the desired posture or movement.

Figure 5-6 is the simplest interpretation of the λ hypothesis that satisfies both the theoretical stability constraints and the experimental observations. In this model the centrally generated equilibrium point is fed directly to the musculo-skeletal system, via the alpha motor neurons. This signal is modified during the course of the movement by sensory feedback. The equilibrium position of the limb is defined by both the threshold of the stretch reflex and the mechanical properties of the muscles.

The point of the foregoing discussion is the following: Figure 5-6 is the only viable formulation of the λ equilibrium point model. At the heart of this formulation is the α model shown in Figure 5-4. One cannot accept the λ hypothesis without accepting the α model as an important component. On the other hand, since the action of reflexes clearly improves the performance of movements, neither should the α model considered in isolation. The two control circuits must work in concert to produce movements. While one might argue about the relative contributions of the muscle vs. reflex elastic properties, the equilibrium point model of motor control is dependent on both of these components.

5.3 Velocity Scaling

While the basic form of equilibrium point control may be adequate for the production of relatively slow movements (as in the case of the deafferented monkey experiments),

some problems may appear as the speed of motion is increased. To move faster along the same path, it is necessary to do one of two things, either increase the stiffness of the muscles or modify the equilibrium point trajectory. In this section I will examine this issue of velocity scaling as it relates to the equilibrium point model of motor control.

Consider the α equilibrium point model of Figure 5-4. The simplest way to produce a desired trajectory with this system is to use the desired trajectory as the reference trajectory input to the system. If the stiffness of the system is sufficiently high relative to the speed of the movement, the actual trajectory produced will be close to (but not exactly equal to) the desired trajectory (Figure 5-7). If the same strategy is used to produce a faster movement, the difference between the actual and desired trajectories may become significant. In particular, the movement may be significantly lower than desired and the velocity profile will no longer be symmetric and bell shaped (Figure 5-8).

5.3.1 Stiffness Scaling

By increasing the stiffness of the system the increase in desired speed can be accommodated. To achieve the same level of performance as for the slower movement, the stiffness must be scaled with the square of the movement velocity. To move four times as fast, the system must be sixteen times as stiff (Figure 5-9).

5.3.2 Equilibrium Trajectory Modification

The speed of movement can be increased without increasing stiffness if the reference trajectory is no longer constrained to be the same as the desired trajectory. Since the reference trajectory need never be achieved, it has been called a *virtual trajectory* [30]. Using this approach, the equilibrium point trajectory will initially lead, then lag the actual desired position during the course of the movement. The equilibrium position may actually overshoot the final desired position (Figure 5-10).

While this formulation of the model increases the efficiency of the system, it

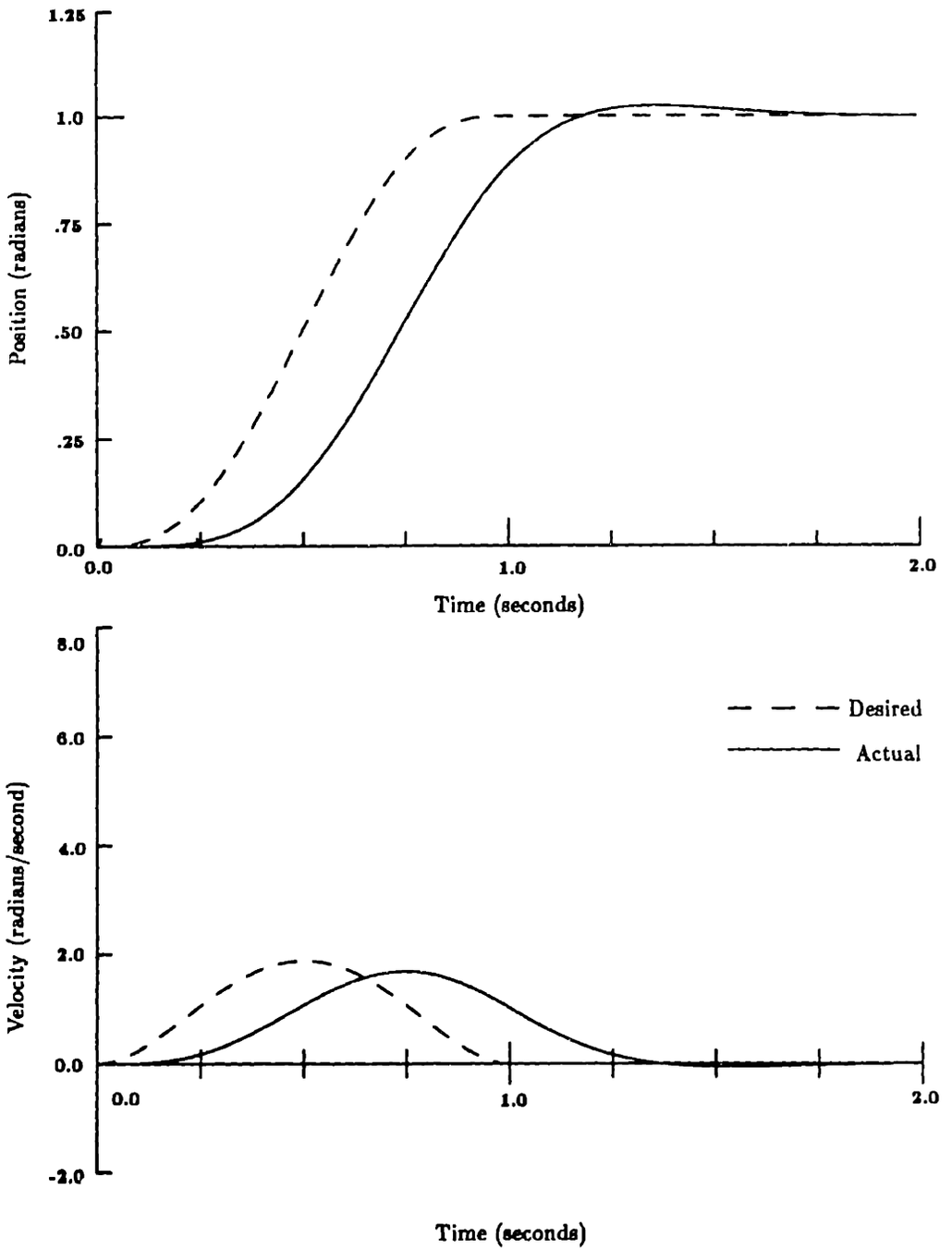

Figure 5-7: Slow movement at low stiffness.
$I = .1$, $K = 4.0$, $B = .88$, $f_0 = 1\text{hz}$. $\zeta = .707$

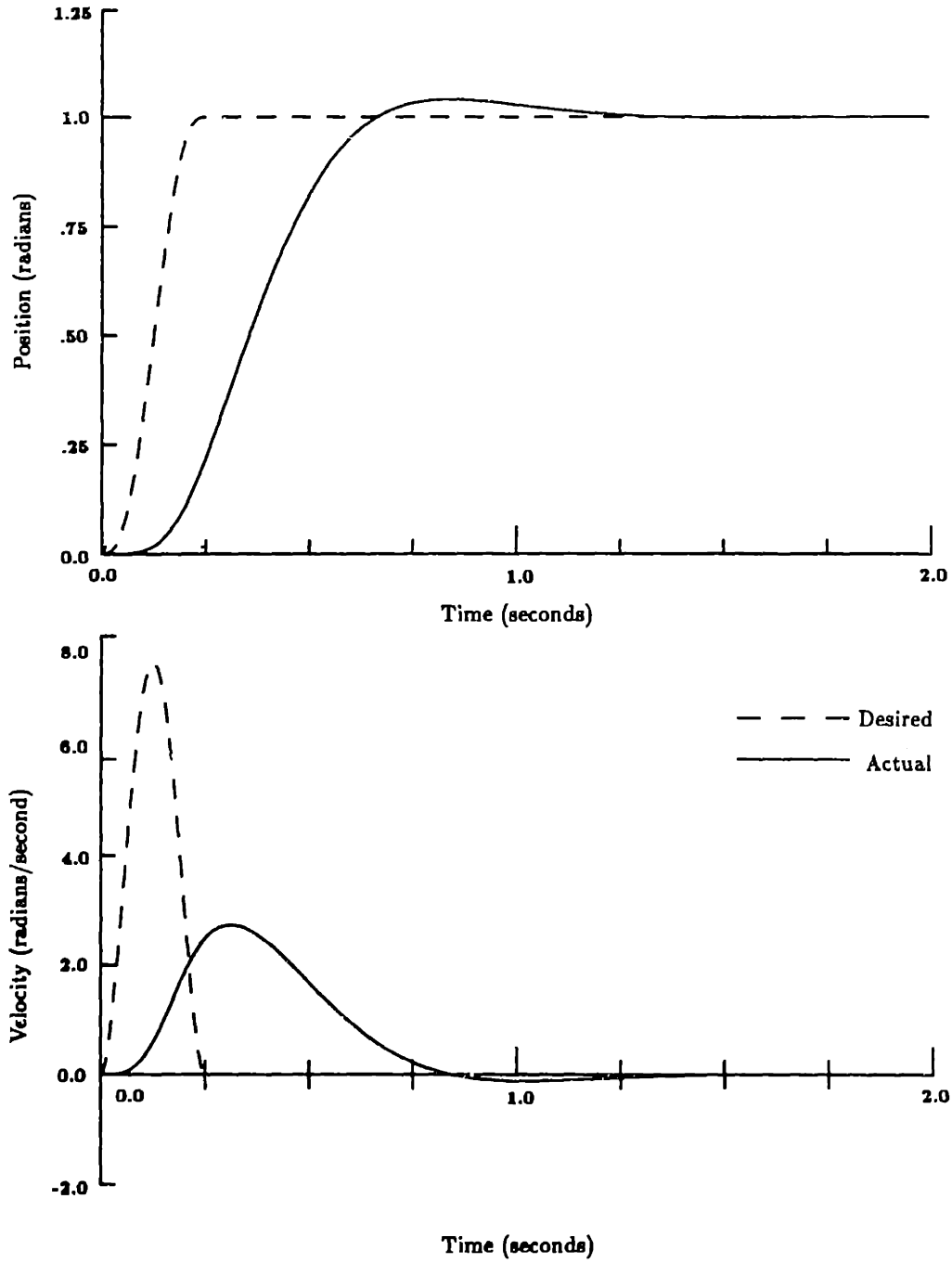

Figure 5-8: Fast movement at low stiffness.
$I = .1,\ K = 4.0,\ B = .88,\ f_0 = 1\text{hz}.\ \zeta = .707$

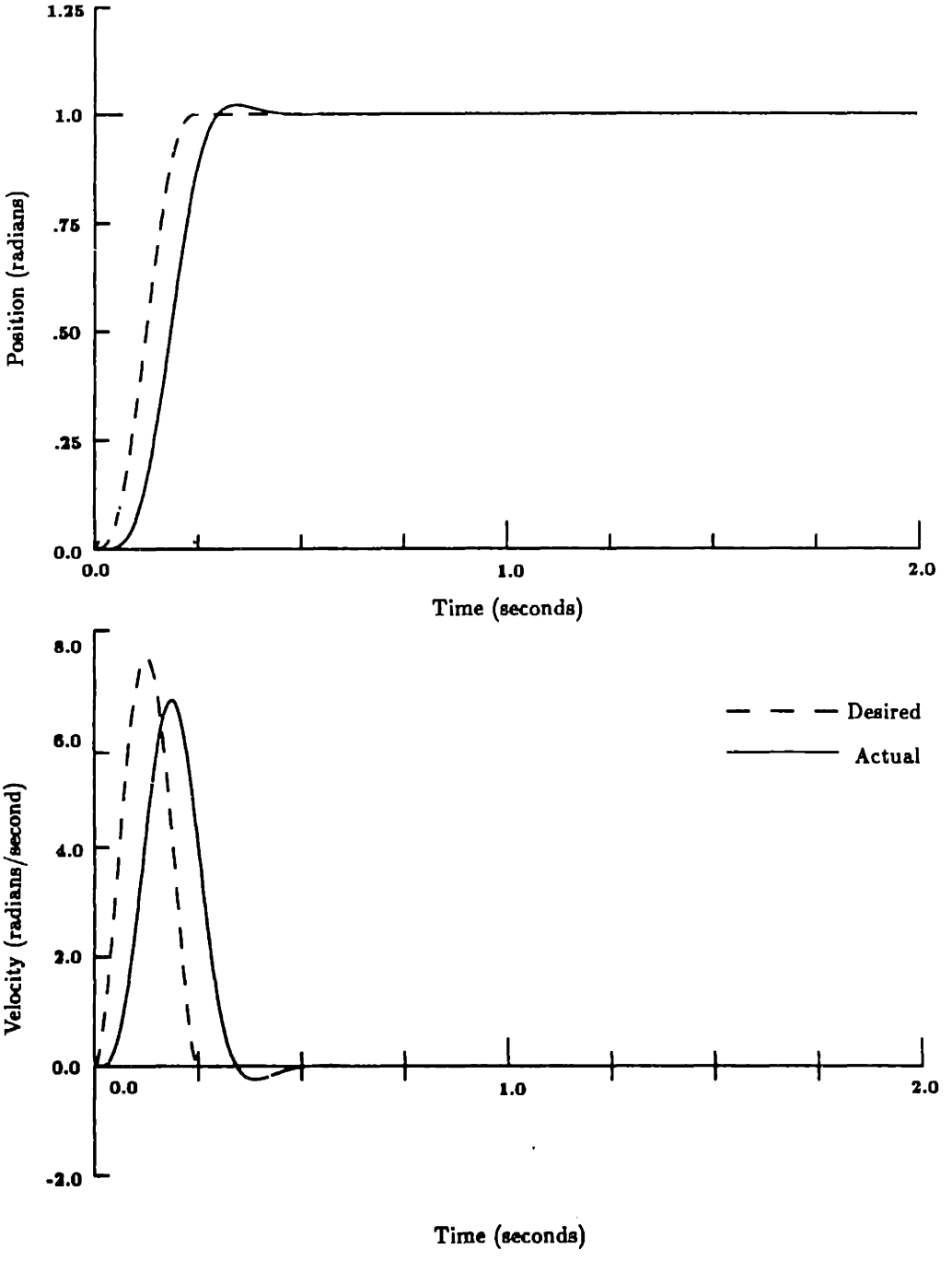

Figure 5-9: Fast movement at high stiffness.
$I = .1,\ K = 64.0,\ B = 3.6,\ f_0 = 4\text{hz}.\ \zeta = .707$

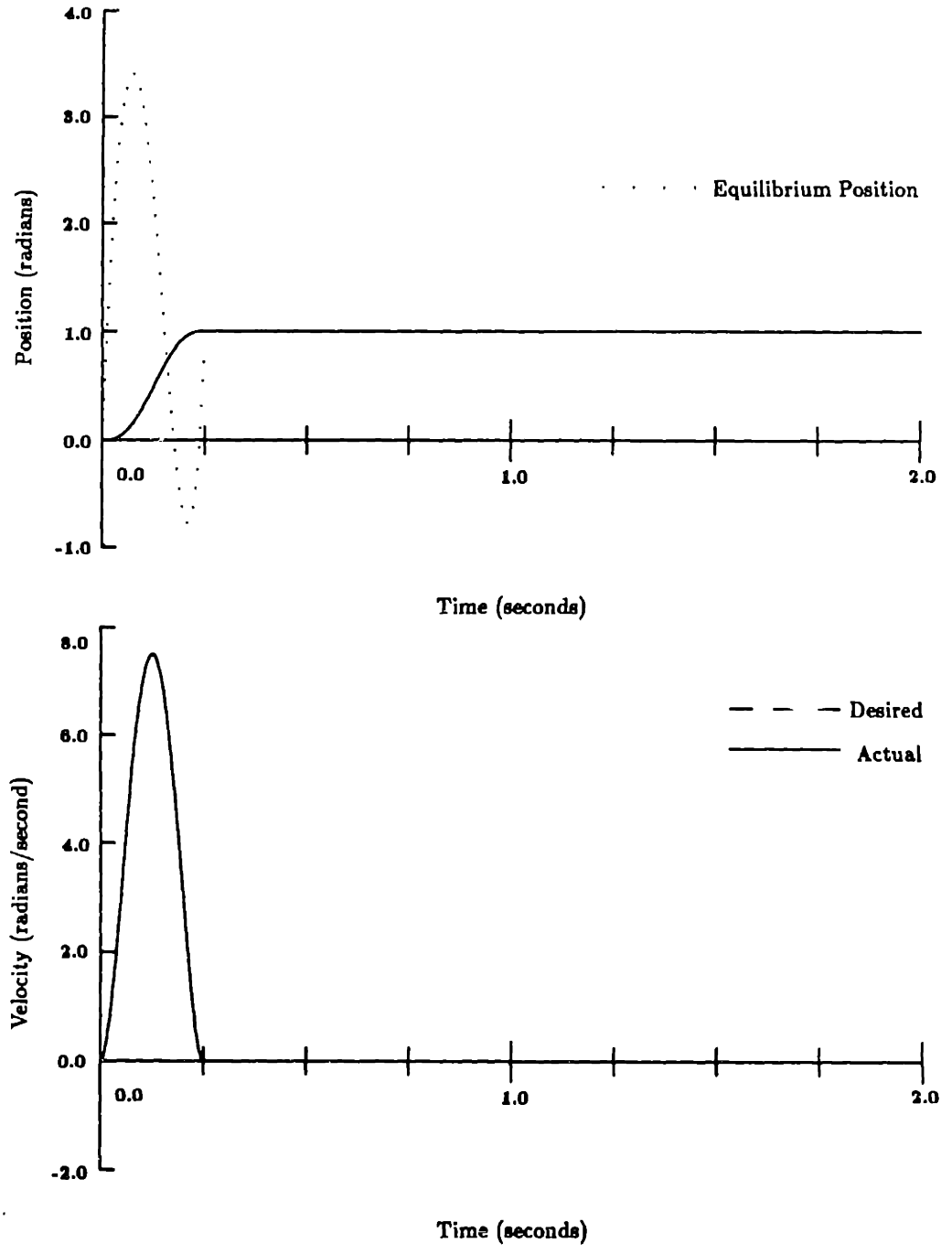

Figure 5-10: Fast movement with computed virtual trajectory.
$I = .1$, $K = 4.0$, $B = .88$, $f_0 = 1\text{hz}$. $\zeta = .707$

also increases the computational complexity of the problem. The equilibrium point trajectory required to produce the movement is no longer simply a copy of the desired movement. The system must solve the inverse dynamics problem in order to generate the appropriate motor command, and it must recompute this command for movements of different speeds and with different loads. By the strict definition of Section 5.1 a system which requires an input of this type does not qualify as a servo system.

5.3.3 Velocity Scaling and the Equilibrium Point Control Models

Can stiffness scaling account for the production of fast movements under the equilibrium point models of motor control? Under the α model, increasing the stiffness corresponds to increasing the level of co-contraction around the joint. While this may be a possible option for increasing speed, it is not necessarily the most efficient. Co-contraction requires an increase in the consumption of metabolic energy [29]. Under the λ model, an increase in stiffness could be achieved by either an increase in muscle stiffness, or an increase in the reflex feedback gain. The latter may, however, be limited by the feedback delays of the system. In either case the level of stiffness that would be required for fast movements of the human arm is relatively high. Figure 5-11 shows the trajectory of the limb produced by a subject asked to move as fast as possible. The duration of this movement is approximately 125 milliseconds, which would require a servo stiffness of approximately 252 newton-meters/radian (for an estimated limb inertia of 0.1 kilogram-meter^2).

The stiffness of the arm can be estimated by measuring the response to disturbances applied during the movement. Experiments such as these estimate that the natural frequency of the elbow is low during the production of fast movements, on the order of 1 – 3 hz. [2, 38]. This corresponds to stiffness values in the range of 4.0 to 36.0 newton-meters/radian. Note that these estimates would include the combined contributions of the muscle mechanical stiffness and the stretch reflex gain.

Hogan computed the virtual trajectory required to produce a movement of a

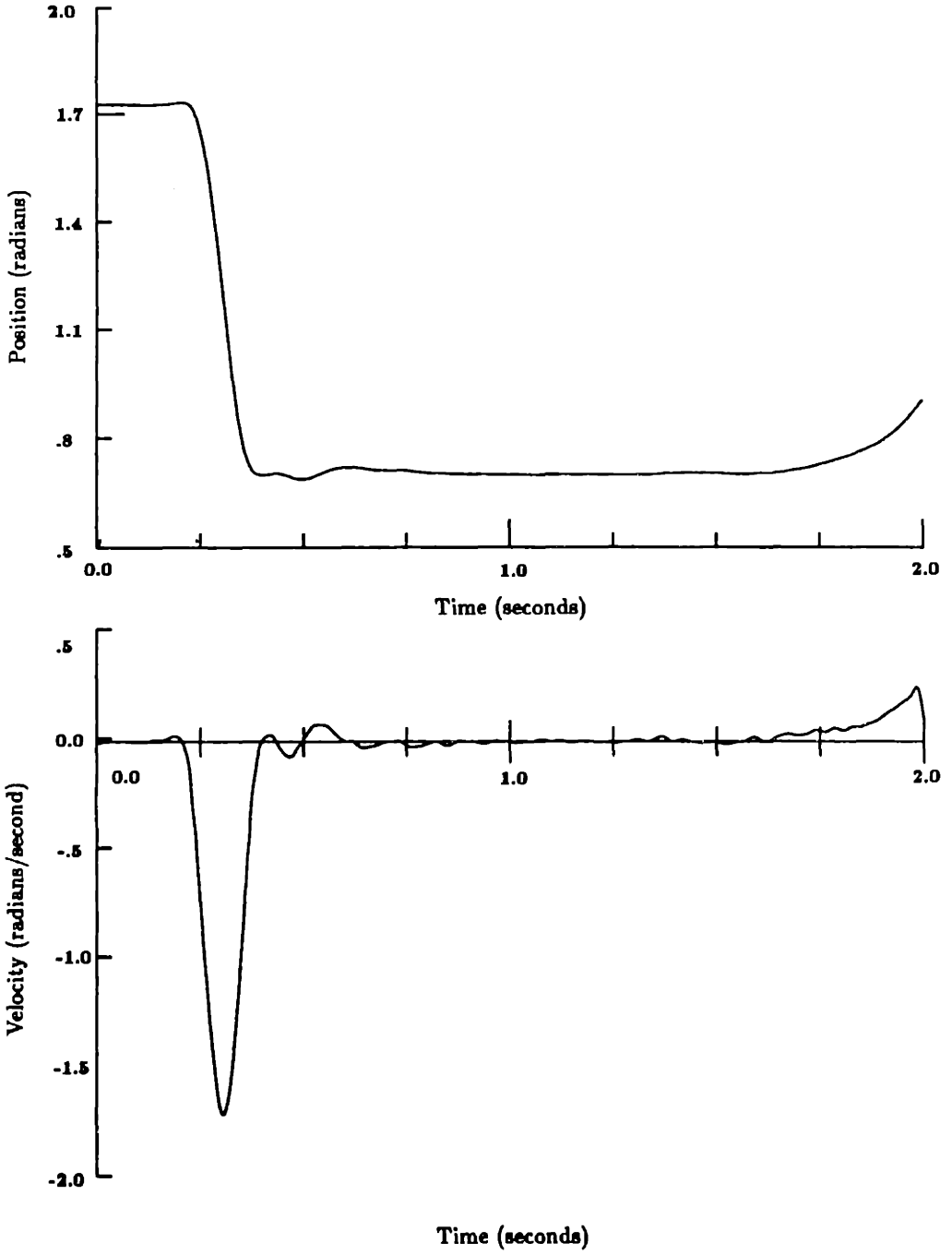

Figure 5-11: Measured actual movement for subject asked to move as fast as possible, after 10 practice trials.

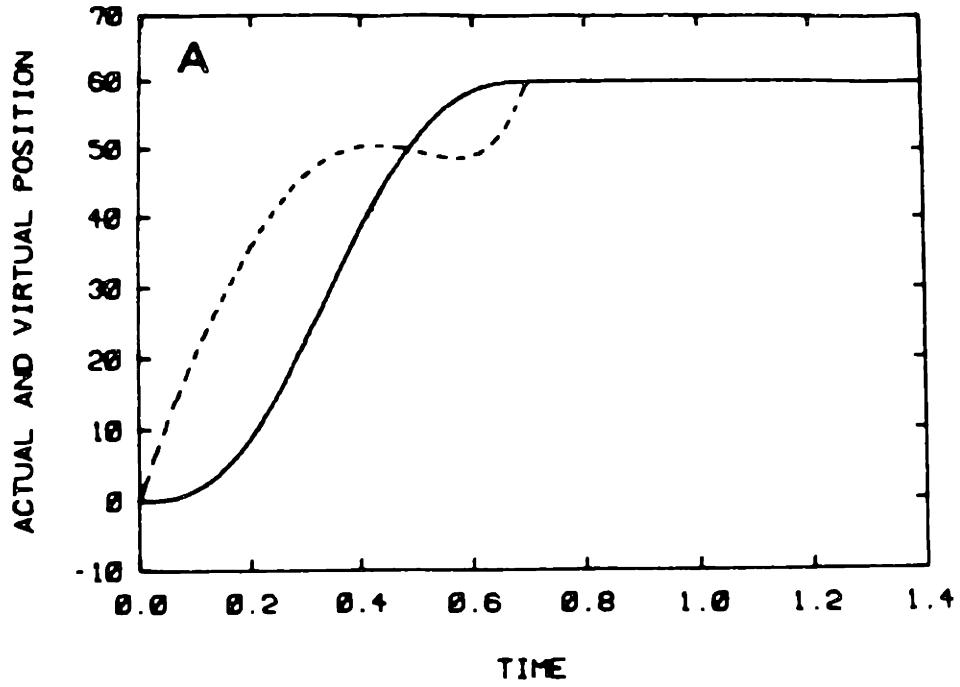

Figure 5-12: Estimation of the virtual trajectory for a monkey arm movement (from Hogan, 1984 [30]). The equilibrium trajectory has a different time course than the actual trajectory.

monkey arm, based on estimates of stiffness for the limb [30], the results of which are shown in Figure 5-12. Even for a slow movement such as this one (700 milliseconds) the virtual trajectory is seen to be significantly different from the actual trajectory.

The evidence suggests that neither formulation of the equilibrium point control model can adequately describe the production of fast arm movements if these models are restricted to act as position servos as defined above. Adequate performance of these models requires the inclusion of a feedforward component in the virtual trajectory command provided by the CNS to the sensory-motor system.

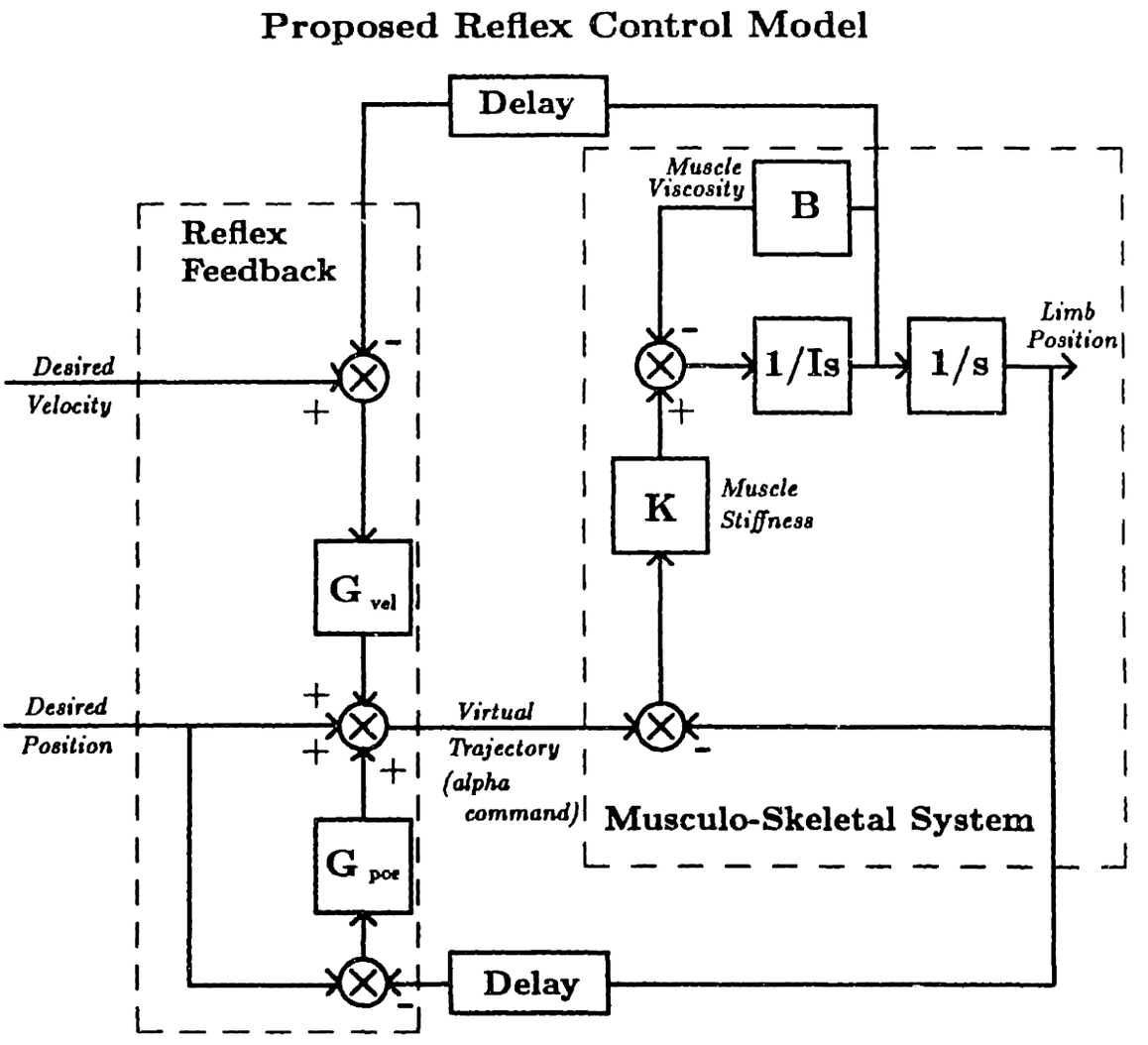

Figure 5-13: Proposed equilibrium point model with reflex feedback.

5.4 Enhancement of the Equilibrium Point Control Model

Can any feedback-only control system adequately account for the known behavior of the human limb? I have proposed a new control structure which defines such a system. (Figure 5-13). The controller is computationally simple in that the CNS need specify only the actual desired trajectory for the limb. The desired trajectory is fed directly to the muscles, as in the α equilibrium point control scheme. This

virtual trajectory is modified, however, by reflex feedback during the execution of the movement.

The proposed model differs from the λ equilibrium control model by the addition of a *velocity reference* signal. The addition of this signal effectively implements a position plus derivative controller which serves to increase the command following performance of the system. This allows the system to produce faster movements at a given level of K and G_{pos}.

5.4.1 Simulation of the Proposed Controller

A potential problem with this approach is that the delays in the reflex pathways limit the feedback gains, and thus the performance level that can be achieved. Computer simulations have been carried out in order to establish the feasibility of such a control scheme.

Figures 5-14 – 5-17 show the results of the simulations for a variety of different system parameters. Table 5.1 shows the parameter values for each of these movements. Estimates of feedback delays are based on values reported in [14] in which a best estimate of a 47 msec. was reported for both reflex paths, and from [15] in which distinct values of 25 msec. and 65 msec. were reported for the velocity and position reflex components, respectively. Reflex parameters were selected by simulating controlled movements while systematically varying the appropriate gain values. The system is stable, where pure reflex feedback would not be, and the system produces fast movements at stiffness levels below those required by the equilibrium point hypothesis alone. In addition, the movements speeds and velocity profiles are comparable to that achieved by a human subject asked to move "as fast as possible" (Figure 5-11).

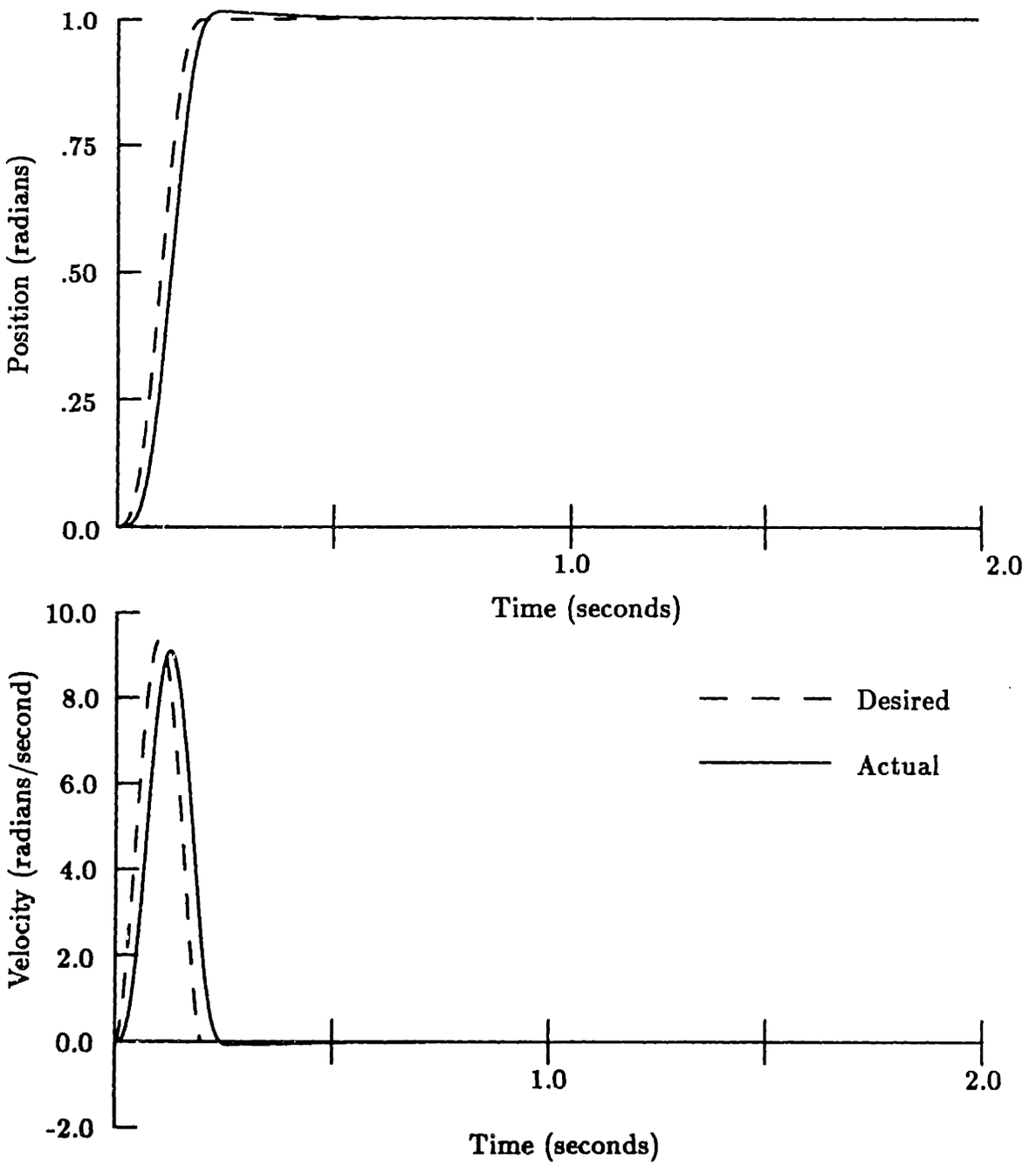

Figure 5-14: Fast movement with proposed reflex feedback model.

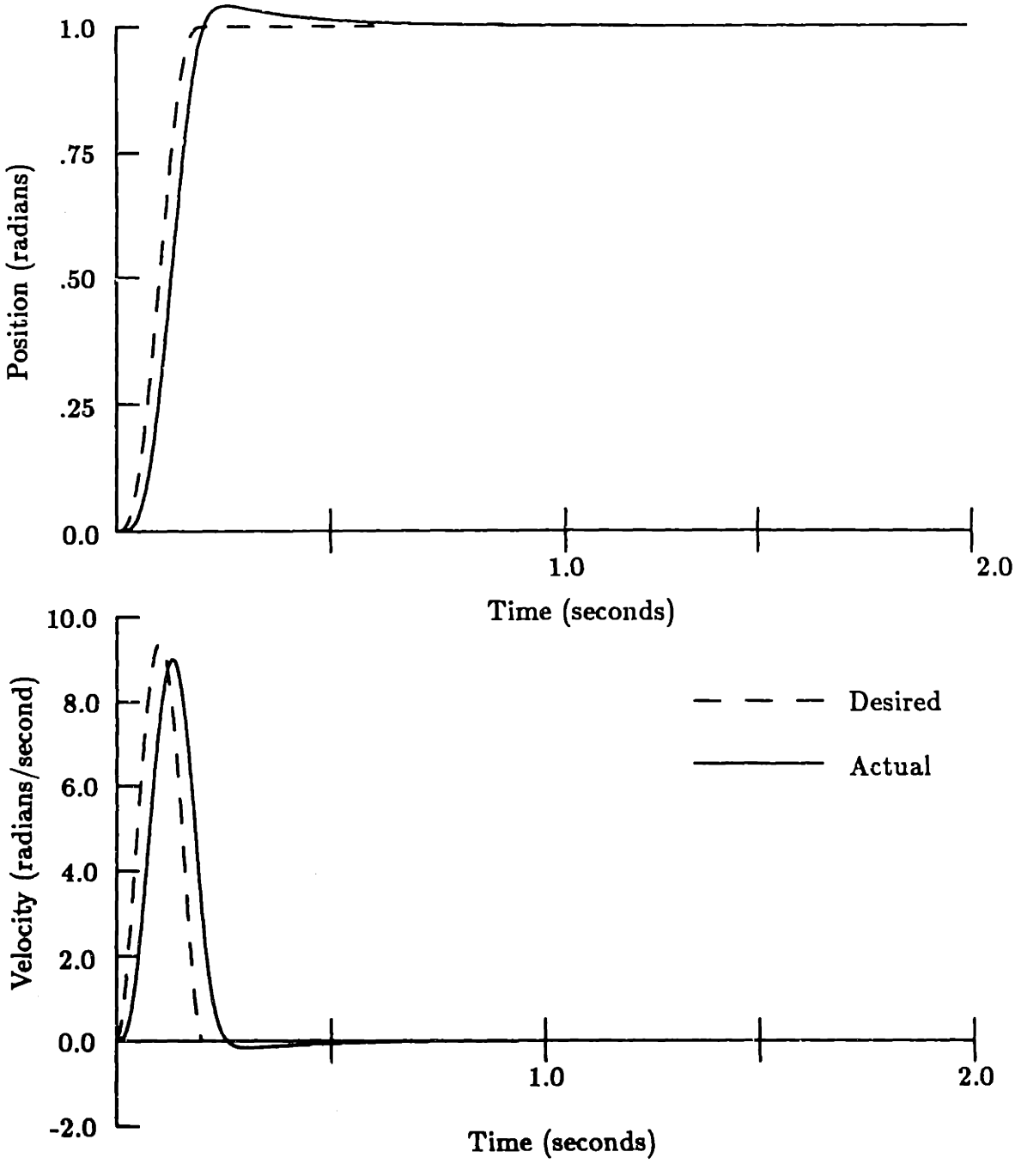

Figure 5-15: Lower muscle damping ratio.

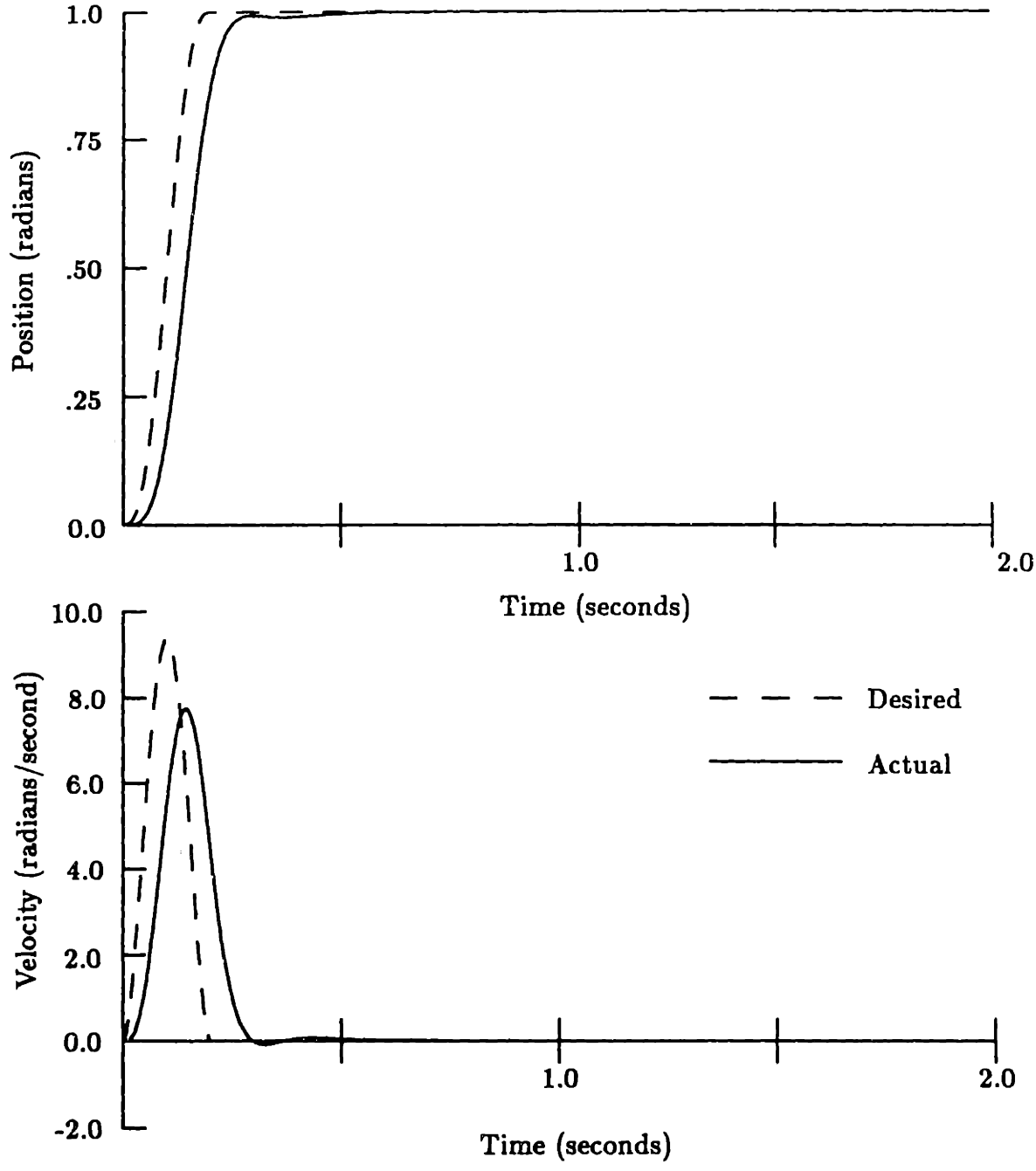

Figure 5-16: Single feedback delay.

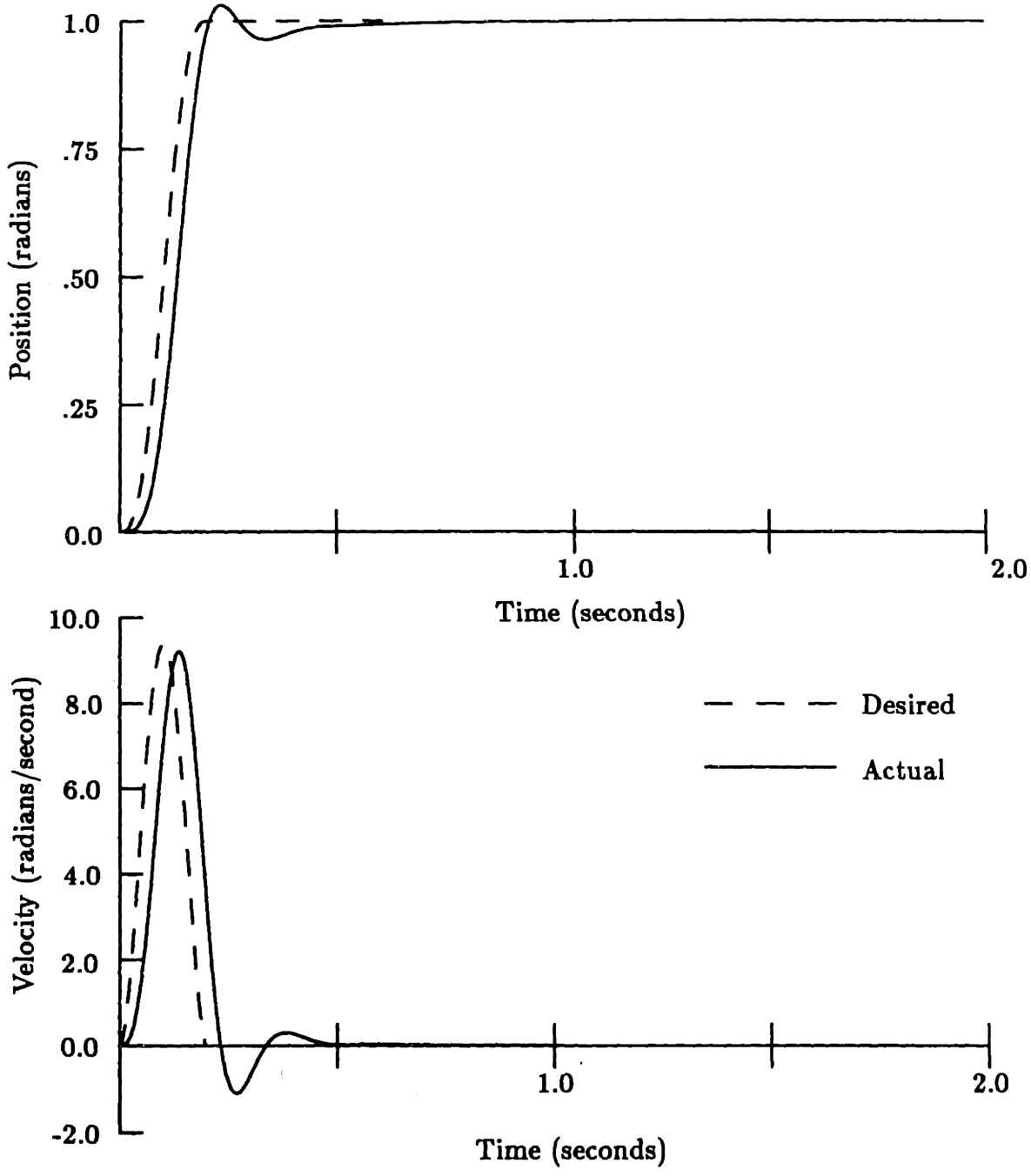

Figure 5-17: Single delay and low damping.

Figure	Muscle Characteristics		Reflex Parameters				Effective
	Natural	Damping	Position		Velocity		Natural
	Freq. (hz.)	Ratio	Gain	Delay (msec)	Gain	Delay	Freq. (hz.)
5-14	1.0	.707	2.5	65	.60	25	1.9
5-15	1.0	.4	1.4	65	.50	25	1.5
5-16	1.0	.707	2.0	40	.30	40	1.4
5-17	1.0	.4	1.5	40	.35	40	1.4

Table 5.1: Control Model Parameters.

5.5 Conclusions

Recent criticism of the equilibrium point hypotheses for motor control have centered on the inability of these models to predict the characteristics of high speed movements. The feedback loop gains (stiffnesses) that would be required for the servo-like production of fast movements are not experimentally observed. Under these models the command input cannot be a simple representation of the desired output. The command must contain a feedforward component based on the dynamics of the system, and thus the computational simplicity of a servomechanism is lost.

In this chapter a new control structure has been proposed which fits the strict definition of a servomechanism. Under this model the CNS need specify only the parameters of the desired trajectory. The model requires a representation of the desired velocity as well as the desired positions to improve the command following performance of the system. Using realistic values for the feedback gains and delays, it has been shown that the proposed controller can produce high speed single joint movements using a pure feedback approach.

Bibliography

[1] K. N. An, F. C. Hui, B. F. Morrey, R. L. Linchield, and E. Y. Chao. Muscles across the elbow joint: A biomechanical analysis. *Journal of Biomechanics*, 14:659–669, 1981.

[2] D.J. Bennett, Y. Xu, J.M. Hollerbach, and I.W. Hunter. Identifying the mechnical impedance of the elbow joint during posture and movement. In *Society for Neuroscience Abstracts*, volume 15, page 396, Pheonix, Arizona, 1989.

[3] M. B. Berkinblitt, A. G. Feldman, and O. I. Fukson. Adaptability of innate motor patterns and motor control mechanisms. *Behavioral Brain Science*, 9:585–638, 1986.

[4] N. Bernstein. *The Co-ordination and Regulation of Movements.* Permagon Press, Oxford, 1967.

[5] E. Bizzi and W.K. Abend. Control of multijoint movement. In F. Strumwasser and M. Cohen, editors, *Comparative Neurobiology: Modes of Communication in the Nervous System*, pages 255–277. Wiley and Sons, New York, 1985.

[6] E. Bizzi, N. Accornero, W. Chapple, and N. Hogan. Postural control and trajectory formation during arm movement. *Journal of Neuroscience*, 4(11):2738–2744, 1984.

[7] E. Bizzi, W. Chapple, and N. Hogan. Mechanical properties of muscles; implications for motor control. *Trends In Neuroscience*, 5(11):395–398, 1982.

[8] E. Bizzi, P. Dev, P. Morasso, and A. Polit. Effects of load disturbances during centrally initiated movements. *Journal of Neurophysiology*, 41(3):542–556, May 1978.

[9] E. Bizzi, A. Polit, and P. Morasso. Mechanisms underlying achievement of final head position. *Journal of Neurophysiology*, 39(2):435–444, March 1976.

[10] Thomas S. Buchanan, David P. J. Almdale, Jack L. Lewis, and W. Zev Rymer. Characteristics of synergic relations during isometric contractions of human elbow muscles. *Journal of Neurophysiology*, 56(5):1225–1241, November 1986.

[11] J.E. Colgate. *The Control of Dynamically Interacting Systems.* PhD thesis, MIT, August 1988.

[12] J.E. Colgate and N Hogan. Robust control of dynamically interacting systems. *International Journal of Control*, 48:65–88, 1988.

[13] R. D. Crowninshield. Use of optimization techniques to predict muscle force. *Journal of Biomechanical Engineering*, 100:88–92, 1978.

[14] J.R. Dufresne, J.F. Soechting, and C.A. Terzuolo. Electromyographic response to pseudo-random torque disturbances of human forarm position. *Neuroscience*, 3:1213–1226, 1978.

[15] J.R. Dufresne, J.F. Soechting, and C.A. Terzuolo. Reflex motor output to torque pulses in man: Identification of short– and long– latency loops with individual feedback parameters. *Neuroscience*, 4:1493–1500, 1979.

[16] J. Dul, M. A. Townsend, R. Shiavi, and G. E. Johnson. Muscle synegism – ii. a minimum-fatigue criterion between synergistic muscles. *Journal of Biomechanics*, 17:675–684, 1984.

[17] S. A. Ellias, J. McIntyre, and E. Bizzi. Trajectory formation and stiffness in multi-joint arm movements. *Biological Cybernetics*, 1989. In Press.

[18] A.G. Feldman. Functional tuning of nervous system with control of movement or maintenance of a steady posture. ii. controllable parameters of the muscles. iii. mechanographic analysis of the execution by man of the simplest motor task. *Biophysics*, 11:565–578,766–775, 1966.

[19] A.G. Feldman. Once more on the equilibrium-point hypothesis (λ model) for motor control. *Journal of Motor Behavior*, 18(1):17–54, 1986.

[20] J. R. Flanagan, A. G. Feldman, and D. J. Ostry. The equilibrium point model for two-joint arm movement control. In *Society for Neuroscience Abstracts*, volume 15, page 173, 1989.

[21] Tamar Flash. The control of hand equilibrium trajectories in multi-joint arm movements. *Biological Cybernetics*, 57:257–274, 1987.

[22] C. C. A. M. Gielen and E. J. van Zuylen. Coordination of arm muscles during flexion and supination: Application of the tensor analysis approach. *Neuroscience*, 17:527–539, 1986.

[23] Simon F. Giszter, Joseph McIntyre, and Emilio Bizzi. Kinematic strategies and sensorimotor transformations in the wiping movements of frogs. *Journal of Neurophysiology*, 62(3):750–767, September 1989.

[24] D. E. Hardt. Determining muscle forces in the leg during normal human walking – An application and evaluation of optimization methods. *Journal of Biomechanical Engineering*, 100:72–78, 1978.

[25] E.C. Hildreth and J.M. Hollerbach. Artificial intelligence: Computational approach to vision and motor control. In F. Plum, editor, *Handbook of Physiology, Section 1: The Nervous System, Volume V: Higher Functions of the Brain, Part II*, pages 605–642. American Physiological Society, 1987.

[26] J.A. Hoffer, A.A. Caputi, I.E. Pose, and R.I. Griffiths. Roles of muscle activity and load on the relationship between muscle spindle length and whole muscle length in the freely walking cat. *Progress in Brain Research*, 80:75–85, 1989.

[27] Neville Hogan. Control and coordination of voluntary arm movements. In *Proceedings of the 1982 American Control Conference 1*, pages 552–558, 1982.

[28] Neville Hogan. Mechanical impedance control in assistive devices and manipulators. In M. Brady, J. M. Hollerbach, T. L. Johnson, T. Lozano-Perez, and M. T. Mason, editors, *Robot Motion: Planning and Control*, pages 361–371. M.I.T. Press, Cambridge, 1983.

[29] Neville Hogan. Adaptive control of mechanical impedance by coactivation of antagonist muscles. *IEEE Transactions on Automatic Control*, AC–29:681–690, 1984.

[30] Neville Hogan. An organizing principal for a class of voluntary movements. *Journal of Neuroscience*, 4(11):2745–2754, 1984.

[31] Neville Hogan. The mechanics of multi-joint posture and movement control. *Biological Cybernetics*, 52:315–351, 1985.

[32] J. M. Hollerbach and K. C. Suh. Redundancy resolution of manipulators through torque optimization. *Proceedings of the IEEE International Conference on Robotics and Automation*, pages 1016–1021, 1985.

[33] J.M. Hollerbach. Computers, brains and the control of movement. *Trends in Neurosciences*, 5(6):189–204, June 1982.

[34] S. C. Jacobsen, E. K. Iversen, D. F. Knutti, R. T. Johnson, and K. B. Biggers. Design of the utah/mit dextrous hand. *Proceedings of the IEEE International Conference on Robotics and Automation*, pages 1017–1023, April 1986.

[35] H. A. H. Jongen, J. J. Denier van der Gon, and C. C. A. M. Gielen. Activation of human arm muscles during flexion/extension and supination/pronation tasks. *Biological Cybernetics*, 61:1–9, 1989.

[36] M. I. Jordan. Supervised learning and systems with excess degrees of freedom. Technical report, COINS, University of Massachusetts at Amherst, 1988.

[37] Charles A. Klein and Ching-Hsiang Huang. Review of pseudo-inverse control for use with kinematically redundant manipulators. *IEEE Transactions on Systems, Man, and Cybernetics*, SMC-13(3):245–250, March/April 1983.

[38] J.M. Lanman. *Movememt and the Mechanical Properties of the Intact Human Elbow Joint.* PhD thesis, M.I.T., 1980.

[39] A. Liegeois. Automatic supervisory control of the configuration and behavior of multi-joint mechanisms. *IEEE Transactions on Systems, Man, and Cybernetics*, SMC-7(12), 1977.

[40] Gerald E. Loeb. Motorneurone task groups: Coping with kinematic heterogeneity. *Journal of Experimental Biology*, 115:137–146, 1985.

[41] J. McIntyre, F.A. Mussa-Ivaldi, and E. Bizzi. Modelling of multi-joint motor systems. *Proceedings of the Annual International Conference of the IEEE Engineering in Medicine and Biology Society*, 11:242–243, 1989.

[42] P. A. Merton. Speculations on the servo control of movement. In *The Spinal Cord.* Little Brown, Boston, MA, 1953.

[43] P. Morasso, F. A. Mussa-Ivaldi, G Vercelli, and R. Zaccaria. A connectionist formulation of motor planning. In R. Pfeifer, Z. Schreter, F. Fogelman, and L. Steels, editors, *Connectionism in Perspective.* Elsevier, Amsterdam, 1989.

[44] F. A. Mussa-Ivaldi and T. Flash. Voluntary variation of stiffness parameters for a two-joint arm. Personal Communications, 1990.

[45] F. A. Mussa-Ivaldi, J. McIntyre, and E. Bizzi. Theoretical and experimental perspectives on arm trajectory formation: A distributed model for motor redundancy. In E. Clementi and S. Chin, editors, *Biological and Artificial Intelligence Systems.* Escom, 1988.

[46] F. A. Mussa-Ivaldi, P. Morasso, N. Hogan, and E. Bizzi. Network models of motor systems with many degrees of freedom. In M. D. Fraser, editor, *Advances in*

Control Networks and Large Scale Parallel Distributed Processing Models. Ablex Publishing Corporation, Norwood, N.J., 1989.

[47] F.A. Mussa-Ivaldi, N. Hogan, and E. Bizzi. Neural, mechanical and geometric factors subserving arm posture in humans. *Neuroscience*, 5:2732–2743, 1985.

[48] T.R. Nichols and J.C. Houk. Improvement in linearity and regulation of stiffness that results from actions of the stretch reflex. *Journal of Neurophysiology*, 39:119–142, 1976.

[49] Katsuhiko Ogata. *Modern Control Engineering.* Prentice–Hall Electrical Engineering Series. Prentice–Hall, Inc., Englewood Cliffs, NJ, 1970.

[50] H. M. Paynter. *Analysis and Design of Engineering Systems.* MIT Press, Cambridge, MA, 1961.

[51] A. J. Pellionisz. Coordination: a vector-matrix description of transformations of over-complete cns coordinates and a tensorial solution using the moore–penrose generalized inverse. *Journal of Theoretical Biology*, 110:353–375, 1984.

[52] D. D. Penrod, D. T. Davy, and D. P. Sigh. An optimization approach to tendon force analysis. *Journal of Biomechanics*, 7:123–129, 1974.

[53] A. Polit and E. Bizzi. Characteristics of motor programs underlying arm movements in monkeys. *Journal of Neurophysiology*, 42(1):183–194, January 1979.

[54] William H. Press, Brian P. Flannery, Saul A. Teukolsky, and William T. Vetterling. *Numerical Recipes in C.* Cambridge University Press, 1988.

[55] P.M.H. Rack and D.R. Westbury. The effects of length and stimulus rate on the tension in the isolated cat soleus muscle. *Journal of Physiology*, 204:443–460, 1969.

[56] A. Seireg and J. Arvikar. A mathematical model for evaluation of forces in lower extremities of the musculo-skeletal system. *Journal of Biomechanics*, 16:313–326, 1973.

[57] G. Strang. *Linear Algebra and Its Applications.* Academic Press, New York, 1980.

[58] A. B. Vallbo. Discharge patterns in human spindle afferents during isometric contractions. *Acta physiol. scand.*, 80:552–566, 1970.

[59] Thomas A. Zeffiro. *Motor Adaptation to Alterations in Limb Mechanics.* PhD thesis, M.I.T., May 1986.